

AD-A174 665

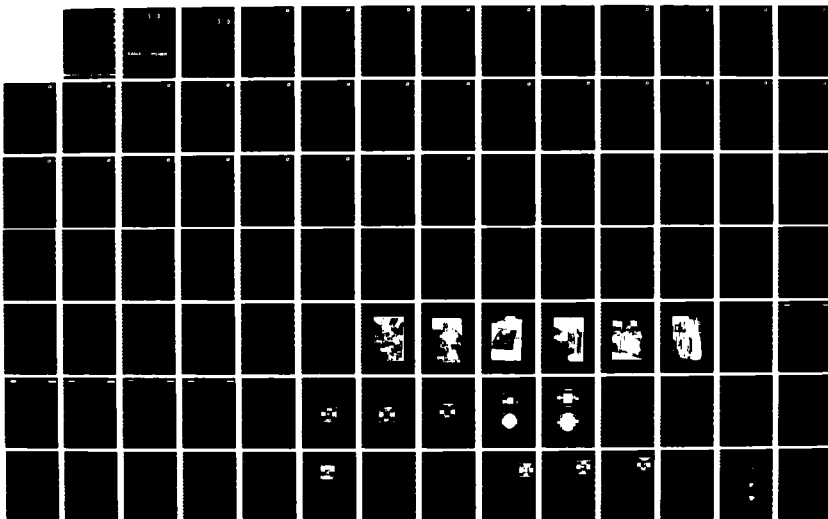
DEVELOPMENT OF A FREE CARRIER ABSORPTION MEASUREMENT
INSTRUMENT FOR INDIU (U) EAGLE-PICKER RESEARCH LAB
MIAMI OK SPECIALTY MATERIALS DIV 27 OCT 86
N00014-85-C-2430 F/G 20/12

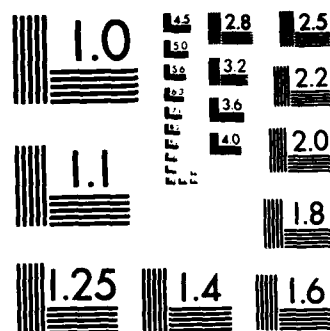
1/2

UNCLASSIFIED

F/G 28/12

NL





MICROCOPY RESOLUTION TEST CHART
NATIONAL BUREAU OF STANDARDS-1963-A

AD-A174 665

DTIC
ELECTE
DEC 03 1986
S D

12

Final Report
Development of a Free Carrier
Absorption Measurement Instrument
For
Indium Phosphide and Gallium Arsenide

EAGLE EPICHER
RESEARCH LABORATORY

This document has been approved
for public release and sale; its
distribution is unlimited.

Specialty Materials Division ✓

86 11 6 052

12

DTIC
ELECTE
DEC 03 1986
S D D

Final Report
Development of a Free Carrier
Absorption Measurement Instrument
For
Indium Phosphide and Gallium Arsenide

Contract No: N00014-85-C-2430

Prepared For: Naval Research Laboratory
4555 Overlook Ave. S.W.
Washington, D.C. 20375-5000

Prepared By: Eagle-Picher Research Laboratory
200 9th Ave. N.E.
Miami, OK 74354

This document has been approved
for public release and sale; its
distribution is unlimited.

27 October 1986



Accession For	
NTIS CRA&I	<input checked="" type="checkbox"/>
DTIC TAB	<input type="checkbox"/>
Unannounced	<input type="checkbox"/>
Justification	
By <i>lth. or file</i>	
Distribution /	
Availability Codes	
Dist	Avail and/or Special
A-1	

FEA FINAL REPORT

I. INTRODUCTION

This work represents ^{an} effort to develop and evaluate a contactless method for determining the spatial variation of the free carrier concentration in compound semiconductor materials. ^{is discussed} The capability of performing such measurements is of particular importance because of the current interest in producing electronic grade wafers from the III-V and II-VI compounds. These materials (particularly the II-VI compounds) tend to be nonuniform due to preferential migration of one of the constituents in the neighborhood of growth defects. All semiconductors which are grown at some finite temperature will contain Frenkel and Schottky point defects; such defects in compounds tend to be of a preferential nature which results in slight deviations from stoichiometry. These deviations can result in significant variations in doping concentrations and type. Defects in the macrostructure such as twin lines, grain boundaries, inclusions and dislocation lines can produce stoichiometric gradations which will also result in doping variations. Utilizing traditional electrical characterization methods on such materials can be misleading. A Hall sample taken from one portion of the wafer may yield results which are not at all descriptive of another portion; or, of more concern, the size of the Hall sample may prohibit a measure of the short range variations which may exist throughout the material. The ability to distinguish short range variations in free carrier concentration ^{is} would be an extremely valuable aid to the crystal grower in the development of a particular growth

process. In particular, a contactless, rapid scanning probe would permit a quick evaluation and should result in a more direct and rapid evaluation of a particular crystal growth scheme.

A contactless method for measuring free carrier concentrations has been investigated at the Eagle Picher Research Laboratory, Miami, Oklahoma. The basis for the instrument is the free carrier absorption of infrared radiation. Infrared absorption by free carriers in semiconductors was ~~first~~ demonstrated by Fan and Becker [1]. If this absorption property is to be exploited as a measurement of free carrier concentration, there are a few items which must be addressed taking into consideration that the instrument will, in its simplest form, measure the variation in an IR beam transmitted through the semiconductor. These items for consideration include:

- (1) a need to ascertain the absence of other dominant absorption mechanisms at the frequency (or band of frequencies) involved;
- (2) establish a direct (preferably measurable) relationship between the transmitted beam intensity and the free carrier concentration;
- (3) a better understanding of the impurity concentration and degree of compensation can be achieved through a knowledge of the dominate scattering mechanisms;
- (4) the material geometry, thickness, and orientation, must be considered;
- (5) the ultimate sensitivity and resolution must determined.

Page 3

One of the most attractive features of FEA in semiconductors is that there is usually a band, $4 < \lambda < 12 \mu\text{m}$, in which the free carrier absorption is the dominate mechanism. Free carrier absorption is characterized by monotonic spectrum which grows as λ^p where p ranges from 1.5 to 3.5 and is determined by the dominate scattering mechanisms. FEA characterization of semiconductors has been preformed previously and of most significance to our effort is the work of Jastrzebski, Lagowski and Gatos [2] which involved the use of a scanning CO_2 laser to obtain spatial resolution of the impurity concentrations in silicon. Boone, Cantwell and Shaw [3] have demonstrated the practicability of using a scanning CO_2 laser for mapping CdS wafers; the work reported here is an extension of that effort which has the objective of demonstrating the feasibility of developing an FEA instrument which can provide an automated, rapid scan of a semiconductor wafer. Further, the measurement is contactless with no wafer preparation such as an antireflective coating.

II. THEORETICAL DISCUSSION

The operation of this FEA instrument is based upon the absorption of a CO_2 beam propagating through a semiconductor wafer. According to classical electromagnetic theory [4] a coherent plane wave normally incident upon a lossy dielectric slab has a transmission coefficient given by

$$(1) \quad T = \frac{[(1-R_{12})^2 + 4R_{12} \sin^2 \delta_{12}] \exp(-\alpha d)}{[1-R_{12} \exp(-\alpha d)]^2 + 4R_{12} \sin^2 (\delta_{12} + K_2 d) \exp(-\alpha d)}$$

where

$$(2) \quad R_{12} = \frac{(K_1 - K_2)^2 + (\alpha/2)^2}{(K_1 + K_2)^2 + (\alpha/2)^2}$$

and

$$(3) \quad \delta_{12} = \tan^{-1} [-K_1 \alpha / \{K_1^2 - K_2^2 + (\alpha/2)^2\}].$$

Where α is the absorption coefficient which is related to the complex conductivity (σ') by the expression $\alpha = \sigma' (\mu/\epsilon)^{1/2}$, K_2 and K_1 are the propagation constants for the semiconductor and free space, respectively, given by $K_2 = w(\mu_o \epsilon_o \epsilon_r)^{1/2}$ and $K_1 = w(\mu_o \epsilon_o)^{1/2}$, where w is the frequency (radians/sec), d is the wafer thickness (cm), μ_o is the free space permeability, ϵ_o is the free space permittivity, μ is the semiconductor permeability and ϵ is the semiconductor permittivity.

Equation (1) indicates that the transmission is critically dependent upon the path length through the semiconductor. Figure 1 is a computer generated curve showing T (%) versus wafer thickness for $r=10.6\mu\text{m}$ and $\epsilon_r=5.4$. This figure clearly shows that for thickness variations of the order of $1\mu\text{m}$, the transmission coefficient can change by 10% to 15% which would match the variations due to free electron absorption. This large variation is the result of wave interactions which are dependent upon the spacing, in wavelengths, between the two air/dielectric interfaces. By adjusting the path length between the two surfaces of the wafer one can maximize the transmission coefficient such that

$$(4) \quad T_{\max} \approx \frac{(1-R_{12})^2 \exp(-\alpha d)}{[1-R_{12} \exp(-\alpha d)]^2}$$

where it has been assumed that $\delta_{12} \approx 0$. Now the fractional change in T_{\max} can be expressed as

$$(5) \quad \Delta T_{\max} / T_{\max} = \frac{-[1 + R_{12} \exp(-\alpha d)] \Delta(\alpha d)}{[1 - R_{12} \exp(-\alpha d)]}$$

and $\Delta(\alpha d) = \alpha \Delta d + d \Delta \alpha$. Thus, one must now evaluate the relative changes in the absorption coefficient (α) as opposed to the wafer thickness (d). If α is simply proportional to n then $\Delta(\alpha d)$ can be expressed as

$$(6) \quad (\Delta \alpha d) / \alpha d = \Delta d / d + \Delta n / n$$

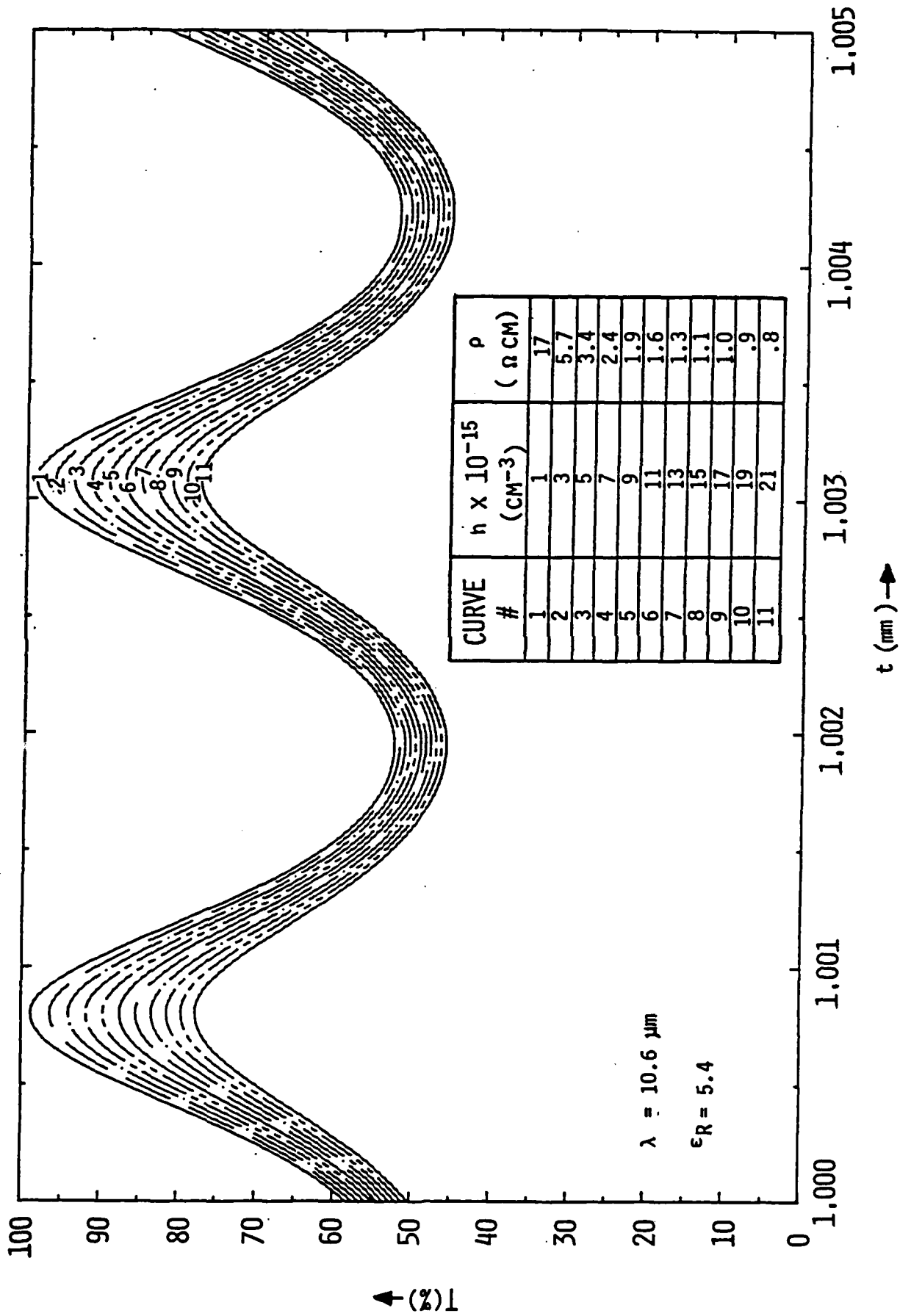


Figure 1 Percent transmission vs thickness for different free carrier densities

which implies that if the objective is to measure Δn then the condition that $\Delta n/n \gg \Delta d/d$ should be maintained. This could place a constraint on the sensitivity. For example if $\Delta d = 1 \mu m$, $d = 1 mm$ and the nominal value for n is $10^{15} cm^{-3}$. Then to ascertain that the measurement is indicating a variation in free carrier density, one must consider only those deviations such that

$$(7) \quad \Delta n \gg n \Delta d/d = 10^{12} cm^{-3}.$$

Of course, this is a 0.1% variation and should represent adequate sensitivity for most measurements. However, the theoretical sensitivity can be significantly improved if the overall thickness variation is held to less than one wavelength ($\approx 3 \mu m$). Since the Δd represents a variation in the path length, the obvious way to avoid thickness limitations on sensitivity is to keep d constant. Figure 2 represents a wafer with thickness variations.

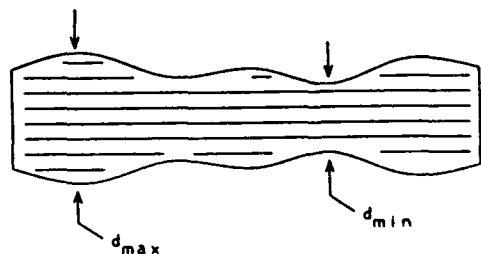


Figure 2: Wafer thickness variations; $d_{max} \leq d_{min} + \tau$

If $d_{max} \leq d_{min} + \tau$ then the beam path length can be held constant by adjusting the angle of incidence such that the path length is constant; further, if the path length is

adjusted to an integer number of wavelengths, the maximum sensitivity will be achieved as described by equation (5). Thus, the smallest angle, θ_{imin} , for which the transmission maximum occurs is determined such that

$$(8) \quad d \cos(\theta_{imin}) = d_{max} \quad \text{with } d = m\tau \text{ and } m = 1, 2, 3, 4, 5, \dots$$

then it must be ascertained that

$$(9) \quad (d_{min}) / \{\cos(\theta_{imax})\} = m\tau$$

this is to insure that the path length stays at $d=m\tau$ and not $(m+p)\tau$ where $p=1, 2, 3, \dots$. The simplest way to insure that equation (9) holds is to make certain that $d_{max} - d_{min} \leq \tau$ which is not a stringent requirement. The actual measurement technique involves rotating the sample through a small angle seeking the transmission maximum nearest $\theta = 0$. Theoretically, the relation between transmission variations and the absorption coefficient becomes

$$(10) \quad \Delta T_{max} / T_{max} = \frac{-\{1 + R_{12} \exp(-\alpha d)\} (\alpha d) (\Delta \alpha / \alpha)}{\{1 - R_{12} \exp(-\alpha d)\}}$$

In this instance, the absorption coefficient, α , is a measure of the attenuation of the infrared beam due to the free electron interactions with incident photons. The photon absorption by the free electrons is a two step process which includes electron-phonon interaction as a necessity for the conservation of momentum. Lattice vibrations, impurities

and lattice defects (acting as scattering centers for free electrons) give rise to absorption. These scattering processes result in small energy variations such that secondary perturbation theory [5] can be used to determine the transition probability for each of the scattering processes. For semiconductors, there are five scattering mechanisms which may be significant depending upon the crystal structure, defects and impurity concentrations. These mechanisms are acoustic phonon, optical phonon, polar optical phonon, piezoelectric and charged impurity scattering. Ridley [5] among others has developed the theoretical expressions for these scattering mechanisms. Of particular significance to this work is the functional dependence of absorption coefficient (α) upon the free electron density and wavelength of the incident radiation. In the wavelength range of free carrier absorption, α can be expressed approximately as a sum of the absorption coefficients due to various scattering process, for most cases of interest (at room temperature),

$$(11) \quad \alpha = \alpha_{op} r^{2.5} + \alpha_{imp} r^{3.5} + \alpha_{ac} r^{1.5} + \alpha_{pz} r^{2.5}$$

where the terms on the right hand side represent the contributions from optical phonons, ionized impurities, acoustical phonons and piezoelectric contributions respectively. The coefficients α_{op} , α_{ac} , and α_{pz} are all linear in n while α_{imp} is proportional to the product $N_I n$ where N_I is the concentration of ionized impurities. Thus, for an uncompensated semiconductor, α_{imp} is proportional to n^2 . In principle, it should be possible to determine the degree of compensation in a doped semiconductor by observing

the dependence of the coefficient α_{imp} on the free electron concentration. This will require the introduction of the temperature as a variable as a means to incorporate variations in n into the measurements. Obviously, it is possible to isolate on various scattering mechanisms by operating over specific temperatures ranges. All of our work performed to date has been done at room temperature although we have conducted extensive studies on the temperature dependence of mobility and free carrier concentrations using conventional measurement techniques [6].

From equation 11 and the equation for the transmission coefficient it is possible to determine the dominate scattering mechanism (if one exists) on the basis of the wavelength dependence of the scattering terms. For most semiconductors at room temperature, piezoelectric scattering is not a significant factor so that each of the common scattering mechanisms has a different wavelength dependence. If an incoherent source such as a scanning IR spectrophotometer is employed;

$$(12) \quad T = \frac{(1 - R_{12})^2 \exp(-\alpha d)}{1 - R_{12}^2 \exp(-2\alpha d)}$$

For the values of R_{12} and αd normally encountered

$$(13) \quad \ln(T) \approx 2\ln(1 - R_{12}) - \alpha d$$

and

$$\begin{aligned}
 (14) \quad \ln[\ln(T) - 2 \ln(1 - R_{12})] &= \ln(\alpha_{op}) + 2.5 \ln(\tau) \\
 &+ \ln(\alpha_{imp}) + 3.5 \ln(\tau) + \ln(\alpha_{ac}) + 1.5 \ln(\tau) \\
 &+ \ln(d) = \ln(\alpha d)
 \end{aligned}$$

therefore, a plot of $\ln(\alpha d)$ vs $\ln(\tau)$ will yield a slope which is characteristic of the scattering process [3]. If the dominate scattering processes are unknown, this procedure should be employed as a basis for the scanning IR measurements.

If it is determined that the dominate scattering is impurity scattering then the relation between the absorption coefficient and free electron concentration must be established. Obviously if

$$(15) \quad \alpha d = A(T, \tau) n^k, \quad 1 \leq K \leq 2$$

a plot of $\ln(\alpha d)$ vs $\ln(n)$ should yield a slope of K which is indicative of the degree of compensation. One approach is to make successive measurements at a constant wavelength at different temperatures; it is possible to calculate the changes in free electron concentration since it is known that

$$(16) \quad n \approx N_c \exp[-(E_c - E_f)/KT]$$

for nondegenerate semiconductors. However, the temperature dependence of the scattering process must be known and taken into consideration when interpreting the data. This report

does not encompass any temperature variations in the FEA measurements; it would appear that such measurements would enhance the value of the FEA instrument.

Returning to equation (10), if αd is assigned an average value, $\alpha_0 d$; then we can write

$$(17) \quad \Delta T_{\max} / T_{\max} = \frac{-[1 + R_{12} \exp(-\alpha_0 d)] (\alpha_0 d) (\Delta \alpha / \alpha_0)}{[1 - R_{12} \exp(-\alpha_0 d)]}$$

where T_{\max} corresponds to $\alpha_0 d$. If $\alpha = A n^k \tau^p$ the ratio $\Delta \alpha / \alpha_0$ can be written as,

$$(18) \quad \Delta \alpha / \alpha_0 = K (\Delta n / n_0)$$

where $K=2$ for uncompensated impurity scattering and $K=1$ otherwise; of course, an effective K between 1 and 2 can be determined for a combination of scattering processes which includes ionized impurities. Generally at room temperature taking a value of $K=1$ will not produce serious error. Since the primary objective of this work has been to explore the limitations on sensitivity and resolution, we have taken the bulk Hall reading from a designated area to establish n and have taken an average T_{\max} over that region to establish T_{\max} .

If equation (17) is used to describe the relation between the transmission coefficient and the free carrier variations, it is apparent that fractional changes have a near linear relationship. Of course $\alpha_0 d$ is directly

Page 12

related to the free carrier density which results in a decrease in sensitivity as the free electron concentration decreases. The fundamental measurements problem becomes one of resolving variations in the transmitted beam. From our measurements on InP, a typical value for $\alpha_0 d$ is 0.1 for a 1mm thick wafer with $n_0 \approx 3 \times 10^{16} \text{ cm}^{-3}$. This yields

$$(19) \quad \Delta T_{\text{max}}/T_{\text{omax}} \approx -0.45 (\Delta n/n_0).$$

Typically, one can expect to resolve a $\Delta T_{\text{max}}/T_{\text{omax}}$ of 0.01 so that for this case

$$(20) \quad \Delta n/n_0 \approx -[0.01/0.45] = -0.022 \text{ or } \approx 2.2\%$$

which should be more than adequate resolution. The sensitivity of the measurement is controlled by αd ; for small αd

$$(21) \quad T_{\text{max}} \approx \exp(-\alpha d).$$

Again, using the InP example, assuming it is possible to "see" a T of 0.99 compared to 1.0 for lossless material,

$$(22) \quad \alpha d \approx \ln(1/T) \approx 0.01.$$

For $d=0.1 \text{ cm}$, using a linear relation between α and n this implies that it is possible to measure a free electron concentration of approximately 1×10^{14} assuming approximately a 1% resolution for T_{max} . If the wafer thickness is increased to 1 cm then the sensitivity should approach 10^{13} cm^{-3} .

Page 13

The ultimate resolution of the transmission coefficient is controlled by the system; some sources of system "noise" are:

- (1) variations in the laser power level due to temperature variation, mode hopping or discharge current instability
- (2) variations in the channel transmission characteristics due to temperature variations in material properties; this includes the air portion of the channels
- (3) fluctuations in the IR detector response due to thermal or mechanical variations
- (4) stray IR radiation entering the system from outside sources
- (5) and, in our system, instabilities in the rotary platform due to mechanical vibration.

The ultimate sensitivity of the system is limited by the ability to resolve small changes in the transmission coefficient which are the result of changes in the absorption. To detect free electron densities less than 10^{13} cm^{-3} will require careful design of the system to minimize the sources of noise described above.

III. THE FEA SYSTEM

IIIA. SYSTEM DESCRIPTION

The system uses a beam splitter made of CdTe to split an incident CO₂ laser beam into a reflected beam for reference beam intensity information and a transmitted beam for probing the sample.

The sample beam is focused using a germanium lens of very short focal length through a pinhole which eliminates any laser speckle that may cause intensity changes across the sample beam. The sample beam is then diffraction-limited by the pinhole size such that the beam diameter is uniform over approximately a one-inch diameter at the sample position. The incoming laser beam is attenuated with a germanium or silicon absorber to a level that will not overdrive the lithium tantalate detectors. The incoming laser beam is also chopped at a frequency of near 200 hertz to provide a pulsed beam for signal processing. The output of the chopper signal is used to trigger a Lock-In Amplifier (LIA). One LIA is used on the reference beam and a different LIA is used to detect the 10.6-micron transmission through a sample.

The sample is mounted on an X,Y,Z,THETA(Y) stage which allows both peaking and mapping of the sample. For each sample the incident face of the sample crystal is placed on the Y-axis using the Z-translation stage. The sample is then brought to the first maximum transmission to the left

Page 15

or right of center using the THETA(Y) rotation. The transmitted 10.6 micron radiation is reflected from the face of a metallized 45° prism through the detector aperture onto the detector.

The sample is mapped using the X,Y translators for each X,Y coordinate. The resolution of the translators is 10-microns, but for this work the resolution was limited by the detector aperture which was 0.037-inches or 940-microns.

The beam-splitter/reference detector module was machined from aluminum and has parallel machined slots at 45° for one, two, or three beam splitters as well as a detector mount and multiple beam attenuator holders. The module also has large circular apertures to limit the amount of beam scatter arriving at the reference detector and the sample detector.

The sample beam from the beam-splitter is focused with a short-focal-length germanium lens (2.1-cm.) onto a pinhole (0.037-inch diameter) machined into a piece of brass shimstock. The spatial filter action of this arrangement decreases beam wander and the speckle normally associated with laser beams. The housing and lens holder for the spatial filter were machined from aluminum. The germanium lens is secured by a threaded end cap and the pinhole is movable in a slot and secured by two cap screws at the focal length of the germanium lens.

The prism/sample-beam-detector module was machined from aluminum. It consists of a level platform and milled slot for the prism and its translator, and a detector holder and slot for the detector aperture. The prism can be translated in the Z-direction to pick off the sample beam at different

spots along the X-axis. The Lithium tantalate detector has an active diameter of 1.25-millimeters and the detector aperture limits the size of the sample beam on the sample to the aperture size.

The CO₂ laser is a Line Lite Laser Model #950 continuous laser with piezostack wavelength selection. The laser is water cooled with a closed system refrigerator/heater heat exchanger and pump system. The output at 10.6-microns is nominally 8-watts.

The chopper system is a Stanford Research Systems Model SR540 with a 6-slot wheel and power supply/controller. The reference signal is output from internal phototransistors in the chopper base. This reference signal is used to trigger two Lock-In Amplifiers-both Stanford Research Systems Model SR510. The reference infrared beam which is reflected from the face of a CdTe beam splitter is attenuated by three FZ silicon crystals before striking a Lithium Tantalate detector (New England Research LTO-1.25T). The signal from the reference detector is amplified by a New England Research Model OPF-L preamplifier before being feed into the "A" input of a Lock-In Amplifier (LIA). The sample beam is transmitted through the CdTe beam-splitter, passed through the spatial filter, passed through the sample, reflected off the face of the 45° prism, passed through the detector aperture, and detected by a Lithium Tantalate detector (New England Research LTO-1.25T). The sample signal is then amplified by a New England Research Model OPF-L preamplifier and feed into the "A" input of the second LIA. The preamplifiers are powered by a (+/-)12 volt power supply. The output of the reference LIA is feed to a strip chart

Page 17

recorder so that the reference signal can be monitored over a long period of time.

The sample X,Y,Z translation stage is a Daedal Model 4474 and the sample theta rotation stage is a Daedal Model 10000. The Model 4474 translators have 2-inch travel with 10-micron resolution. The prism translator is a Daedal Model 4504 with 1-inch travel and 0.001-inch resolution.

The drawings package is included in Attachment #1 and photographs of the actual experimental arrangement are included in Attachment #2.

IIIB. SYSTEM PERFORMANCE

The laser must reach thermal stability at the power level and line chosen. This normally takes from one to four hours depending on the manner in which the laser is peaked and on the ambient temperature of the laser mainframe. The laser output will oscillate on and off the desired laser line until thermal stability is reached. The beam attenuating crystals (Ge or Si) must also reach thermal equilibrium and be supported in an extremely stable holder. If the attenuation crystals vibrate or are subject to uneven cooling they will produce noise in the laser beam. The chopper must be run at frequency for nearly an hour before it stabilizes. When the output voltage of the reference detector is nearly a straight line on the chart recorder the system is ready for operation. Typical variations run about 1% in voltage output of the reference detector and slightly less than 1% in the output of the signal detector. These

variations set the limits on the resolution of the FEA system to changes in transmission as detected by the sample detector.

After the reference signal has stabilized the output of the sample detector is routed to the chart recorder and the spacial filter elements are adjusted for both sample beam intensity and beam uniformity. The sample beam is monitored for at least 15-minutes before the sample is placed in the sample holder. The output of the reference detector is then placed back on the chart recorder to provide a constant monitor of the beam intensity.

The sample is first scanned on an infrared (IR) spectrophotometer over the range from 2.5 to 50-microns to obtain a baseline for the IR transmission at 10.6-microns(see Attachment #3). The sample is placed in an aluminum holder that will bolt directly to the FEA sample stage and a photocopy made of the sample. The area to be mapped is then placed on a X,Y grid with the X,Y translation micrometer settings forming the axes of the grid. The transmission signal voltage is peaked at each X,Y position by rotating the sample to the left or right of center until the first interference maximum is reached. This rotation peaking eliminates or at least minimizes variations in thickness across the sample. The step size can range from 100-microns and up with with the present detector apertures. The process is repeated in a criss-cross fashion until the desired area is mapped. The sample is then removed and the sample detector output again routed to the chart recorder to check any beam intensity wonder. On a given run the sample detector output stays within 1% over several hours of measurements.

Page 19

The sample is then compared to the wafer map and van der Pauw samples are either diced or sonic-milled from selected regions of the sample for Hall measurements. The Hall data is used to provide free carrier densities for correlation with the IR transmission data.

IIIC. THE EXPERIMENT

For the proof of concept runs three CdS wafers with different free carrier densities, one GaAs wafer, and one InP wafer were polished to a one-micron or better finish on both faces. The wafers were scanned from 2.5 to 50-microns in an IR spectrophotometer to establish the presence or lack of observable free carrier absorption near 10.6-microns. The three CdS crystals were chosen with room temperature resistivities of 0.69, 7.67, and 19.7-ohm-cm. These resistivities correspond to free carrier densities, as determined from room temperature Hall data, of 2.8×10^{16} , 2.2×10^{15} , and 8.1×10^{14} per cubic centimeter respectively. The 0.69-ohm-cm (2.8×10^{16}) shows a pronounced free carrier absorption at 10.6-microns producing nearly a 25% loss in transmission. The 7.67-ohm-cm (2.2×10^{15}) sample shows only a 2% loss in transmission due to free carrier absorption at 10.6-microns. The 19.7-ohm-cm (8.1×10^{14}) sample shows no detectable loss in transmission at 10.6-microns. The GaAs wafer with a room temperature free carrier density of (1.2×10^{11}) and the InP wafer with room temperature free carrier density of 2.8×10^{16} per cubic centimeter were scanned on an infrared

Page 20

spectrophotometer. The GaAs wafer gave no detectable absorption at 10.6-microns, but the InP wafer gave an absorption of nearly 6% at 10.6-microns (see Attachment #3).

While the FEA system was stabilizing the samples were mounted on an aluminum fixture and a photocopy made of the samples (see Attachment #4). The photocopy is fitted with the nearest (X,Y) grid for mapping. A sample is placed on the X,Y,Z,THETA(Y) stage and the "Z" adjustment used to place the incident face of the sample on the THETA(Y) axis. The "X" adjustment was used to locate the edges of the crystal sample and holder by noting when the beam was not blocked or was blocked respectively-these positions were read from the "X" micrometer and transferred to the (X,Y) grid wafer map. The "Y" adjustment was used to locate the top and bottom of the crystal and holder and these positions recorded on the (X,Y) wafer grid map (see Attachment #5). The voltage read from the sample beam detector was peaked at the smallest angle from the center for each (X,Y) position within a predetermined sub-grid and the peak value recorded at the appropriate (X,Y) position on the wafer grid map. The raw data for all samples measured is shown in Attachment #5 and produces a wafer map of the 10.6-micron transmission, peaked for thickness interference, as a function of position on the wafer. The incident beam intensity was obtained by removing the sample and recording the sample detector voltage as I_0 on the wafer grid map.

Hall data was taken on wafers adjacent to the three CdS sample wafers prior to making FEA measurements. Whole-wafer Hall measurements were made on each CdS sample wafer after

Page 21

FEA testing. The GaAs sample wafer was cleaved and Hall measurements made on the pieces cleaved from the round wafer. Five van der Pauw crosses were sonic-milled from the InP sample wafer after FEA testing and Hall measurements made on all five crosses. The Hall data for all samples is given in Attachment #6.

IIID. DEFICIENCIES IN THE SYSTEM

By far the largest source of error in the system is the incident CO₂ laser beam intensity. The laser is very hard to stabilize and even when the reflected reference beam was stable, competition for different line-locks made the beam wander enough to change the intensity over a small region. The spatial filter did a good job of cleaning up the speckle in the beam; however, when the beam was line-hopping it would cause the intensity passing through the tiny hole in the spatial filter to change. A good feedback system to the wavelength control on the laser to hold a particular line would greatly improve the time required before measurements can be made.

The laser output is nearly 8-watts at 10.6-microns and can only be adjusted down to about 4-watts because the laser is unstable below about 4-watts due to mode-hopping. This means that, in order to keep from locally heating a sample, the beam must be attenuated or diverged to lose several orders of magnitude of intensity at the sample position. Diverging the beam before spatial filtering increases the speckle and decreases the uniformity of the beam.

Page 22

Introducing the raw beam into the spatial filter resulted in several melted pinholes--attenuators are cheaper than precision pinholes. Any crystalline attenuators tried (Ge and Si and CdTe and CdS) were extremely sensitive to temperature, mechanical vibrations, and angle in the beam. Using multiple reflections between parallel polished crystals produced multiple beams and a lot of back-scatter. The best attenuator was an unpolished piece of very thin germanium. This piece of Ge would get very hot, but would equalize within about one hour or less. Since this was a factor of two to four better than the time required to stabilize the laser it was not a real problem, but in a system with a better laser it would be a problem.

The task of taking data once the incident beam is stable is extremely labor intensive. In order to map a 1mm by 1mm area using 0.1mm (100-micron) steps requires 100 manual micrometer adjustments and 100 manual angular adjustments. The data must be recorded by hand on an X,Y grid for each measurement. These measurements require approximately two man-hours of attended time. The measurements would benefit greatly from computer automation.

IIIE. RECOMMENDATIONS FOR IMPROVEMENTS

The entire system should be enclosed in a thermally stable environment to ensure a quick and reliable 10.6-micron beam. Both the laser mainframe and the attenuation crystal must be able to reach thermal equilibrium in a area without drafts or other means to conduct spurious heat to or

Page 23

from them. Also the spatial filter must be allowed to reach thermal equilibrium as the germanium lens warms slightly and the pinhole can receive a large heat load if it distorts and absorbs some of the laser beam. The biggest problem with the pinhole is that thermal expansion moves the pinhole into the beam as the temperature changes.

The micrometer movements and the data recording should be computerized. The system is quite adaptable to computer control as the micrometers could easily be replaced with encoded drives. The output of the Stanford Research Systems LIA is fully compatible with both GPIB-PC parallel and RS232C serial busses.

IV. EXPERIMENTAL RESULTS

The FEA experiments were performed on the system as described in Section III. The subsequent data analysis requires that the average reflection coefficient and absorption coefficient must be determined by spectrophotometer measurements. In addition, the room temperature scattering mechanisms, average free electron concentration and degree of compensation should be known for the material under test. Obviously, absolute measurements will be unattainable since this method does not permit point to point direct measurements of the free electron density.

The approach taken here is to make Hall and conductivity measurements on the same sample which are used

for the FEA measurements; ultimately we would like to eliminate the necessity for conventional measurements by establishing calibration tables.

The samples utilized in the experiments were the wafers of InP, GaAs and CdS described in Section III. The measured properties of these wafers are shown in Attachment #3 (incoherent IR transmission) and Attachment #6 (resistivity, mobility and electron density).

The IR spectrophotometer measurement on the test wafers indicate that the primary scattering mechanisms for the InP and CdS samples is ionized impurity scatter since it was determined that the wavelength dependence of the absorption coefficient is approximately

$$(4.1) \quad \alpha_{\text{imp}} = b n_e N_I \tau^{3.5}.$$

This was determined by a plot of $\ln(\alpha d)$ versus $\ln(\tau)$ [3]. The GaAs sample showed little (if any) absorption so that nothing can be said relative to the scattering processes. Previous studies [3] indicate that both CdS and InP tend to be heavily compensated such that it is justifiable to assume that α is linearly related to the free electron density.

The data obtained from the FEA Instrument (Attachment #5) produces a mapping of the 10.6 μm transmission coefficients which are related to the absorption coefficients by the equation

Page 25

$$(4.2) \quad T_{\max} = \frac{(1 - R_{12})^2 \exp(-\alpha d)}{[1 - R_{12} \exp(-\alpha d)]^2}$$

Since these measurements are not absolute, it is necessary to establish a reference value. The procedure used here is to determine an (αd) based upon the incoherent spectrophotometer data at $10.6\mu\text{m}$ then using the equation

$$(4.3) \quad (\alpha d)_0 = C_0(\tau, d, T_0) n_0^K.$$

to determine a C_0 at $T=300\text{K}$ and $\tau=10.6\mu\text{m}$. We have taken $K=1$ for all the samples and d is common to all measurements.

First, $(\alpha d)_0$ is determined from the equation

$$(4.4) \quad T_0 = \frac{(1 - R_{12})^2 \exp(-\alpha d)_0}{[1 - R_{12}^2 \exp\{-2(\alpha d)_0\}]}$$

where T_0 is the incoherent transmission coefficient at $10.6\mu\text{m}$ and R_{12} is determined from the short wavelength data ($\alpha d \approx 0$);

$$(4.5) \quad R_{12} = (T_{\text{sw}} - 1) / (T_{\text{sw}} + 1)$$

where T_{sw} is the short wavelength transmission coefficient. Equation (4.4) can be solved for $(\alpha d)_0$ so that;

$$(4.6) \quad C_0 = (\alpha d)_0 / n_0$$

where n_0 is determined from the Hall measurements.

Page 26

Subsequently, the values for the free electron density at each sampled point are determined by solving equation (4.2) for κd and using

$$(4.7) \quad \kappa d = C_0 n .$$

This procedure yields a value relative to n_0 . Attachment #7 contains the free electron density maps for the wafers tested.

V. DISCUSSION OF RESULTS AND CONCLUSIONS

An analysis of the data taken on the CdS, GaAs and InP samples reveals a range of results which indicate the somewhat varying levels of success which have been achieved in this work.

The FEA data on CdS with doping levels in the 10^{15} to 10^{16} per cm^3 range correlate very well with results taken from Hall and spectrophotometer measurements. The variations in doping concentrations in sample CDS-1 (0.69 μ -cm) indicate that large deviations in stoichiometry may occur over short distances. There is good correlation between the average value of $n = 2.8 \times 10^{16} \text{ cm}^{-3}$ and the FEA values which range from 1.01×10^{16} to $8.46 \times 10^{16} \text{ cm}^{-3}$. Sample CDS-2 (7.67 μ -cm) gave good correlation between the average measured Hall free electron density of $2.2 \times 10^{15} \text{ cm}^{-3}$ and the FEA data which ranged between 4.6×10^{14} and

Page 27

$1.0 \times 10^{16} \text{ cm}^{-3}$. Sample CDS-3 (19.2 Ω -cm) demonstrates the limits of resolution obtainable for CdS with a thickness of 0.055cm and an average measured Hall free electron density of $8.1 \times 10^{14} \text{ per cm}^{-3}$. This CdS sample indicated no detectable loss in transmission at 10.6 μm on the spectrophotometer scan. The FEA data gave values that ranged mostly in the upper 10^{14} and lower $10^{15} \text{ per cm}^{-3}$ with several values that indicated no absorption. At this level edge effects and slight deviations in sample beam intensity became critical.

The GaAs sample was taken from the conducting end of an undoped semi-insulating boule. The spectrophotometer scan showed no detectable absorption at 10.6 μm and Hall measurements yielded an average free carrier density of $1.17 \times 10^{11} \text{ per cm}^{-3}$ with a resistivity of $1.56 \times 10^4 \Omega\text{-cm}$. The sample was 0.06cm in thickness and the FEA data clearly shows that this level of carrier concentration is beyond the sensitivity of the instrument. About the only thing that can be said for the FEA data from this sample is that it demonstrates the level of "noise" in the instrument.

The 0.06 cm thick InP sample was taken from the most uniform section of an LEC boule that was unintentionally doped with silicon from the InP polycrystalline starting material. The average resistivity was 0.056 $\Omega\text{-cm}$ with a average measured free carrier density of $2.87 \times 10^{16} \text{ per cm}^{-3}$. The FEA data from five sections of this wafer were very consistent; however, the free electron densities calculated from the FEA data do not seem to correlate well with spectrophotometer and Hall data. There seems to be a nearly constant factor of approximately two (2) difference between

the free carrier density as determined by FEA measurements and those determined by Hall measurements. The surprising thing is that this is not just a difference in optical and electrical measurements, but is also a difference between the absorption as seen with the spectrophotometer at 10.6 μm and the absorption as seen with the FEA instrument at 10.6 μm . The (αd) product determined from spectrophotometer measurements is approximately 0.1 whereas the (αd) product for the FEA values averages nearly 0.2. Since both measurements measure the optical absorption at 10.6 μm the reason for the difference is not known at this time. The only differences between the two measurements that are readily apparent are:

1. the bandpass of the CO_2 laser is much narrower than the glow bar source of the spectrophotometer,
2. the 10.6 μm beam of the laser is highly polarized while the spectrophotometer source is not,
3. the laser beam is coherent while the spectrophotometer source is not.

Apart from the offset, which continues to be studied, the ability to map the InP wafer is apparent. The measured Hall free carrier densities for five locations by van der Pauw crosses show a variation from 2.82×10^{16} per cm^{-3} to 3.0×10^{16} per cm^{-3} . The FEA data gives average values over the five positions that range from 5.7×10^{16} to 7.6×10^{16}

Page 29

per cm^{-3} in excellent agreement with the spread in Hall values. In addition the FEA measurements indicate fairly large variations in free electron density within the five individual 6mm by 6mm blocks.

An manually scanning FEA instrument has been designed, constructed and tested. The results indicate the practicality of developing an automated FEA instrument for use in evaluating the free carrier concentrations and variations in free carrier concentrations in electronic semiconductor crystals that are doped in excess of 10^{14} per cm^{-3} . The initial testing of the FEA instrument has indicated that the instrument can resolve free electron concentration variations of $\pm 0.1\%$ relative to the average concentration in wafers of the order of 0.06cm in thickness. The only wafer preparation required is a lum polish and the measurement is a non-contact, non-destructive test. A calibration procedure has been achieved to convert FEA data to free electron concentrations for CdS crystals, but a calibration procedure is still needed for InP and GaAs before absolute measurements of the free electron densities can be made. Relative measurements are possible at this time on InP wafers; however, the conversion factors to compute free electron concentrations from the FEA data must be established. Without significant reduction in the system "noise" the FEA instrument will not address semi-insulating semiconductor wafers.

The ultimate sensitivity of the FEA instrument is limited by the stability of the CO_2 laser, the stability of the beam attenuators, the stability of the beam defining apertures, the stability of the sample movement stages, and

Page 30

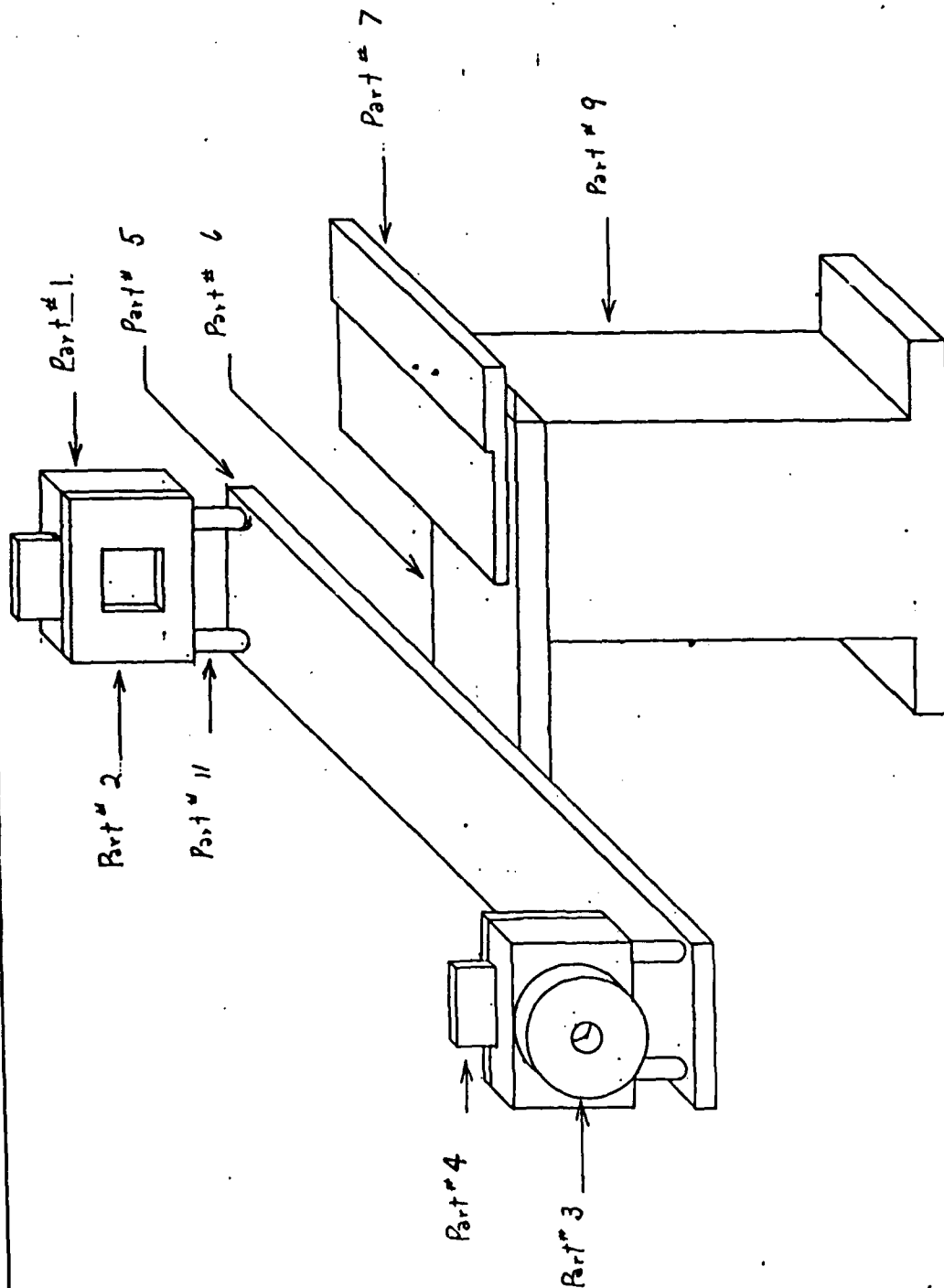
the stability of the detectors. In order to make the speed of testing with the FEA instrument compatible with industry the sample translations, rotations, and measurements will require computer automation. We strongly urge the continued development of this instrument for making contactless measurements on doped semiconductor wafers.

REFERENCES

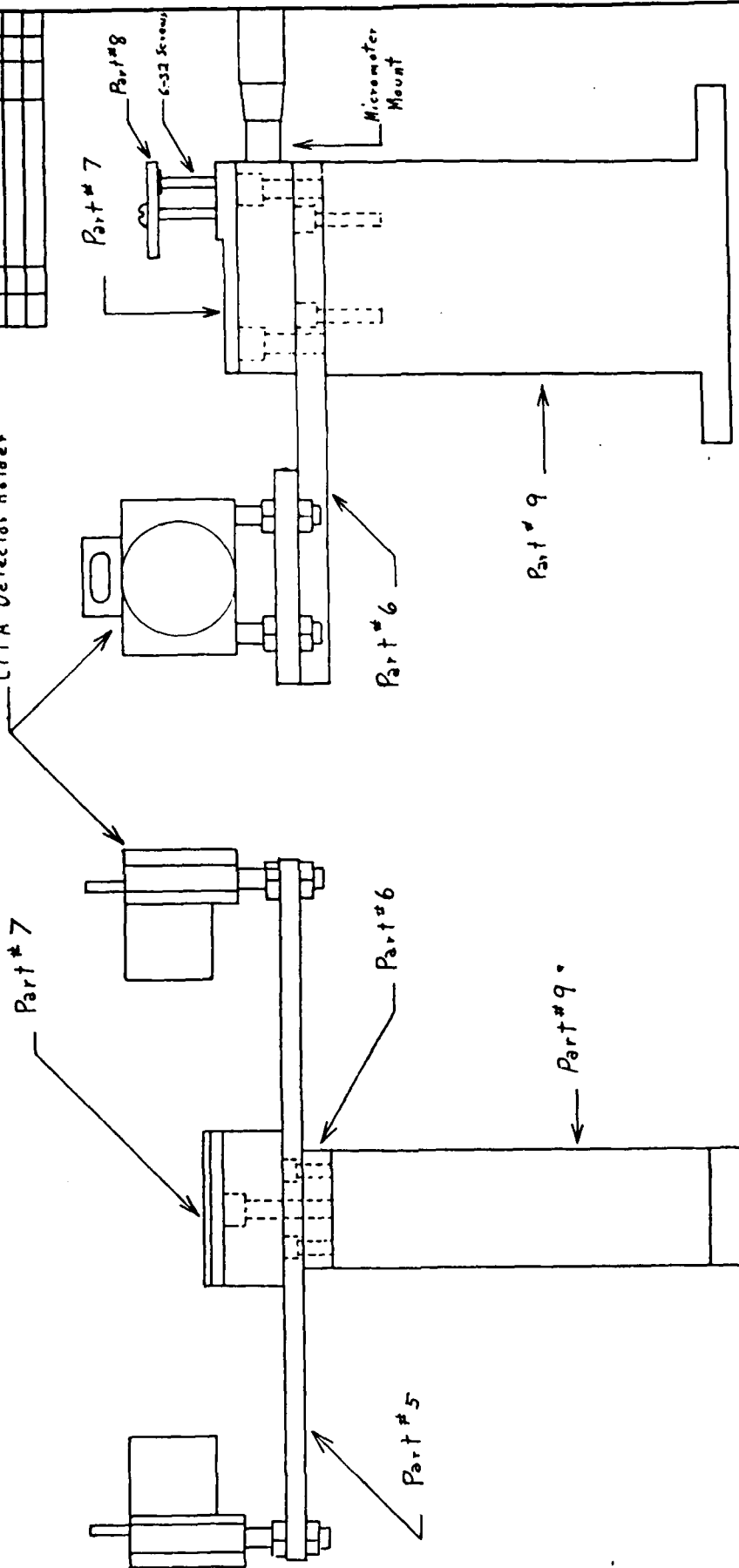
1. H.Y.Fan & M. Becker, "Semiconducting Materials", (Academic Press, New York, 1951), p. 132.
2. L. Jastrzebski, J. Lagowski, and H.C. Gatos, J. Electrochem. Soc. 126, 260(1979).
3. J.L. Boone, G. Cantwell, M.D. Shaw, J. Appl. Phys. 58, 2296(1985).
4. J.A. Stratton, "Electromagnetic Theory", (McGraw-Hill, New York, 1941), p. 511.
5. B.K. Ridley, "Quantum Processes in Semiconductors", (Clarendon, Oxford, 1982), p. 217.
6. J.L. Boone and G. Cantwell, J. Appl. Phys. 57, 1171(1985).


ATTACHMENT #1
(0.64 Reduction Factor)

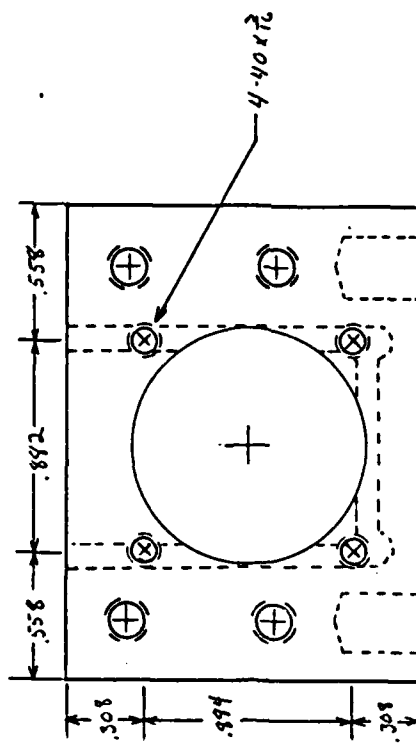
Page #	Title	DRW #
A1-1	Prism/Sample Beam Detector Mod.	RD-1438
A1-2	Prism/Sample Beam Detector Mod.	RD-1439
A1-3	Part #1	RD-1431
A1-4	Part #2 Cover #3 Adjuster #4 Detector Apertures	RD-1432
A1-5	Part #5 Wing	RD-1433
A1-6	Part #6 Extension #7 Prism Holder #8 Hold Down	RD-1434
A1-7	Part #9	RD-1435
A1-8	Part #10 Light Shield #11 Stud	RD-1436
	LITA Detector Holder	RD-1437
A1-9	Beam Splitter/Ref. Detector Mod.	RD-1444
A1-10	Part #12 Base #13 Stand	RD-1440
A1-11	Part #14 Base, Alignment	RD-1441
A1-12	Part #15 Beam Splitter Holder	RD-1442
A1-13	Part #16 Double Filter Holder #17 Single Filter Holder	RD-1443
A1-14	Spacial Filter Assembly	RD-1447
A1-15	Auxiliary Beam Deversion Mod.	RD-1452
A1-16	Part #18 Base #19 Stand, Lower #20 Stand, Upper	RD-1445
A1-17	Part #21 Body, Right Half #22 Body, Left Half	
	#24 Cap, #25 Lens Holder	RD-1446
A1-18	Part #25 Base #26 Stud #27 Nut	RD-1448
A1-19	Part #28 Body	
A1-20	Part #29 Small Lens Holder #30 Lens Holder Cap	RD-1450
A1-21	Part #31 Large Lens Holder #32 Large Lens Holder Cap	RD-1451
A1-22	Part #33 XYZ THETA stage Sample Stage	RD-1453
A1-23	Part #34 Sample Holder Base #35 Sample Holder	RD-1454
A1-24	Part #36 XYZ Base	RD-1455




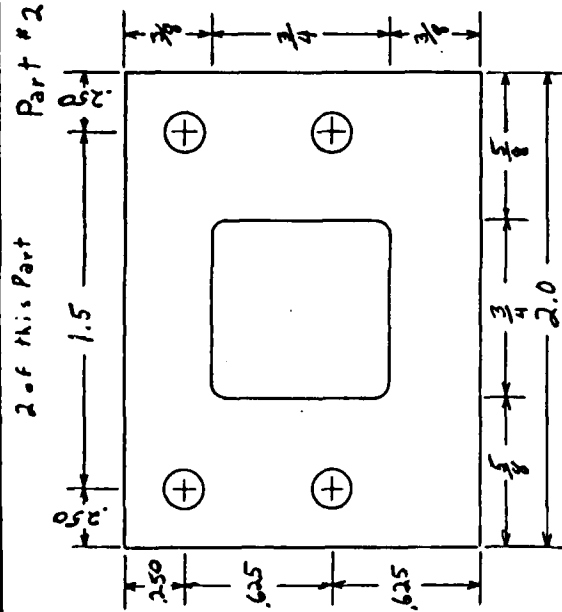
EAGLE-PICHER INDUSTRIES, INC. SPECIALTY MATERIALS DIVISION MIAMI RESEARCH LABORATORY		SCALE	NA	APPROVED BY <i>[Signature]</i>	DATE	9-26-86	DRAWING NUMBER	RD-1438	REV.	0
TOLERANCES DEPT AS NOTED	ORIGINAL	ANGULAR	NA	FRACTIONAL	NA	PRISM/SAMPLE BEAM DETECTOR MOD.	DATE	9-26-86	DRAWING NUMBER	RD-1438

LITA Detector holder

 EAGLE-PICHER INDUSTRIES, INC. SPECIALTY MATERIALS DIVISION MIAMI RESEARCH LABORATORY		DRAWN BY <i>R. Macgister</i> APPROVED BY <i>Michael G. Gaur</i>	
TOLERANCES (EXCEPT AS NOTED)		DECIMAL .0001	SCALE 1" = 1"
Assembled View		TITLE Prism/sample Detector Mod.	
DATE 9-26-86		DRAWING NUMBER RD-1439	REV. 0
ANGULAR .0001			

[illegible]

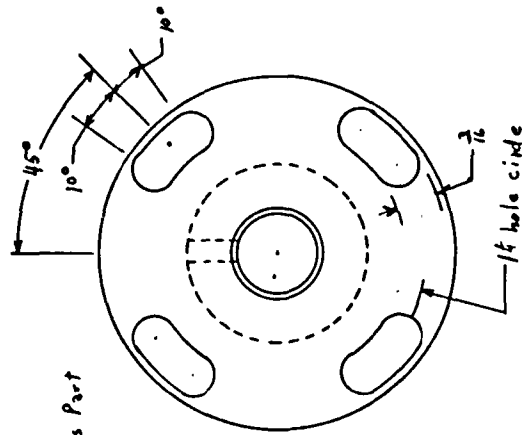
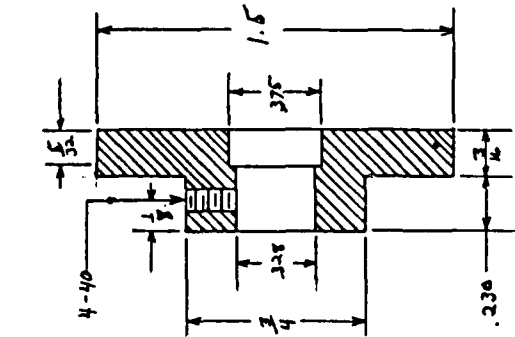
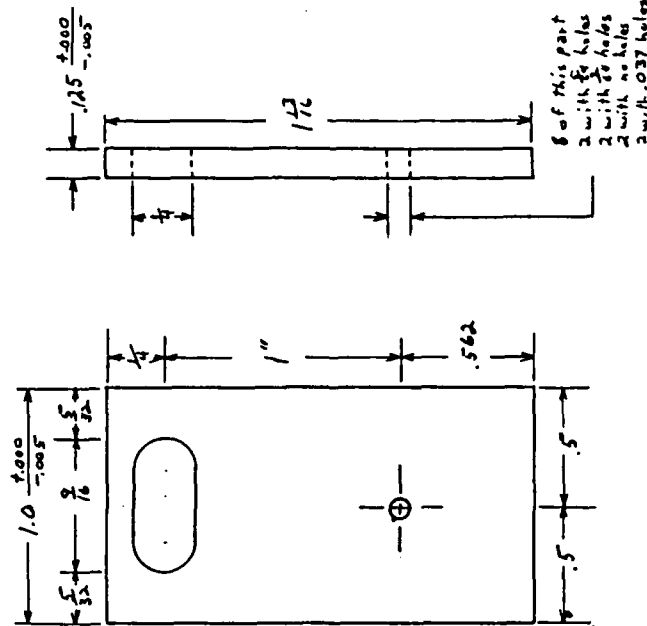
TOLERANCES (EXCEPT AS NOTED)		 EAGLE-PICHER INDUSTRIES, INC. SPECIALTY MATERIALS DIVISION MIAMI RESEARCH LABORATORY			
DECIMAL	Part #1	SCALE	DRAWN BY <i>J.P. Moore</i> APPROVED BY <i>J.P. Moore</i>		
1/1000	Aluminum	2" = 1"			
FRACTIONAL	TITLE Part + Body				
1/1000	Prism/sample Detector Mod.				
ANGULAR	DATE	DRAWING NUMBER	REV.		
1/1000	9/26/66	RD-1431	0		




2 of this Part



De 174

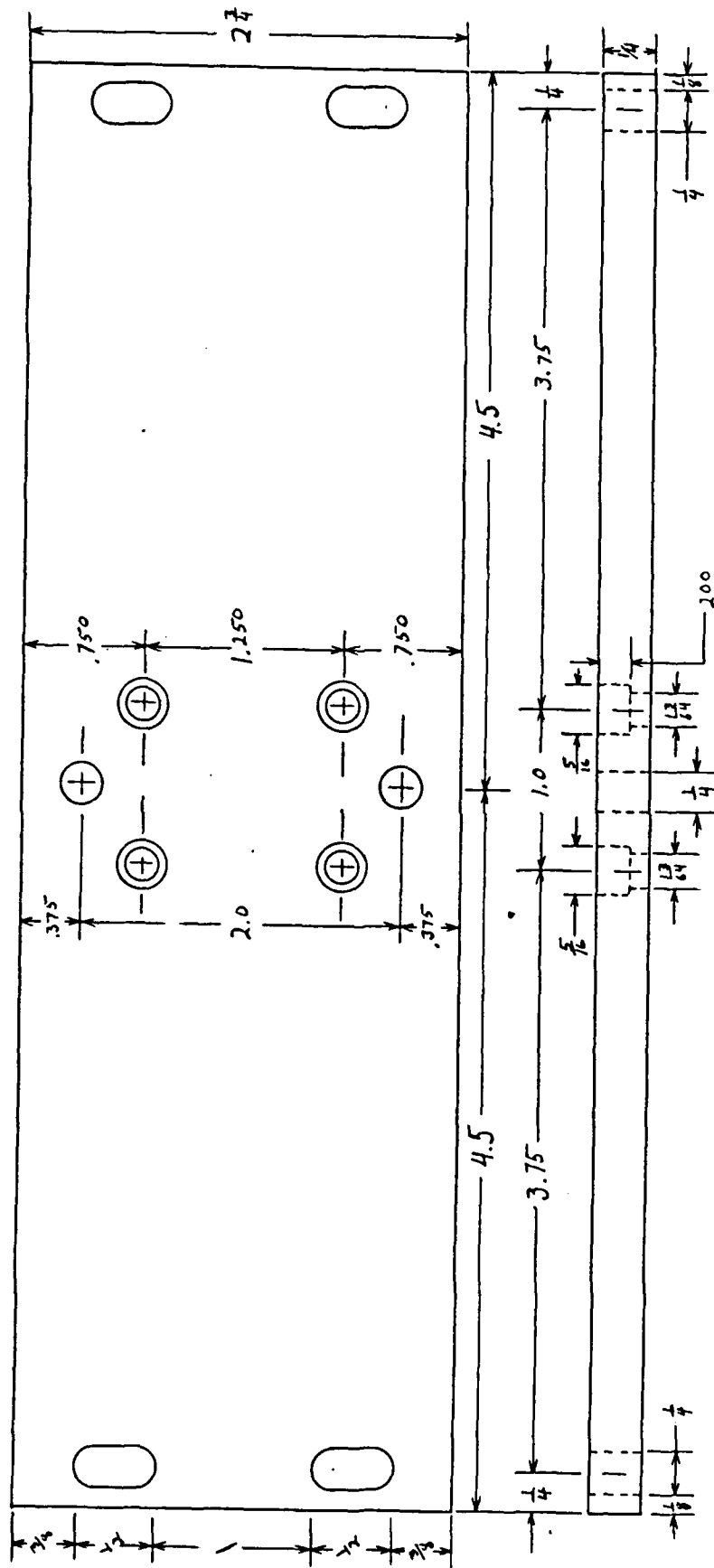


2 of this Part
Part #3

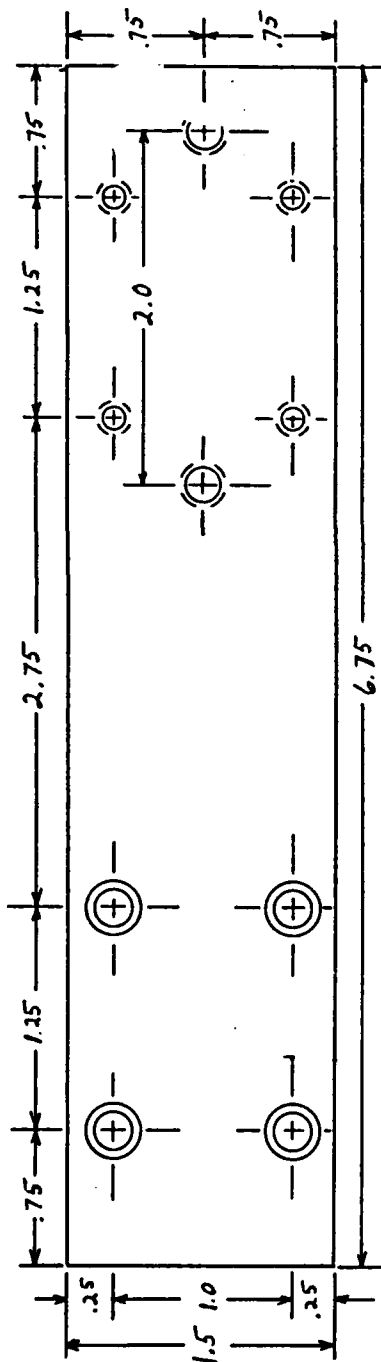
TOLERANCES (EXCEPT AS NOTED)		 EAGLE-PICHER INDUSTRIES, INC. SPECIALTY MATERIALS DIVISION MIAMI RESEARCH LABORATORY			
DECIMAL	$\pm .005$	SCALE	2" = 1"		
FRACTIONAL	$\pm \frac{1}{64}$	DRAWN BY		J. H. Morris	
TITLE #2 COVER #3 ADJUSTOR #4 DETECTOR APERTURES		APPROVED BY		J. H. Morris	
Prism/Sample Beam Detector Mod.					
ANGULAR	$\pm \frac{1}{2}^\circ$	DATE	DRAWING NUMBER		REV.
	9-26-86		RD-1432		0

NAME TO THE 10-40 INCHES

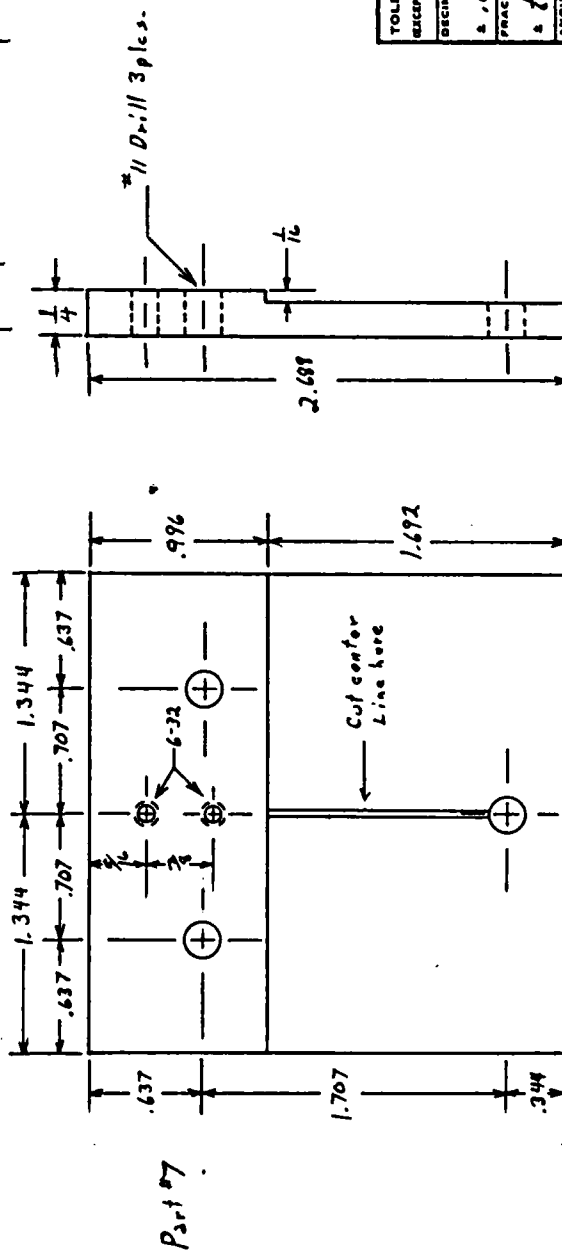
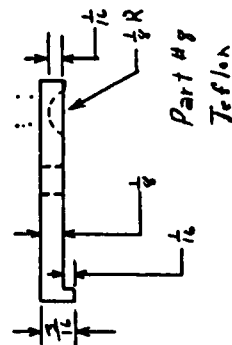
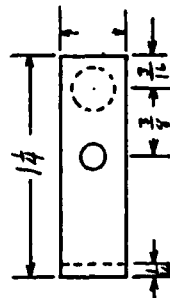
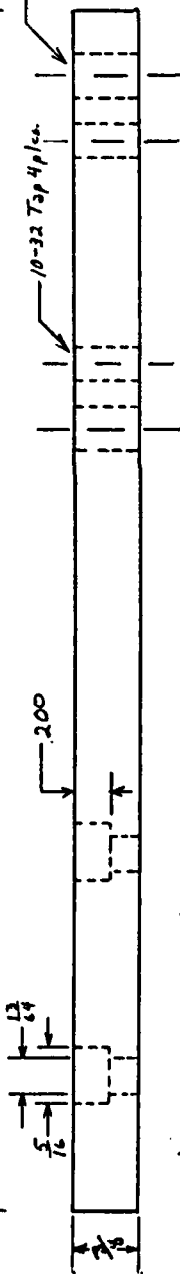
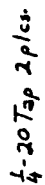
DATE	BY	REVISION RECORD	AUTH.	DL	CL



TOLERANCES EXCEPT AS NOTED	EAGLE-PICHER INDUSTRIES, INC.	SPECIALTY MATERIALS DIVISION	MIAMI RESEARCH LABORATORY
ORIGINAL	Part # 5	SCALE	DRAWN BY / J. L. Smith
Δ .005	ALUMINUM	1/2 = 1	APPROVED BY / J. L. Smith
FRACTIONAL	TITLE #5 Wing		
Δ 1/4	Prism / Sample Det. Mod.		
ANGULAR	DATE	DRAWING NUMBER	REV.
Δ -	9.26.86	RD-1433	0

[illegible]

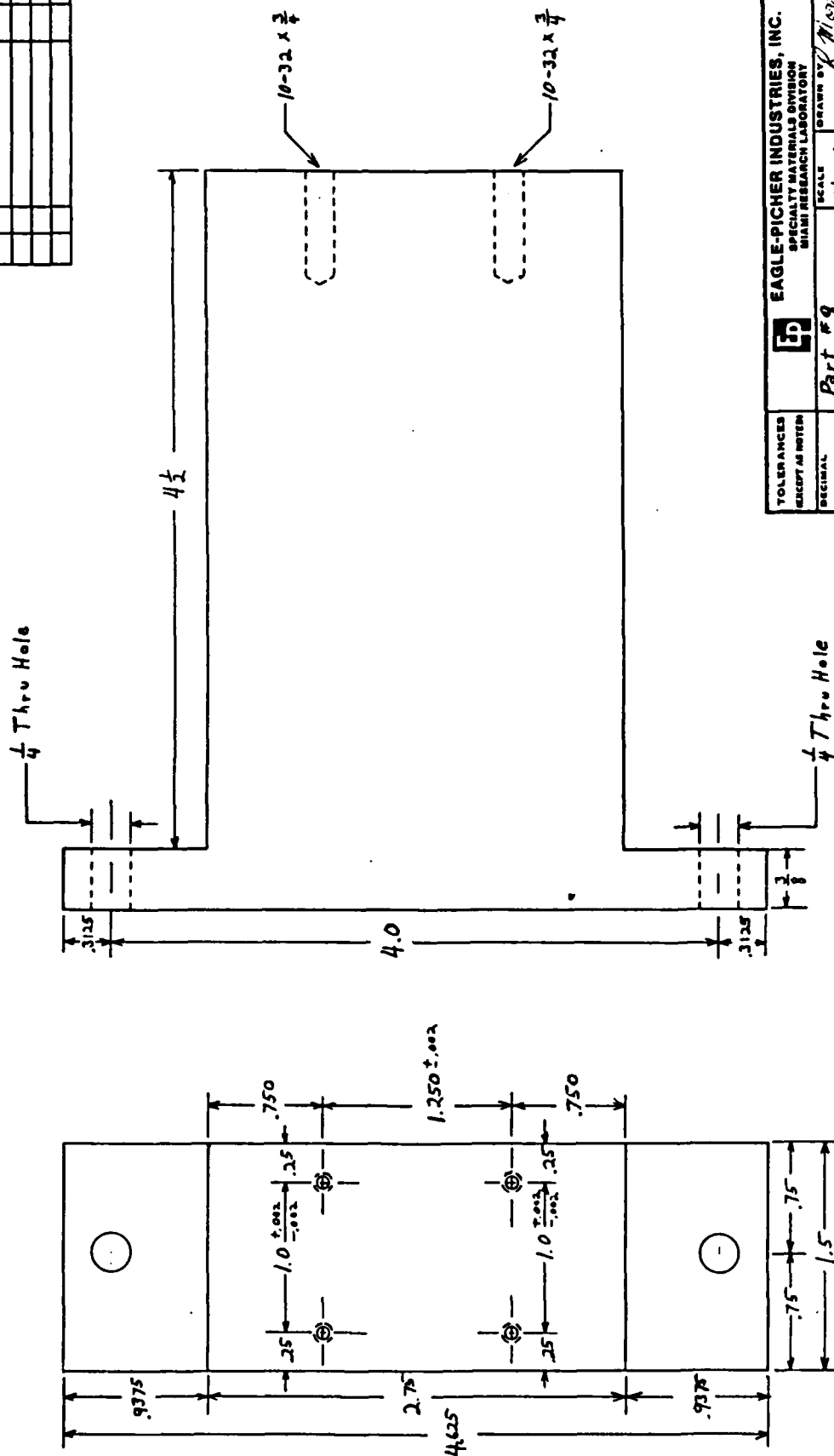
Part #6



TOLERANCES EXCEPT AS NOTED		EAGLE-PICHER INDUSTRIES, INC. SPECIALTY MATERIALS DIVISION MIAMI RESEARCH LABORATORY			
DECIMAL	Part # 6-7-8	SCALE	DRAWN BY <i>K. Picard</i>		
2.004	Aluminum Teflon	1/2 = 1	CHECKED BY <i>W. J. Brown</i>		
FRACTIONAL	TITLE #6 Extension	TITLE #6 Extension			
2 & 4	Prism/sample Beam Detector Mod.	TITLE #6 Extension			
ANGULAR	DATE	DRAWING NUMBER	REV.		
2	9-26-86	RD-1434	0		

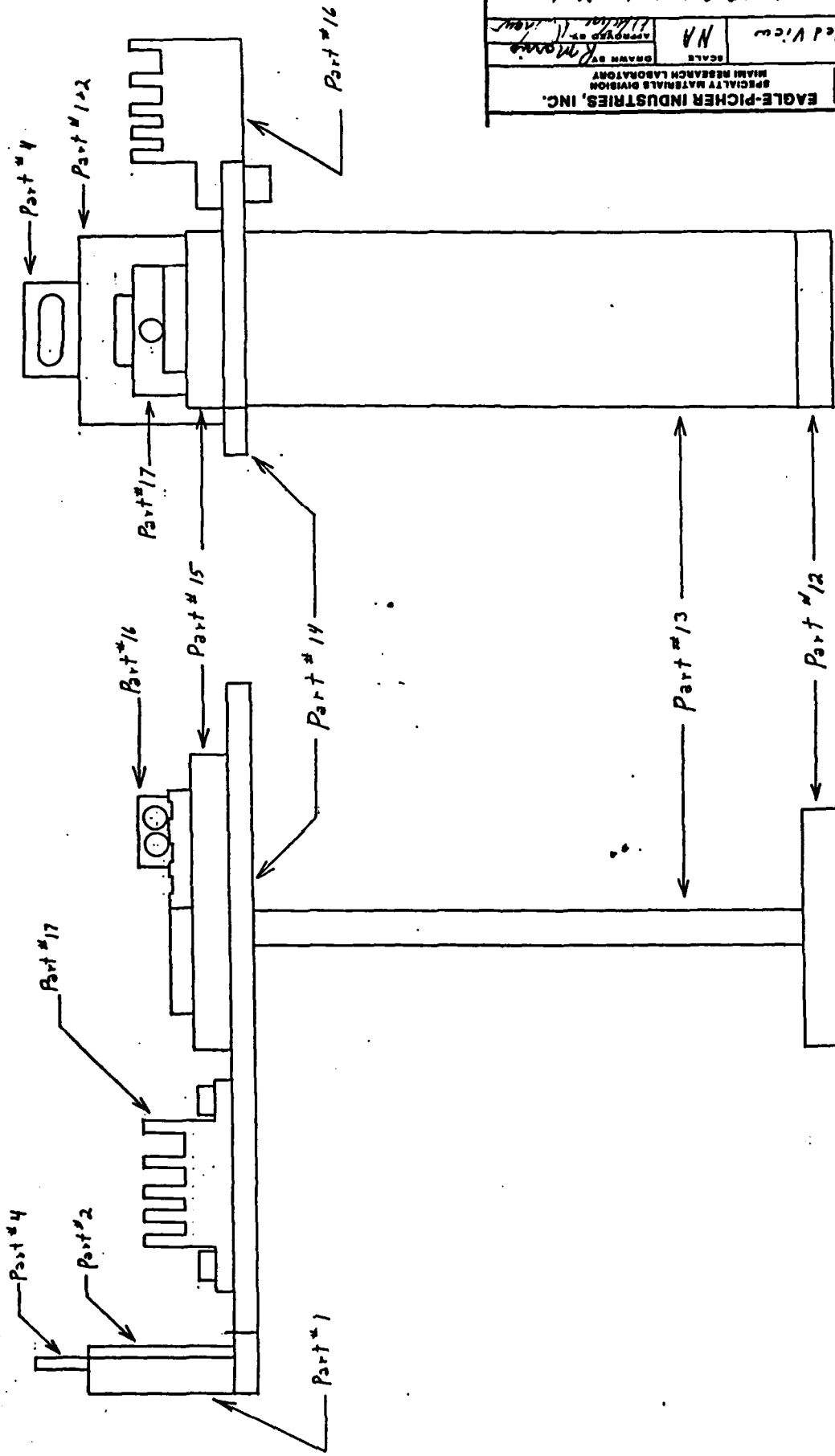
SCALE IN THIS DRAWING

DATE	BY	REVISION RECORD	AUTH.	CHK.



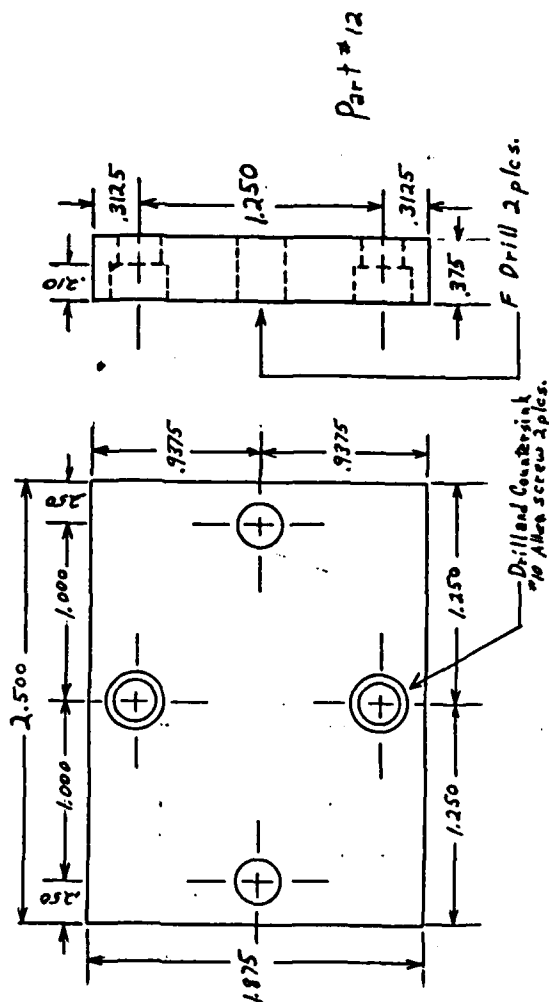
TOLERANCES EXCEPT AS NOTED		EAGLE-PICHER INDUSTRIES, INC.	
DECIMAL		SPECIALTY MATERIALS DIVISION	
FRACTIONAL		MIAMI RESEARCH LABORATORY	
± .005	Part #9	SCALE	1 1/2" = 1"
± 1/64	Aluminum	DRAWN BY	R. Morris
ANGULAR	TITLE #9	APPROVED BY	R. Morris
± 1	Prism/Sample Beam Detector Mod.	DATE	9-26-86
		DRAWING NUMBER	RD-1435
		REV.	0






TOLERANCES UNLESS OTHERWISE SPECIFIED		EAGLE-PICHER INDUSTRIES, INC. SPECIALTY MATERIALS DIVISION MIAMI RESEARCH LABORATORY	
DECIMAL	ANGULAR	DATE	DRAWING NUMBER
NA	NA	9-26-86	RD1424
FRACTIONAL	FRACTIONAL	Beam Splitter/Ref. Detector Mod.	
ASSEMBLY	ASSEMBLY	SCALE	REV.
NA	NA	1:1	0

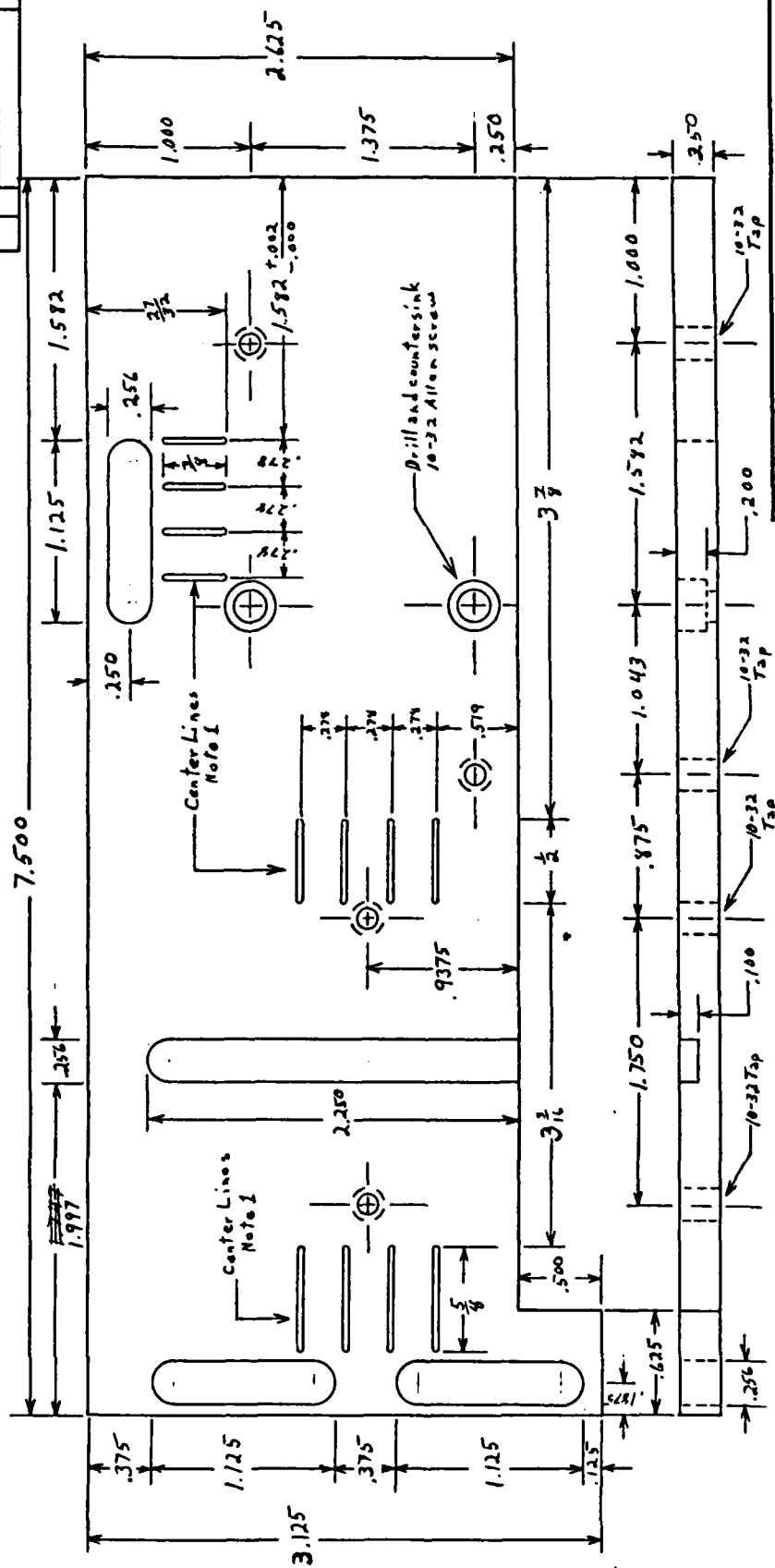
Beam Splitter/Ref. Detector Mod.



TOLERANCES (EXCEPT AS NOTED)	 EAGLE-PICHER INDUSTRIES, INC. SPECIALTY MATERIALS DIVISION MINNEAPOLIS LABORATORY			
DECIMAL	Parts # 12, 13	SCALE	DRAWN BY <i>H. Menist</i> APPROVED BY _____	
± .005	ALUMINUM	1/8" = 1		
FRACTIONAL	TITLE #12 Base ± .013 Stand			
± 1/4	Beam Splitter/Ref Detector Mod			
ANGULAR	DATE	DRAWING NUMBER	REV.	
—	9-26-86	RD-1440	0	

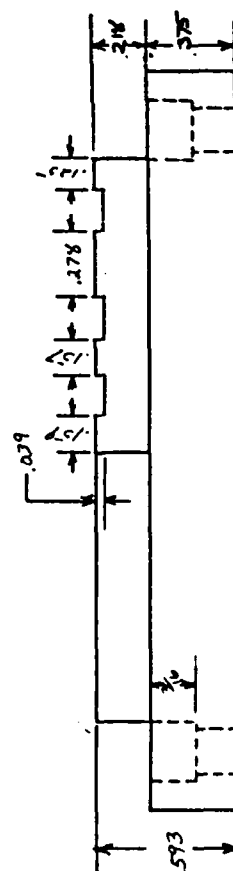
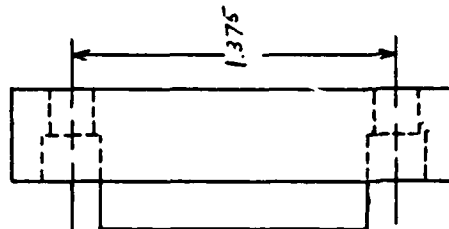
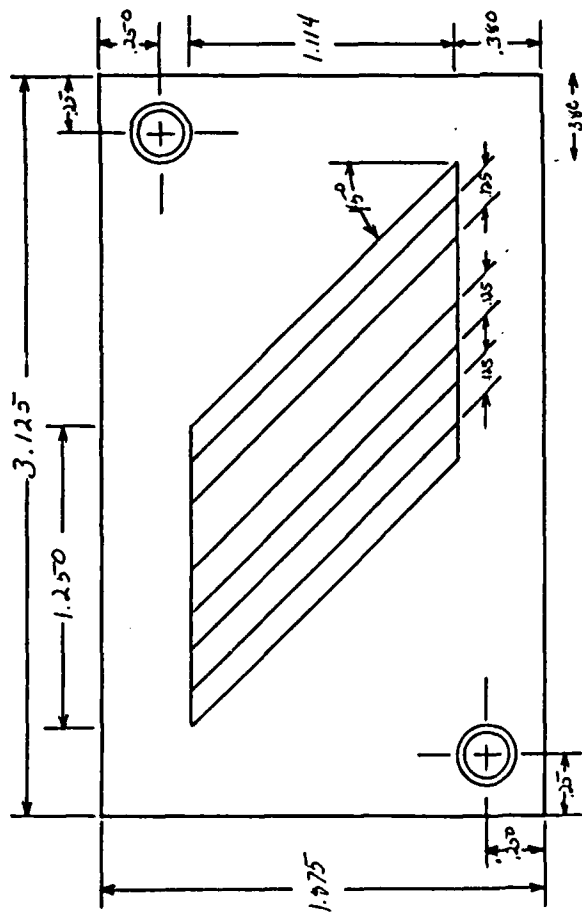
PLEASE TO THIS DRAWING METHOD

DATE	TYPE	REVISION RECORD	APP'D.	BY	CO.




TOLERANCES EXCEPT AS NOTED		EAGLE-PICHER INDUSTRIES, INC.		SPECIALTY MATERIALS DIVISION		MIAMI RESEARCH LABORATORY	
DECIMAL	± .005	PART #	14	SCALE	1/2" = 1"	DRAWN BY	R. M. M. M.
FRACTIONAL	± 1/4	MATERIAL	Aluminum	TITLE #	14	APPROVED BY	R. M. M. M.
ANGULAR	± 1/4	DESCRIPTION	Beam Splitter / Ref. Detector Mod.	DATE	9-26-86	DRAWING NUMBER	RD-1441
							REV.
							0

Note 1. All center lines
Cut with 3/32 Ball end mill
.005 Deep



Drill and counter sink
for #10-32 Allen screw
2 pcs.

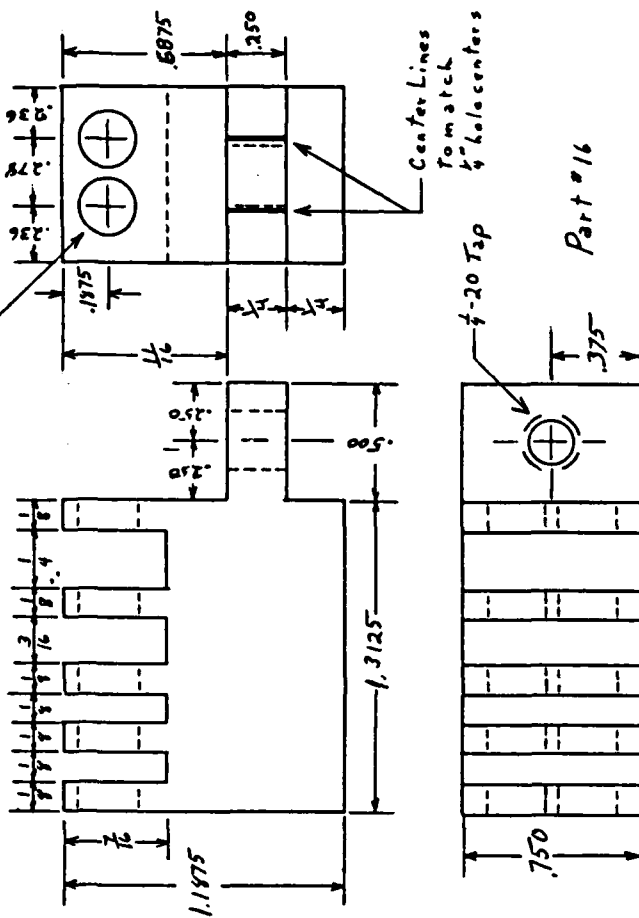
TOLERANCES EXCEPT AS NOTED		 EAGLE-PICHER INDUSTRIES, INC. SPECIALTY MATERIALS DIVISION MIAMI RESEARCH LABORATORY			
DECIMAL	<i>Part #15</i>	SCALE	DRAWN BY <i>R. M. Hest</i> APPROVED BY <i>[Signature]</i> <i>11-1-51</i>		
<i>± .004</i>	<i>Aluminum</i>	<i>2" = 1"</i>			
FRACTIONAL	TITLE #15 Beam Splitter Holder				
<i>± .01</i>	Beam Splitter/Ref. Detector Mod.				
ANGULAR	DATE		GRATING NUMBER		REV.
<i>± 0</i>	9-26-86		RD-1442		0


Part #17

Center line to match 4" hole center

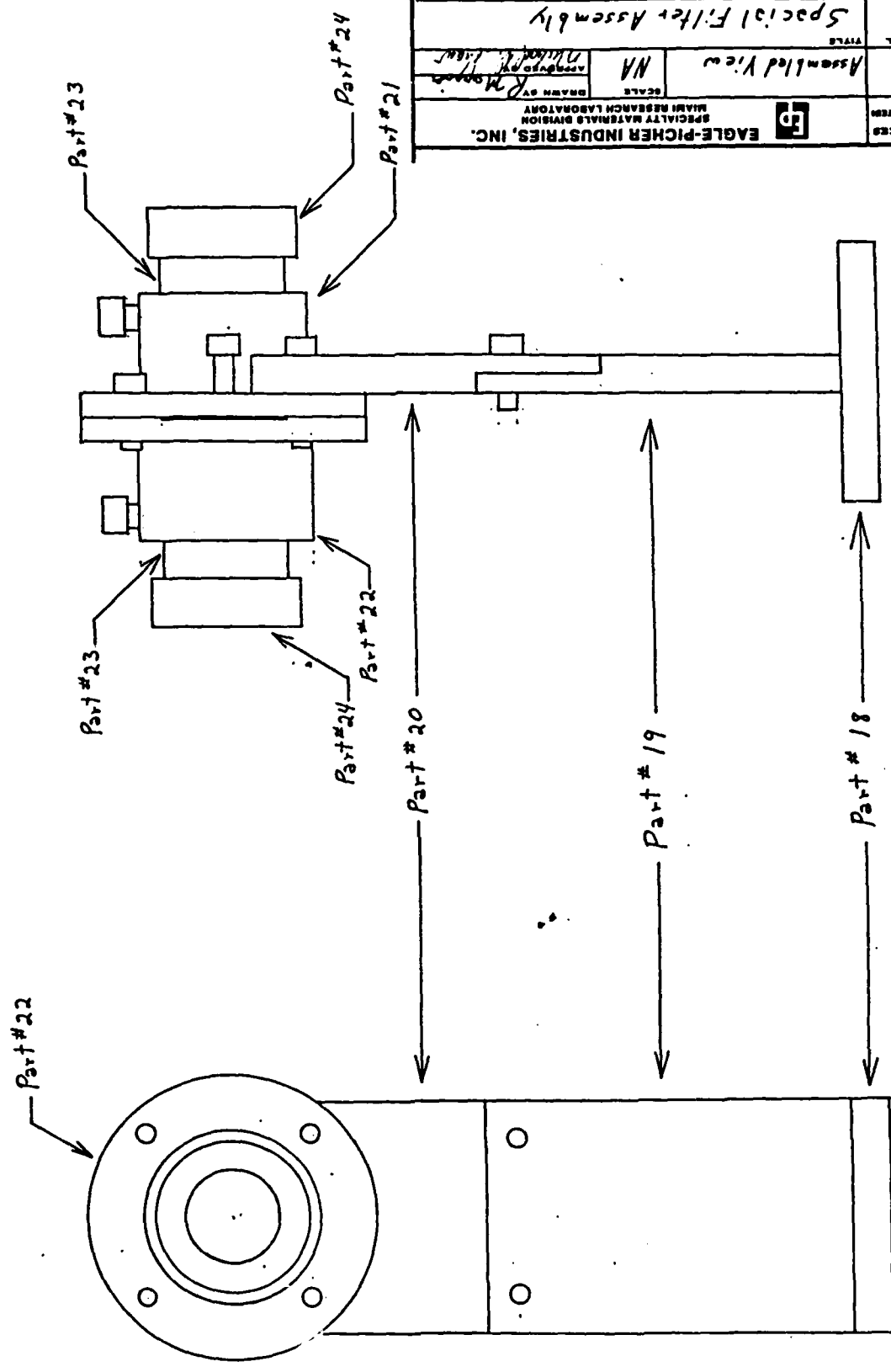
4" hole Ream

Dimensions: .6875, .9375, .1875, .750, .1875



TOLERANCES (EXCEPT AS NOTED)		 EAGLE-PICHER INDUSTRIES, INC. SPECIALTY MATERIALS DIVISION MIAMI RESEARCH LABORATORY			
DECIMAL	<i>Parts # 16-17</i>	SCALE	DRAWN BY <i>R. M. Menden</i>		
<i>± .005</i>	<i>Aluminum</i>	<i>2" = 1"</i>	APPROVED BY <i>[Signature]</i>		
FRACTIONAL	TITLE # 16 Double Filter Holder w/ 17 Single Filter Holder				
<i>± .005</i>	<i>Beam Splitter / Ref. Detector Mod.</i>				
ANGULAR	DATE	DRAWING NUMBER	REV.		
<i>—</i>	<i>9-26-86</i>	<i>RD-1443</i>	<i>0</i>		

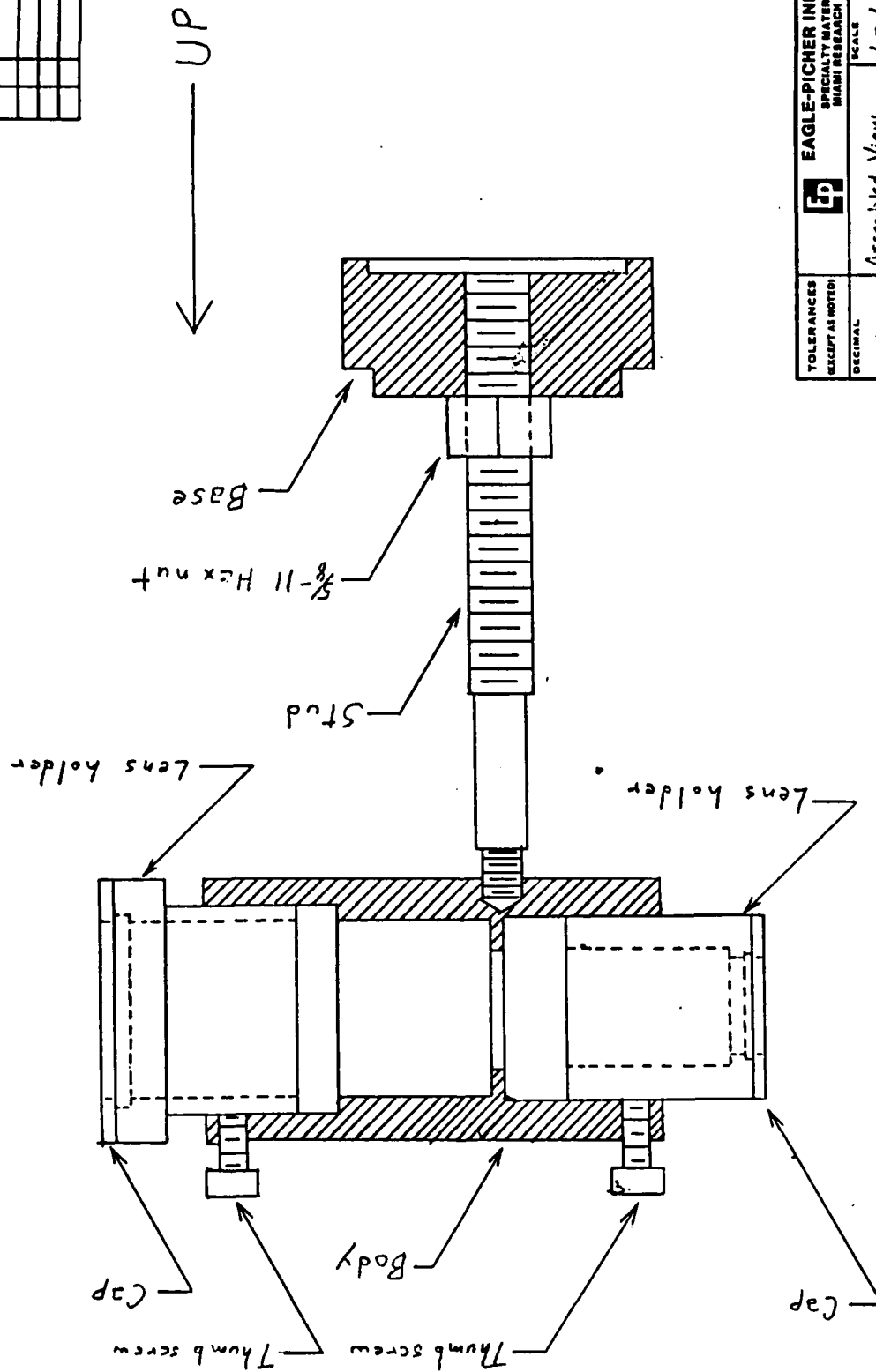
TOLERANCES UNLESS NOTED		EAGLE-PICHER INDUSTRIES, INC. SPECIALTY MATERIALS DIVISION MADE IN U.S.A.		SCALE AS SHOWN	DATE 9-26-86	DRAWING NUMBER RD/1447	REV. 0
PARTIAL		NA		ASSEMBLED VIEW	SPECIAL Filter Assembly		
NATIONAL		NA		TITLE			
DRAWN BY R. M. P.		NA		CHECKED BY J. M. P.			



Special Filter Assembly

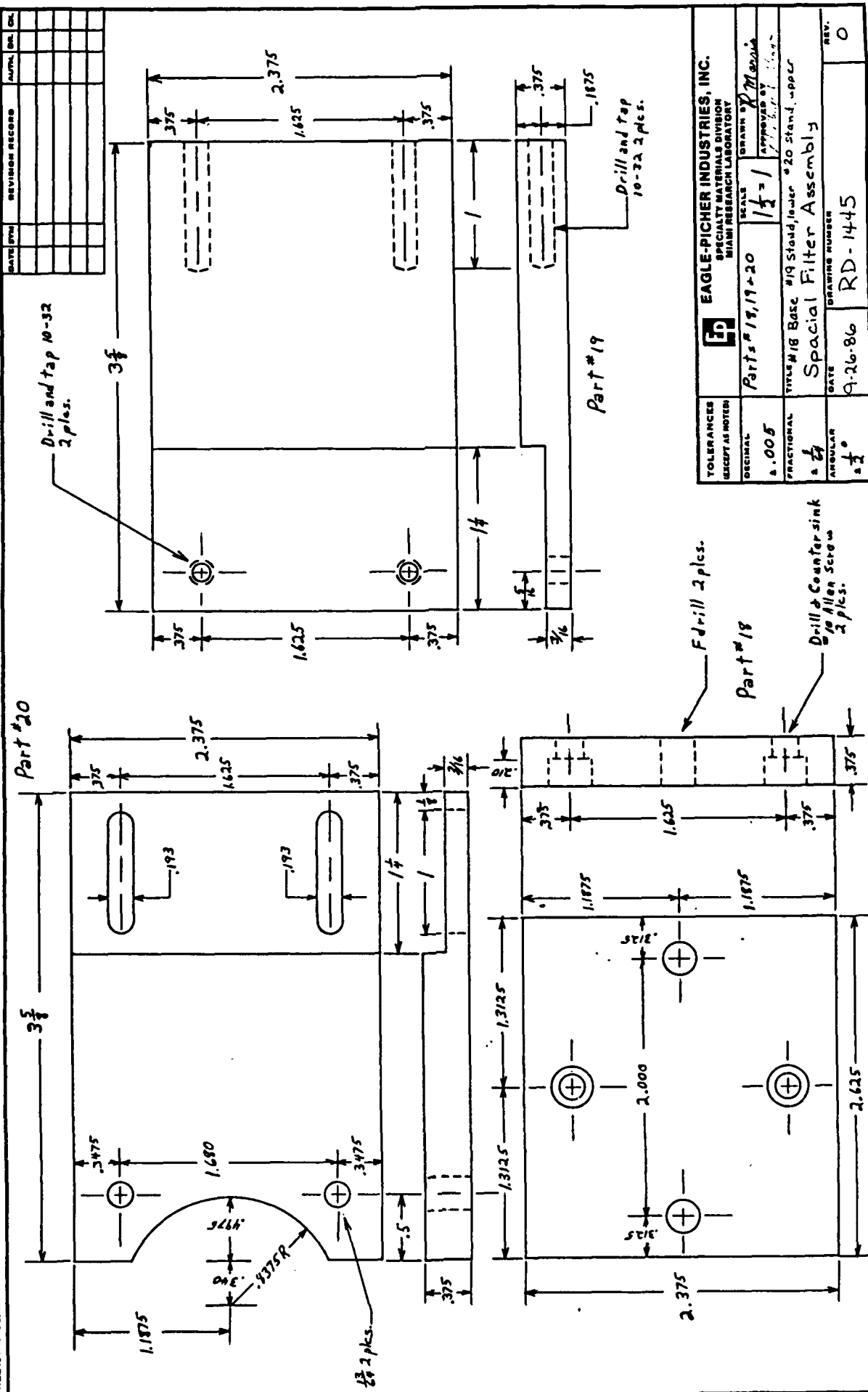
READ TO VIEW ISOP SECTION

DATE	REVISION	RECORD	APPROVAL	DATE



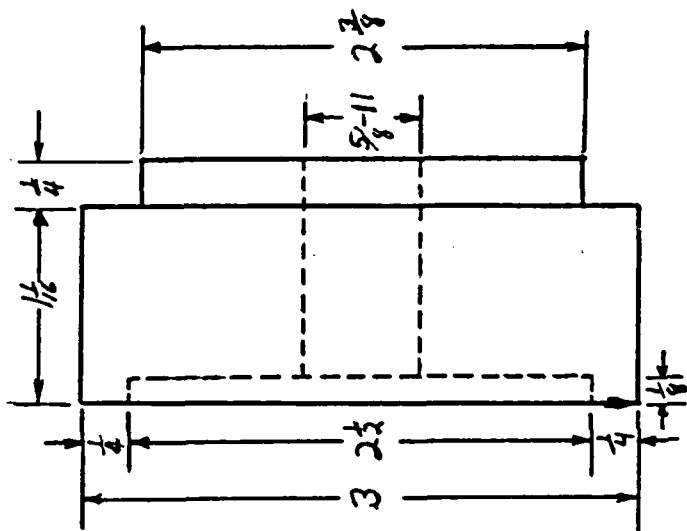
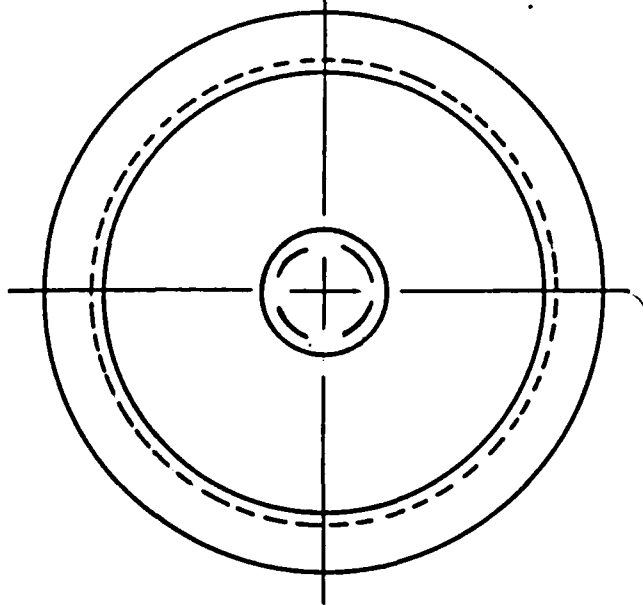
TOLERANCES EXCEPT AS NOTED:		EAGLE-PICHER INDUSTRIES, INC.	
DECIMAL		SPECIALTY MATERIALS DIVISION	
FRACTIONAL		MIAMI RESEARCH LABORATORY	
ANGULAR		SCALE	
± .0012	ASSEMBLED VIEW	1 = 1	DRAWN BY J. M. JONES
± .0012	TITLE	APPROVED BY J. M. JONES	DATE
± .0012	Auxiliary Beam Deversion Mod.	DATE	REV.
± .0012	DATE	9-26-86	0
± .0012	DRAWING NUMBER	RD-1452	

READ IN THE 15-40 SECTION

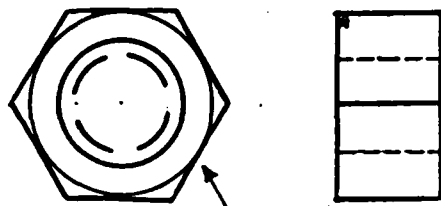


TOLERANCES UNLESS NOTED		EAGLE-PICHER INDUSTRIES, INC.	
DECIMAL	± .005	SPECIALTY MATERIALS DIVISION	MIAMI RESEARCH LABORATORY
FRACTIONAL	± $\frac{1}{64}$	Part # 19, 19-20	SCALE $\frac{1}{2} = 1$
ANGULAR	± 1°	TITLE #18 Base #19 Stand, lower #20 Stand, upper	APPROVED BY <i>R. M. ...</i>
DATE	9-26-86	Special Filter Assembly	REV. 0
DRAWING NUMBER	RD-1445		

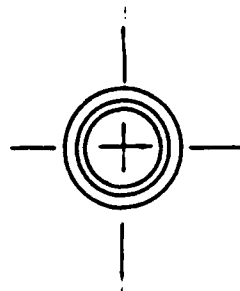
Part # 25



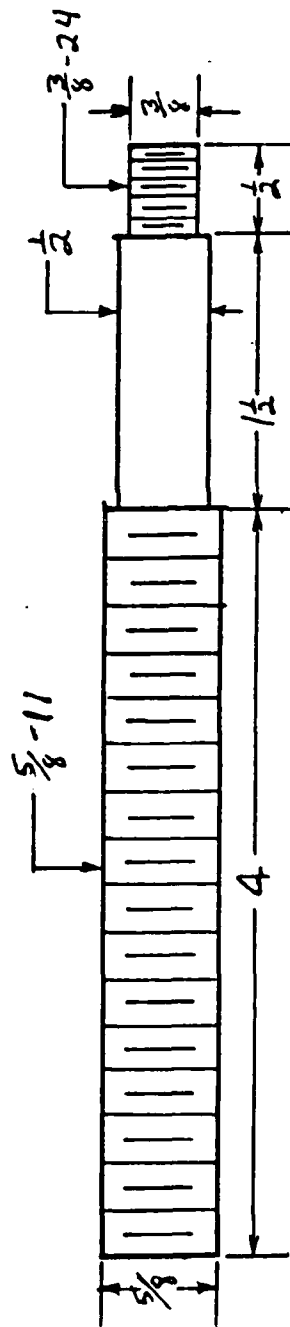
Part # 27

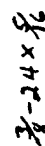


5/8-11 Hex Nut

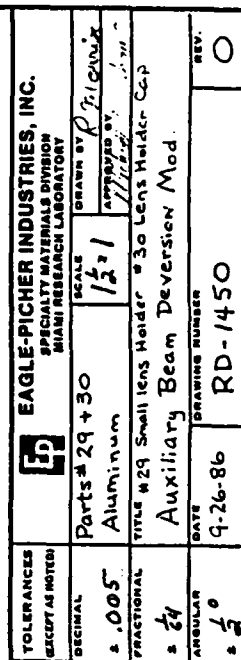


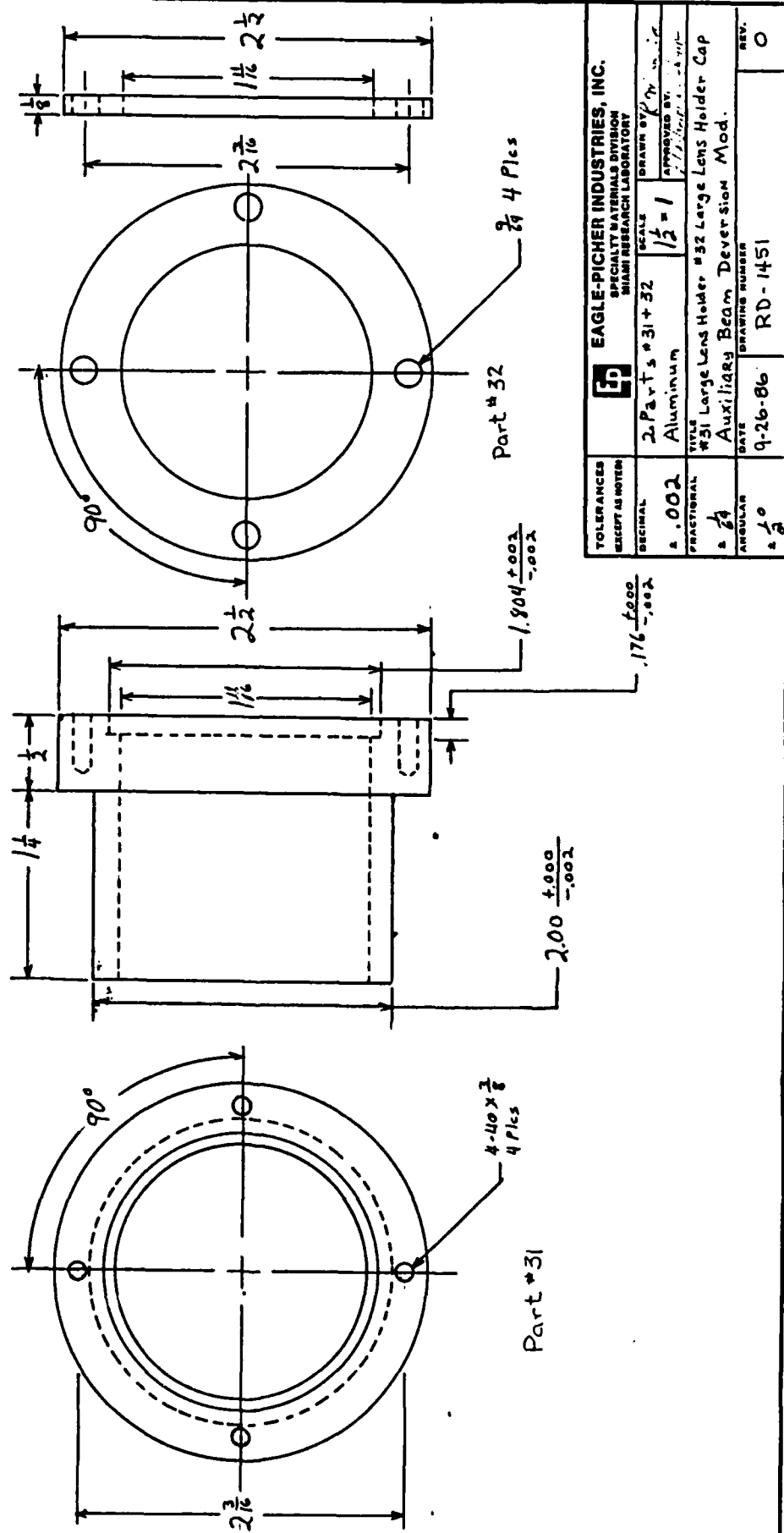
Part #26

[illegible]



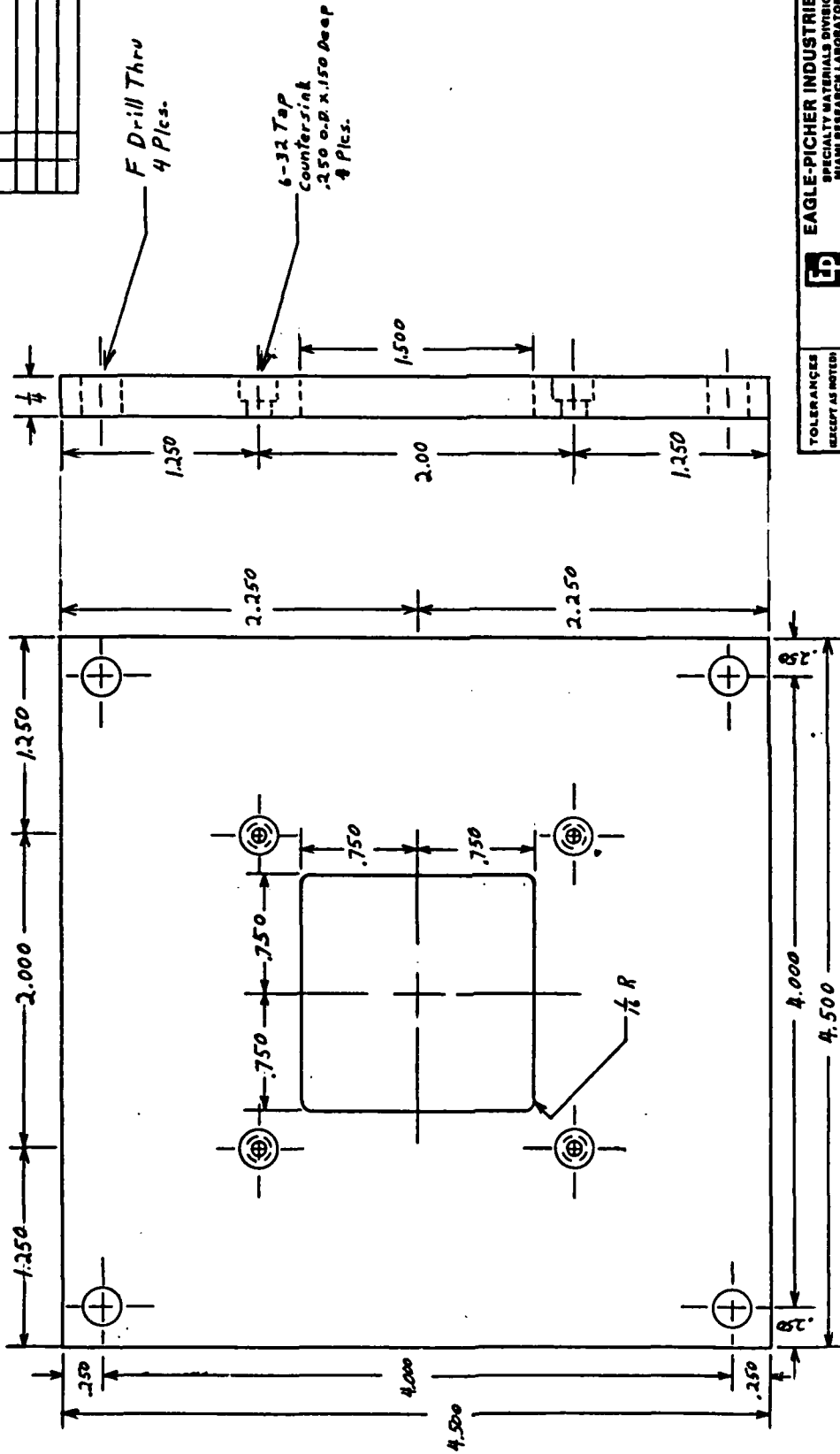
TOLERANCES (EXCEPT AS NOTED)		EAGLE-PICHER INDUSTRIES, INC. SPECIALTY MATERIALS DIVISION MIAMI RESEARCH LABORATORY			
DECIMAL	Part #28	SCALE	DRAWN BY	APPROVED BY	REV.
± .005	Aluminum	1/2" = 1"	W. H. HARRIS	W. H. HARRIS	0
FRACTIONAL	TITLE # 28 Body Auxiliary Beam Deversion Mod.				
± 1/16	DATE	DRAWING NUMBER			
ANGULAR	9/26/86	RD-1449			
±					


[illegible]



NAME IN THIS SPACE

DATE	BY	REVISION	RECORD	AUTH.	DL.



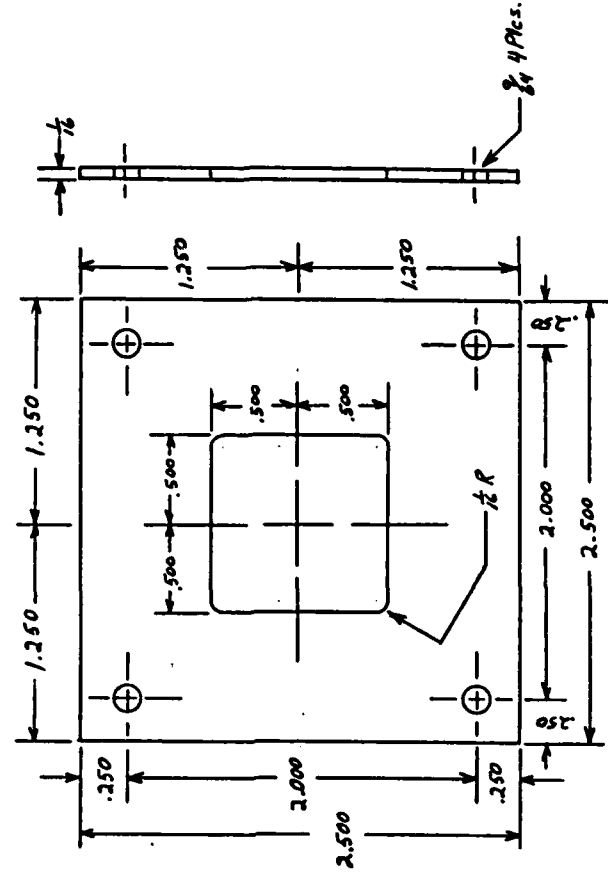
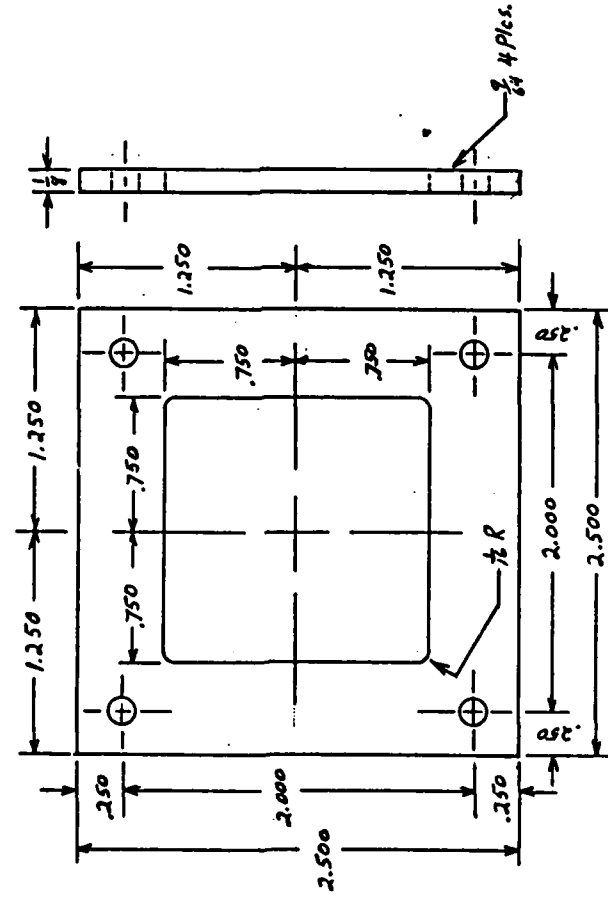
EAGLE-PICHER INDUSTRIES, INC.					
SPECIALTY MATERIALS DIVISION					
MIAMI RESEARCH LABORATORY					
					
TOLERANCES (EXCEPT AS NOTED)	Part # 33	SCALE	DRAWN BY R. Morris		
DECIMAL	Aluminum	1/4" = 1"	APPROVED BY W. Morris		
.005	TITLE #33 Sample Stage				
FRACTIONAL	XYZ THETA Stage				
1/4	DATE 9-26-86				
ANGULAR	DRAWING NUMBER				REV.
.5	RD-1453				0

READ TO Y100 15-40 INCHES

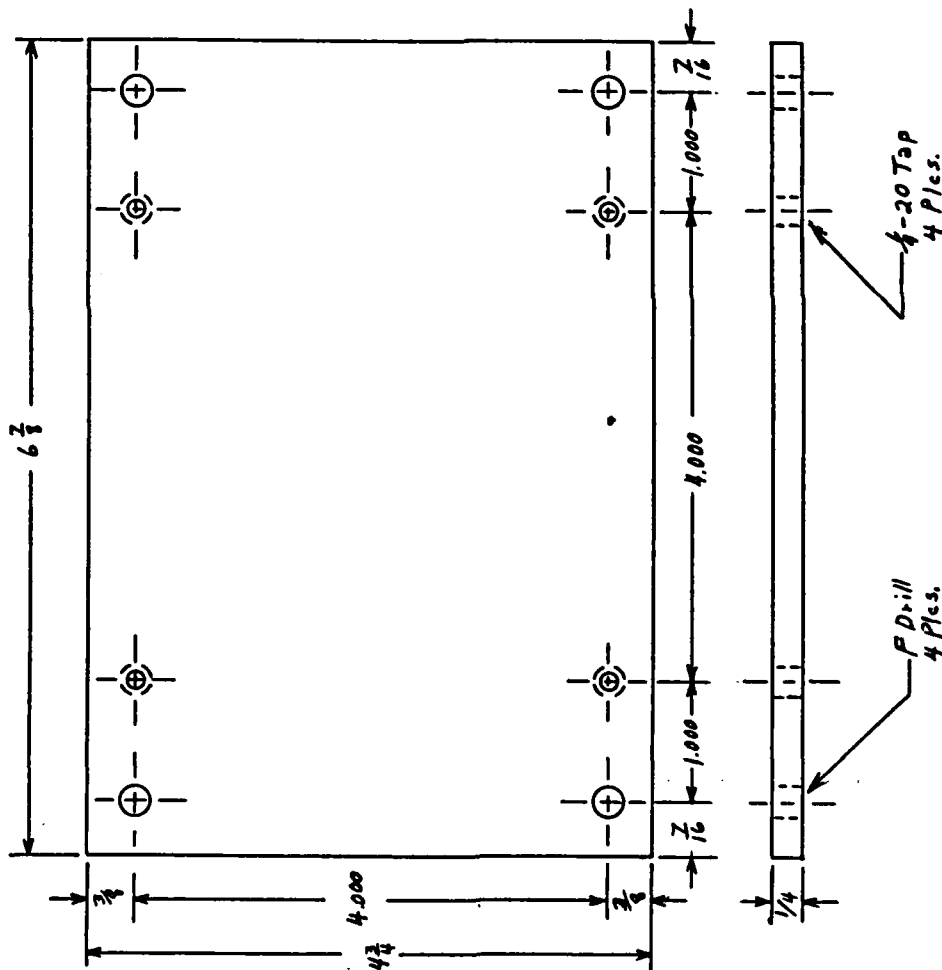
Part #34 5 Reqd.
 1/4" Center sq hole
 20MM " " "
 15MM " " "
 10MM " " "

Part #35 4 Reqd.
 1" Center sq hole
 20MM " " "
 15MM " " "
 10MM " " "

DATE	BY	REVISION	RECORD	AUTH.	COL.



EAGLE-PICHER INDUSTRIES, INC.		SPECIALTY METALS DIVISION		BRIEN RESEARCH LABORATORY	
TOLERANCES EXCEPT AS NOTED	DECIMAL	Parts #34 & 35	SCALE	DRAWN BY	APPROVED BY
	.005	Aluminum	1/2" = 1"	McGee	McGee
FRACTIONAL	1/16	TITLE #34 Sample holder Base #35 Sample holder			
ANGULAR	1/2	XYZ THETA Stage			
		DATE	DRAWING NUMBER	REV.	
		9-26-86	RD-1454	0	

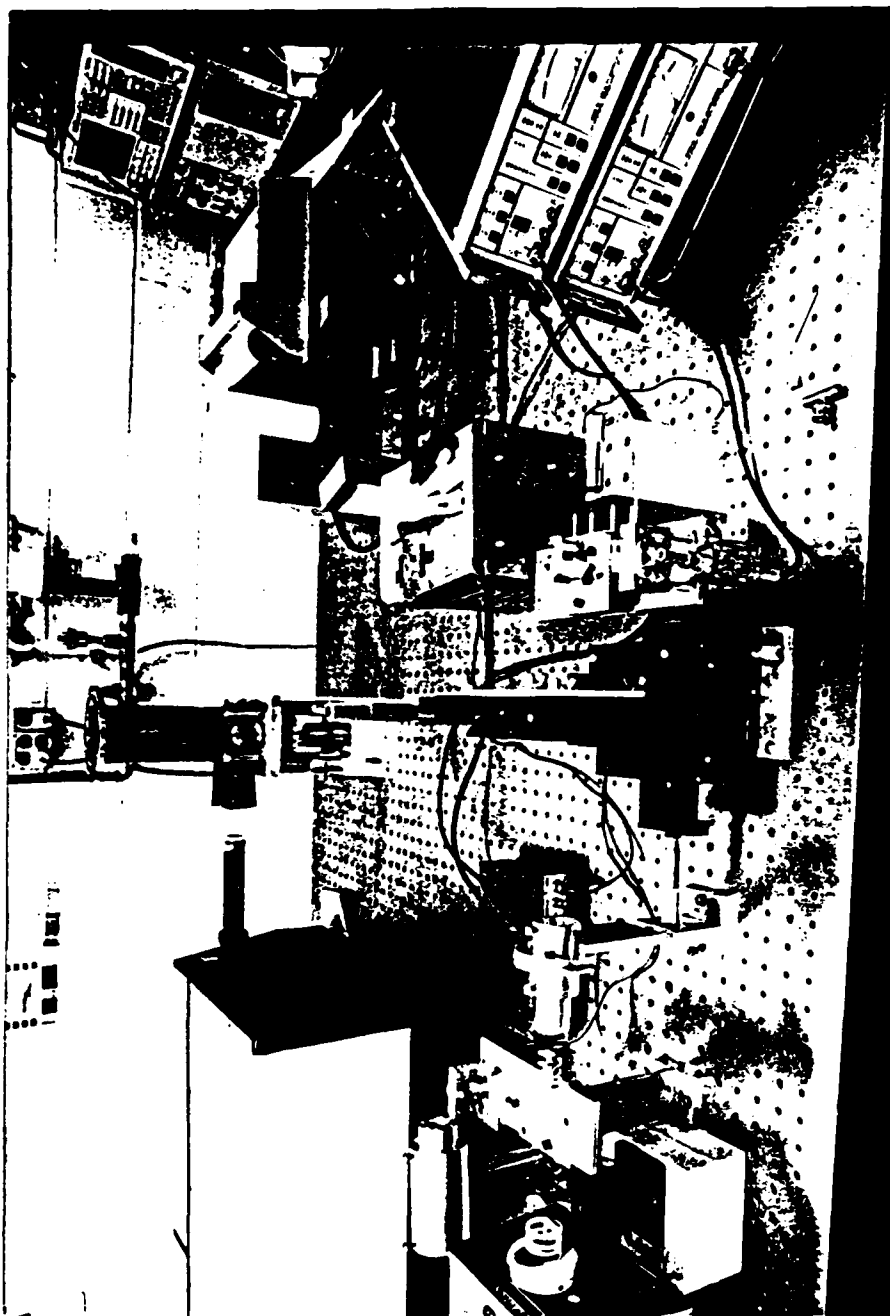


DATE	BY	REVISION	RECORD	APPROV.	REL.

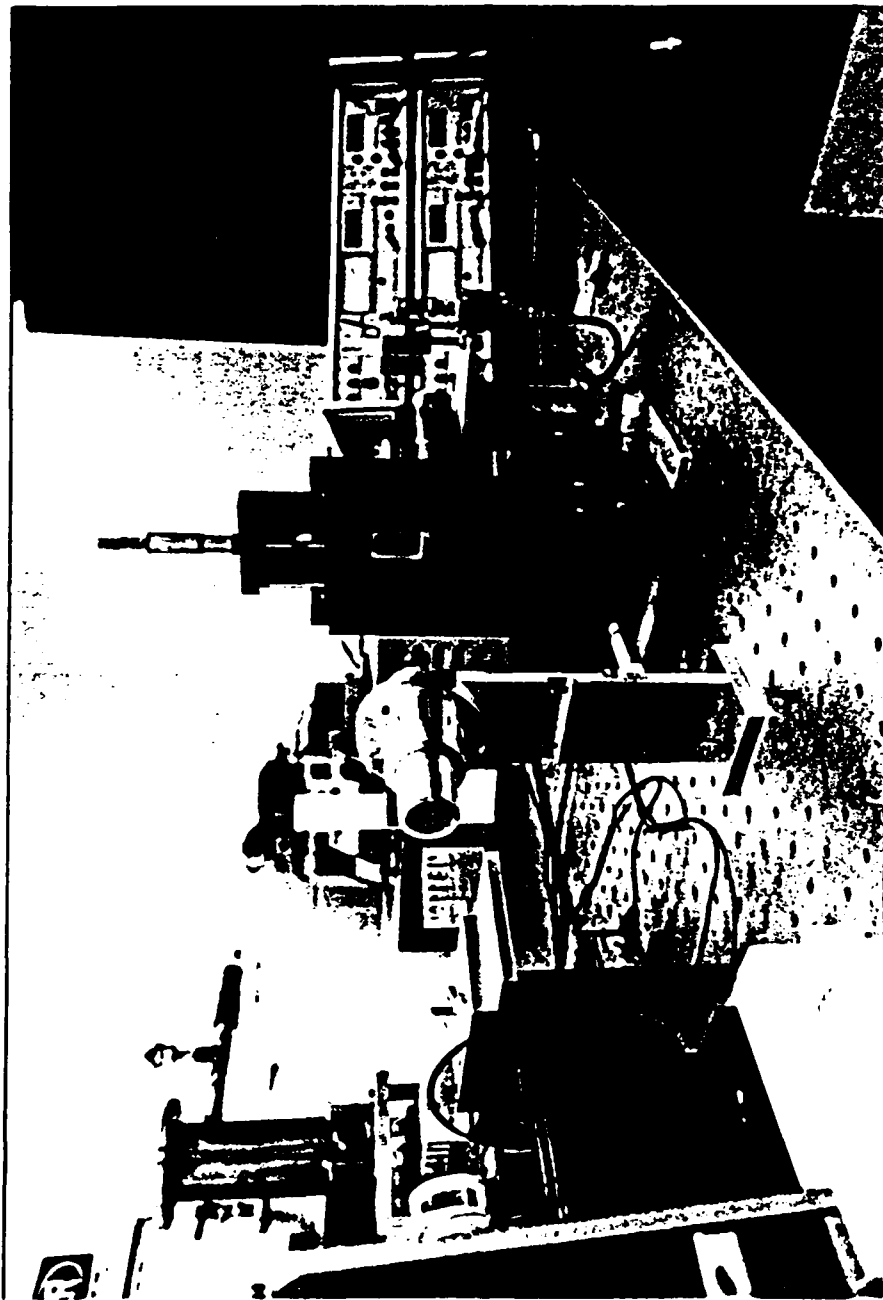
TOLERANCES EXCEPT AS NOTED	EAGLE-PICHER INDUSTRIES, INC. SPECIALTY MATERIALS DIVISION BRIGHT RESEARCH LABORATORY	Part #36 Aluminum	SCALE Full	DRAWN BY K. M. Grier	APPROVED BY W. H. Grier
DECIMAL ±.005		TITLE XYZ THETA Stage			
FRACTIONAL ±.01		DATE 9-26-86			
ANGULAR ±		DRAWING NUMBER RD-1455			REV. 0

ATTACHMENT #2

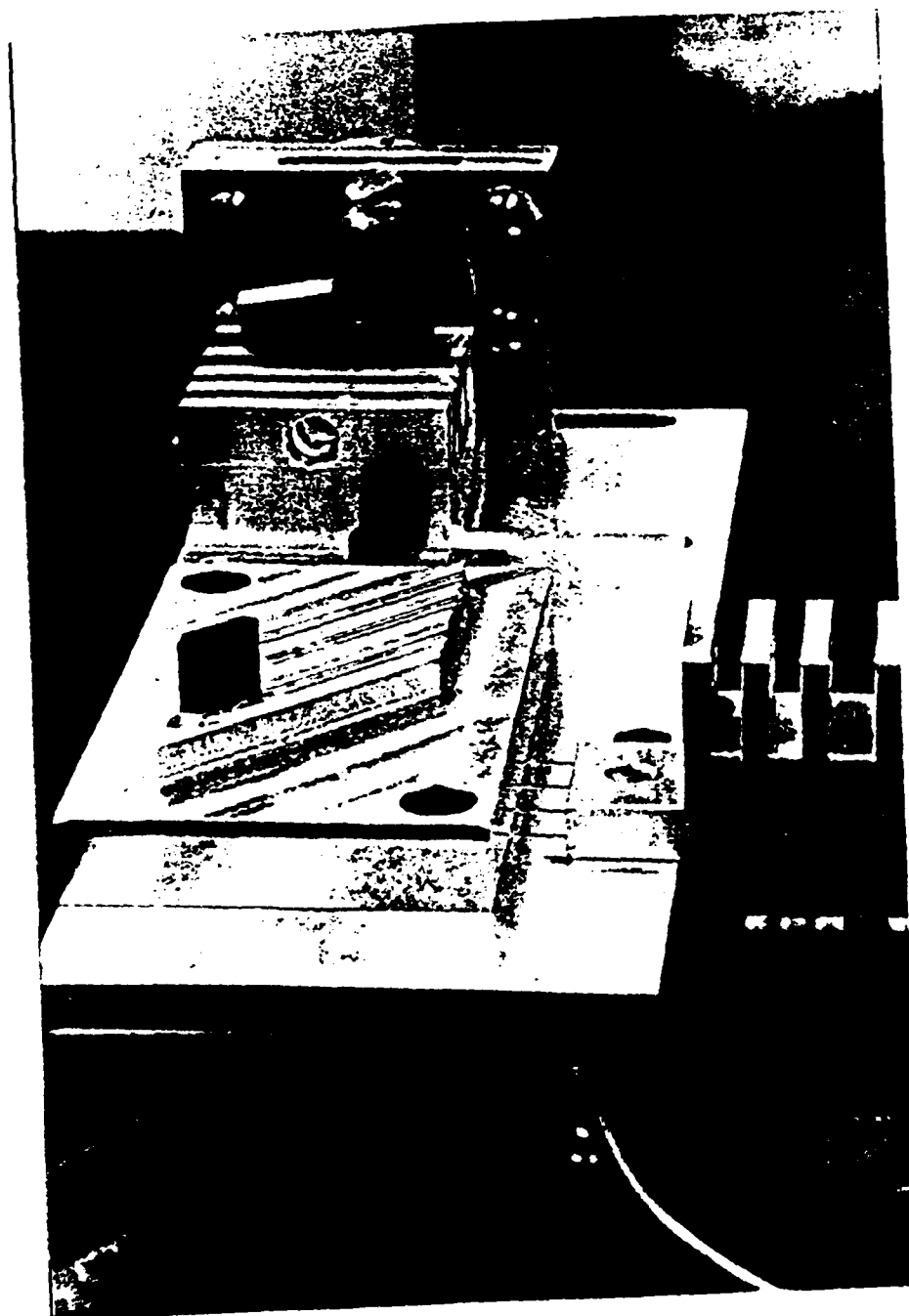
Page #	Title
A2-1	The FEA Set-Up
A2-2	Looking from the laser through the chopper and spatial filter toward the sample stage
A2-3	A close look at the CdTe beam splitter toward the reference attenuators and reference detector
A2-4	Another look at the beam splitter block with the chopper and reference detector in view
A2-5	Looking from behind the sample stage toward the laser
A2-6	Looking from behind the sample beam detector into the metalized prism



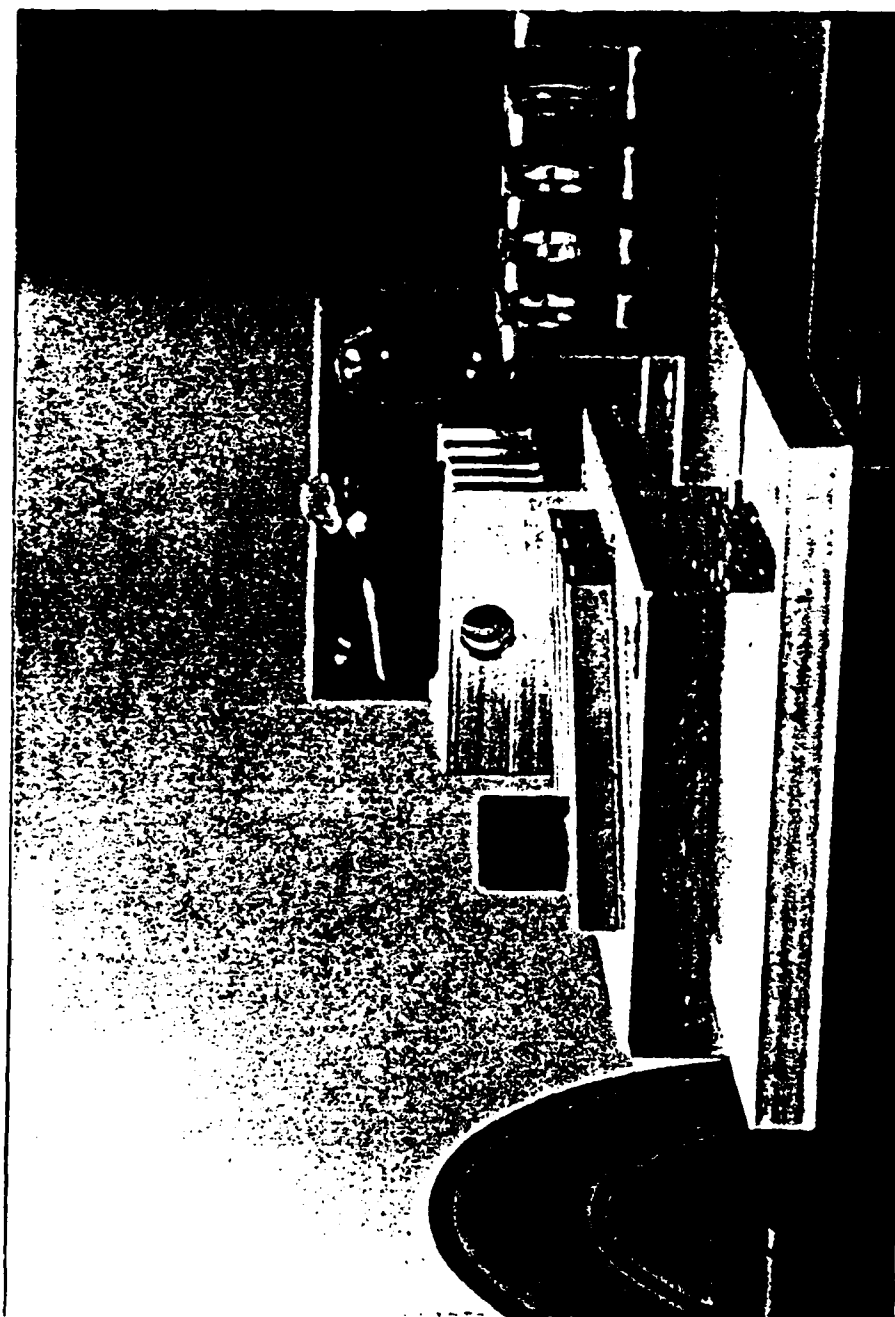
The FEA Set-Up



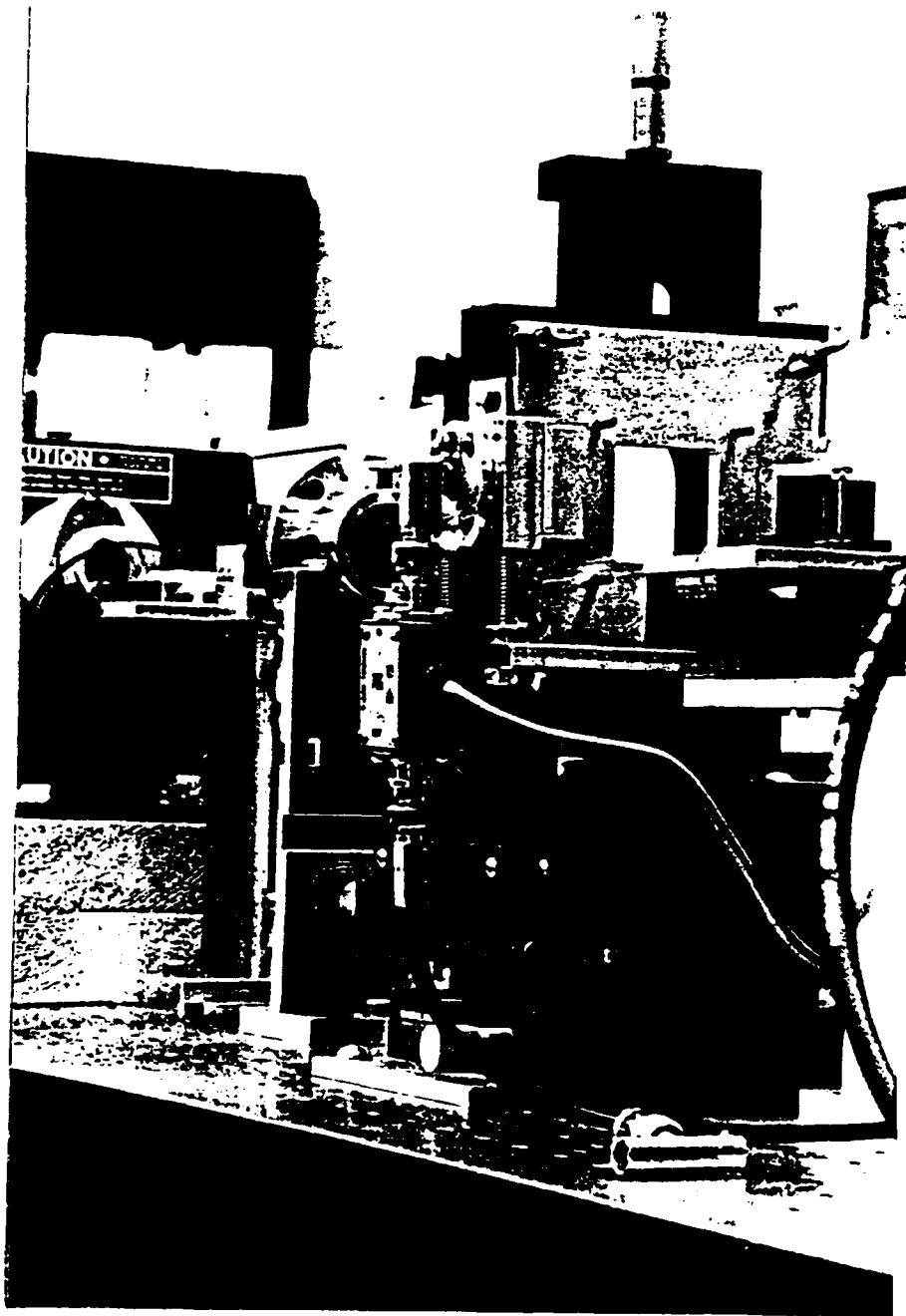
Looking from the laser through the chopper and spatial
filter toward the sample stage



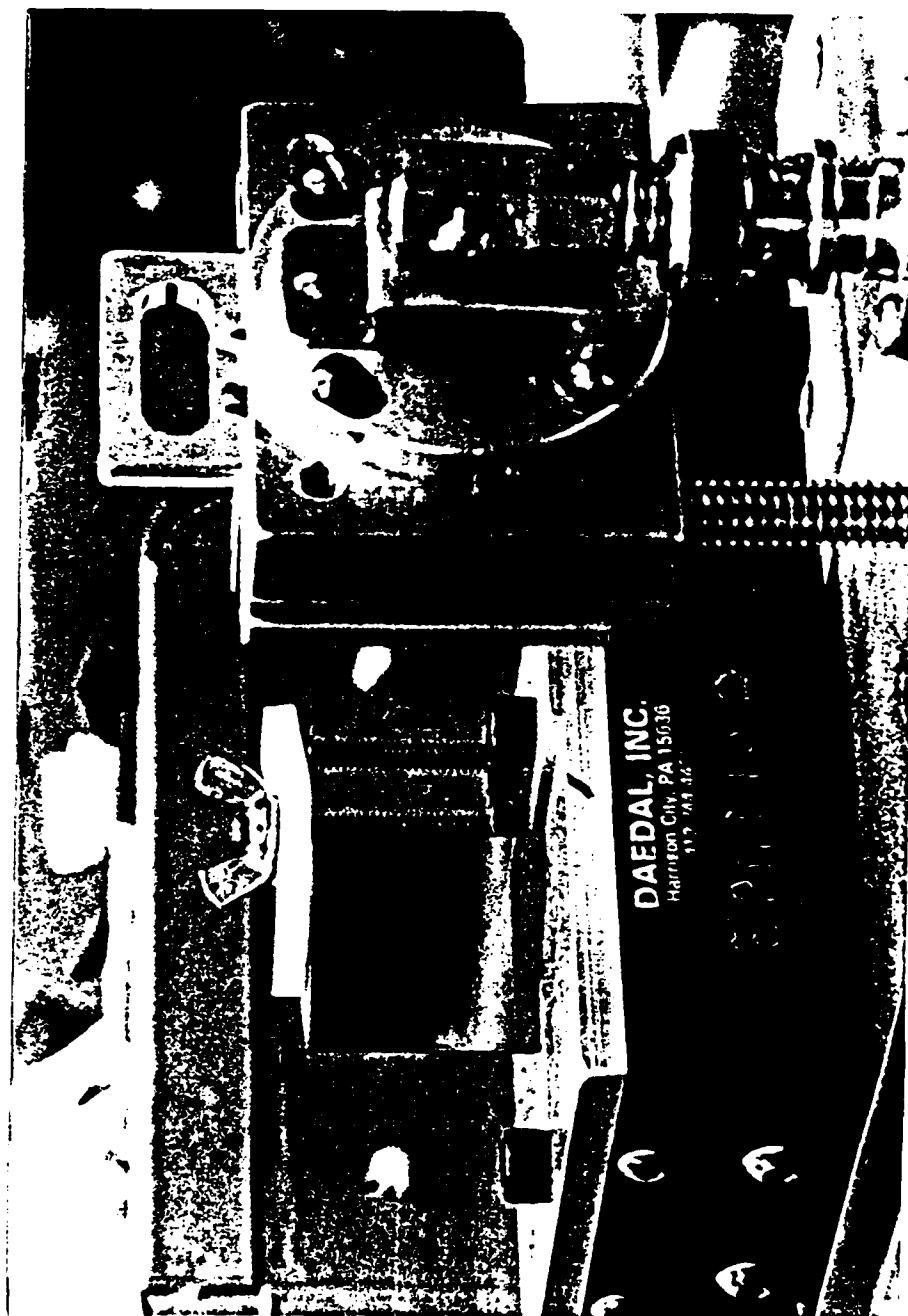
A close look at the CdTe beam splitter toward the reference attenuators and reference detector



Another look at the Beam Splitter block with the
chopper and reference detector in view



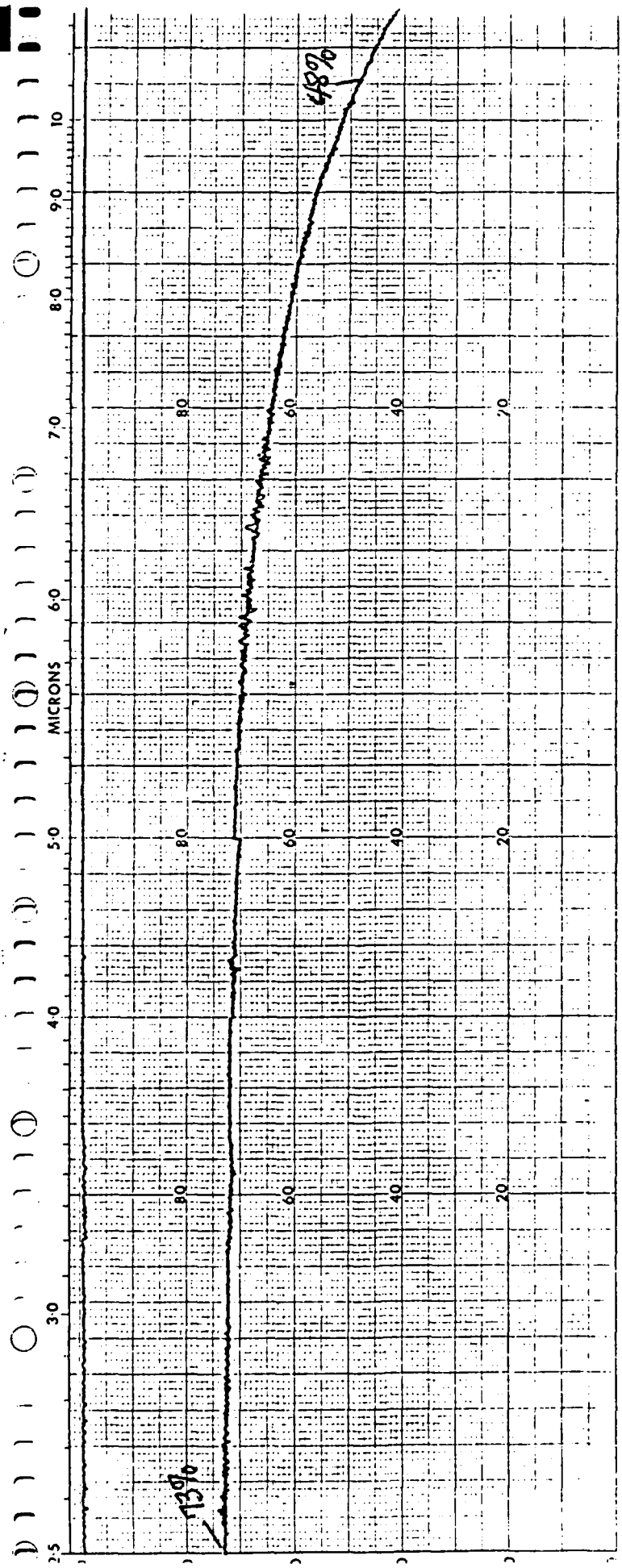
Looking from behind the sample stage
toward the laser



Looking from behind the sample beam detector
into the metalized prism

ATTACHMENT #3

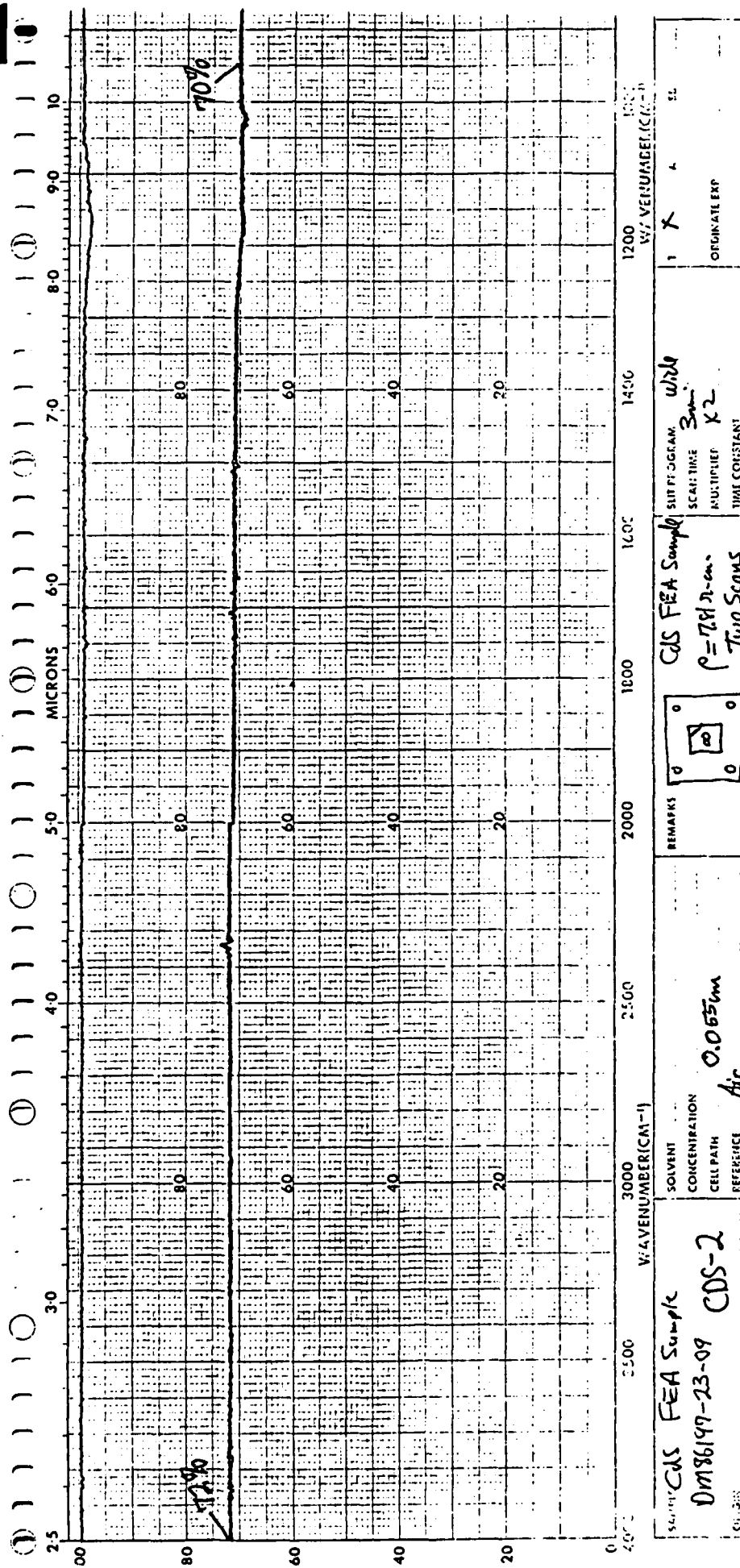
Page #	Title
A3-1	IR Scan of CdS-1 Sample
A3-2	IR Scan of CdS-2 Sample
A3-3	IR Scan of CdS-3 Sample
A3-4	IR Scan of InP Sample
A3-5	IR Scan of GaAs Sample



SAMPLE: DE86016-03-20 CDS-1		WAVENUMBER (CM⁻¹)		WAVENUMBER (CM⁻¹)		WAVENUMBER (CM⁻¹)	
CDS FEA Sample		0.055cm		CDS FEA Sample		CDS FEA Sample	
0.83μm		0.83μm		0.83μm		0.83μm	
A ₁		A ₁		A ₁		A ₁	
SOLVENT		CONCENTRATION		SCATTER		SCATTER	
CELL PATH		REFERENCE		SCATTER		SCATTER	
TIME CONSTANT		MULTIPLIER		SCATTER		SCATTER	
WAVELENGTH		WAVELENGTH		WAVELENGTH		WAVELENGTH	
WAVELENGTH		WAVELENGTH		WAVELENGTH		WAVELENGTH	

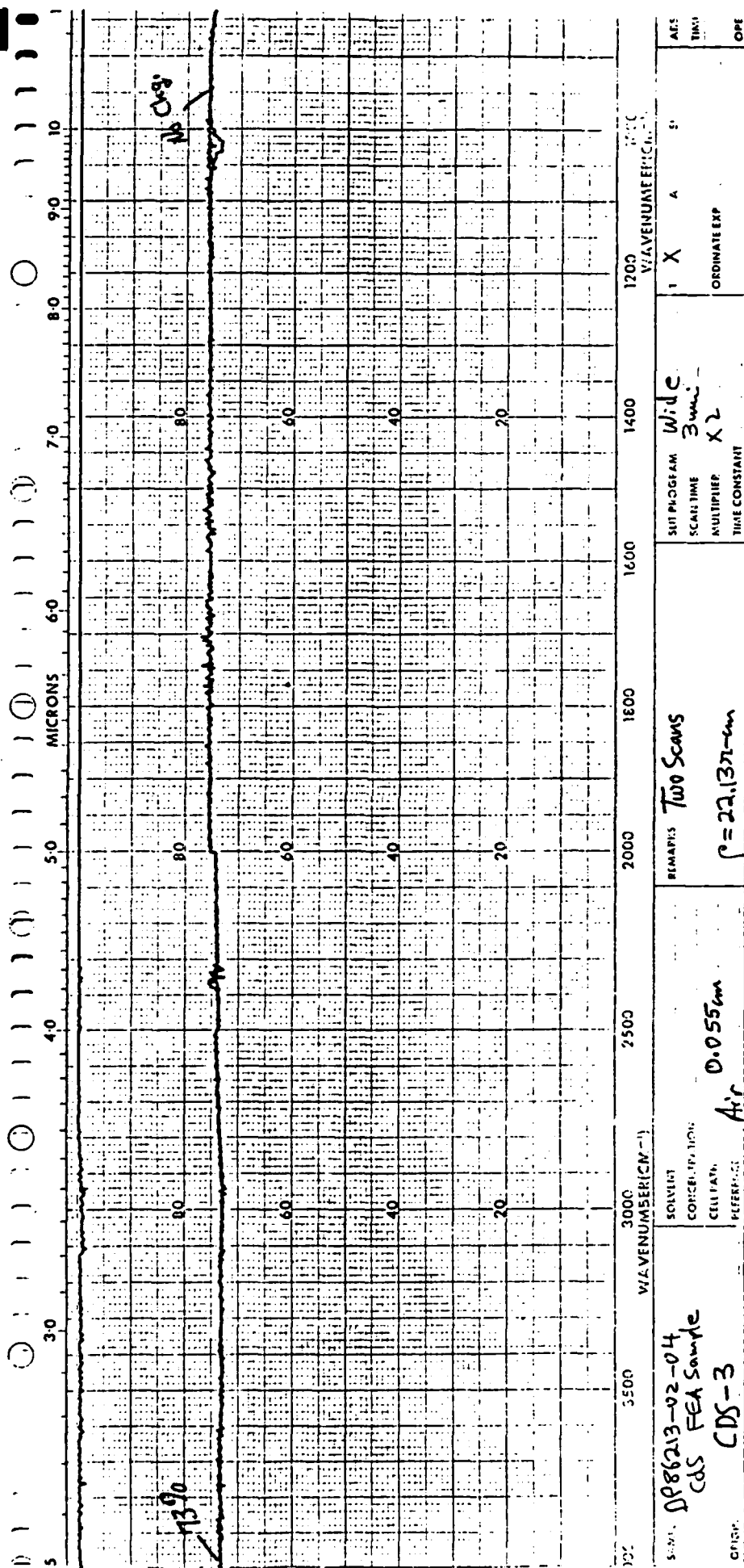
IR scan of CdS-1 Sample

A3-1



SAMPLE: CDS FEA Sample DM86197-23-09 CDS-2		REMARKS:		CDS FEA Sample P=72.9-70.9 Two Scans		SPLIT PROGRAM: wide SCALE: TIME 3m MULTIPLIER: X2 TIME CONSTANT		1 X 4 SL ORIGINATE EXP	
SOLVENT: Air CONCENTRATION: 0.055m CELL PATH: 0.055m									

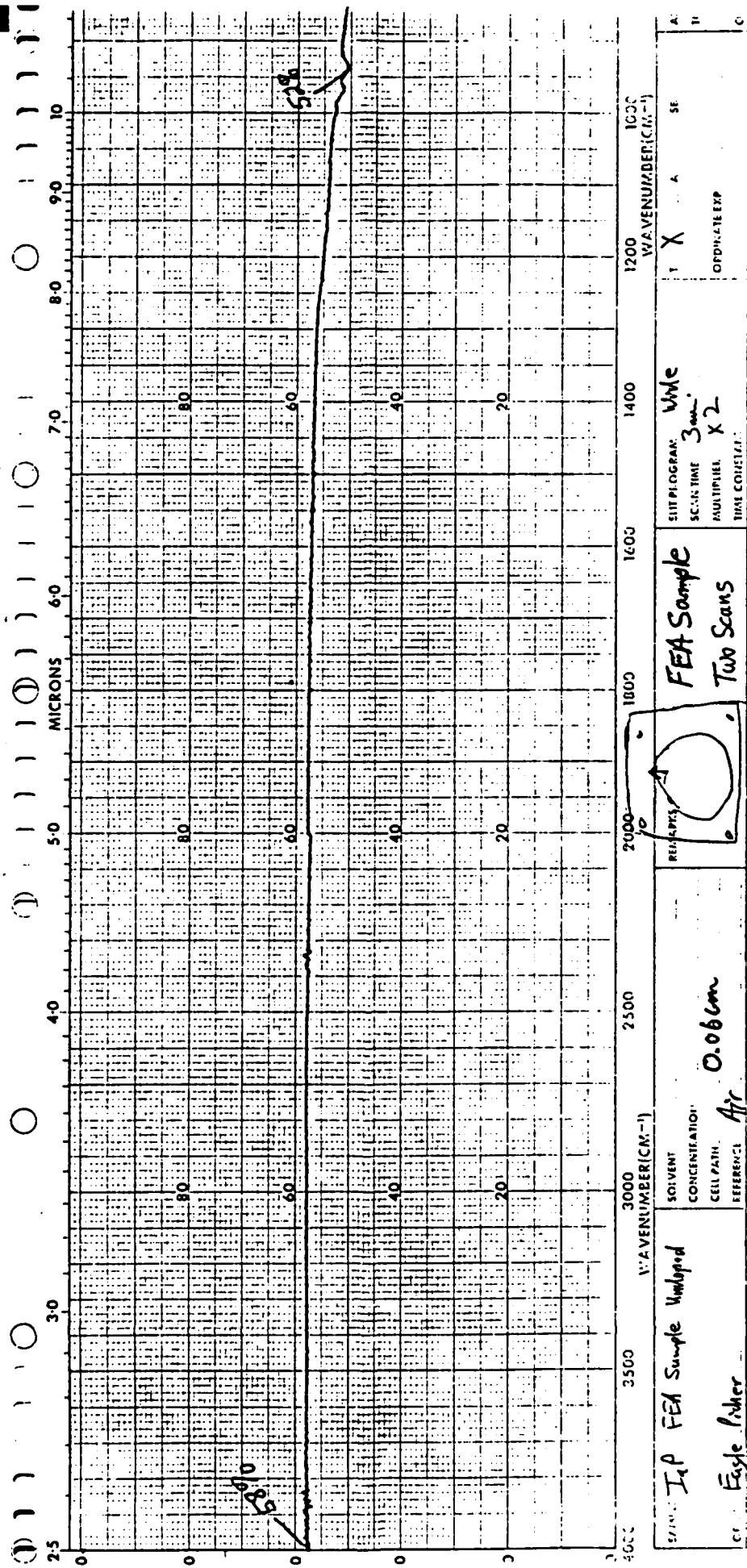
IR scan of CDS-2 Sample
A3-2



DATE: 086213-02-04	WAVELENGTH (MICRONS)	1 X	4	5	10
SAMPLE: CDS FEA Sample	WAVELENGTH (MICRONS)	1 X	4	5	10
ORIGIN: CDS-3	WAVELENGTH (MICRONS)	1 X	4	5	10
SOLVENT	REMARKS	SIT PROGRAM	WIDE	TIME	TIME
CONCENTRATION	Two Scans	SCANS TIME	3 min	ORDINATE EXP	ORDINATE EXP
CELL PATH	$\rho = 22.137 \text{ cm}$	MULTIPLIER	X 2	TIME CONSTANT	TIME CONSTANT
REFERENCE	0.055 cm	TIME CONSTANT			
	Air				

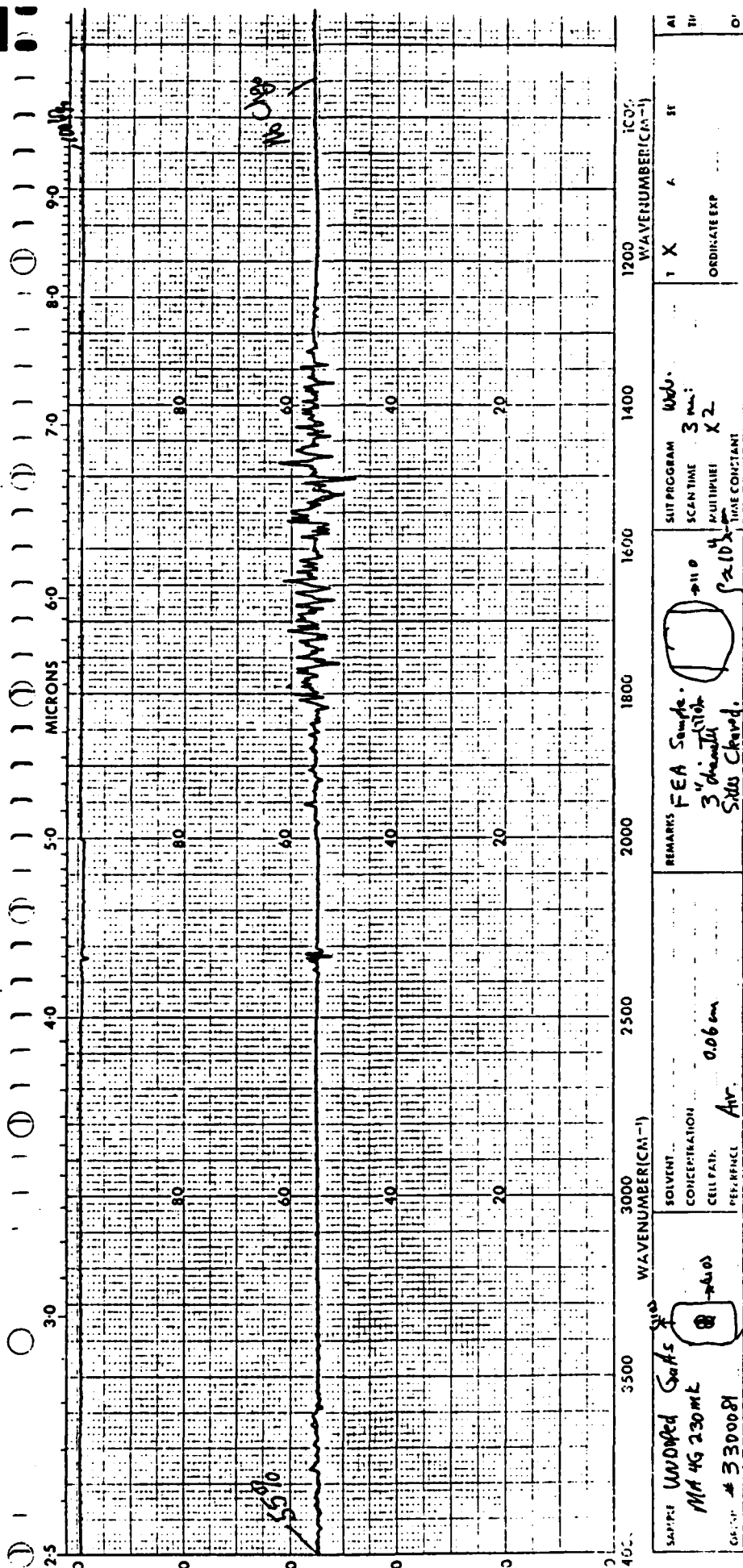
IR Scan of CdS-3 Sample

A3-3



SAMPLE: I.P. FEA Sample Undoped		3000 WAVENUMBER(CM-1)		2500		1800		1600		1400		1200 WAVENUMBER(CM-1)		1000	
SOLVENT		CONCENTRATION		CELL PATH		REFERENCE		0.06cm		Air		FEA Sample		Two Scans	
SCANS TIME		MULTIPLIER		TIME CORRECTION		REMARKS				SPLIT PROGRAM		SCANS TIME		MULTIPLIER	
Feyle Fiber		Feyle Fiber		Feyle Fiber		Feyle Fiber		Feyle Fiber		Feyle Fiber		Feyle Fiber		Feyle Fiber	

IR scan of InP sample



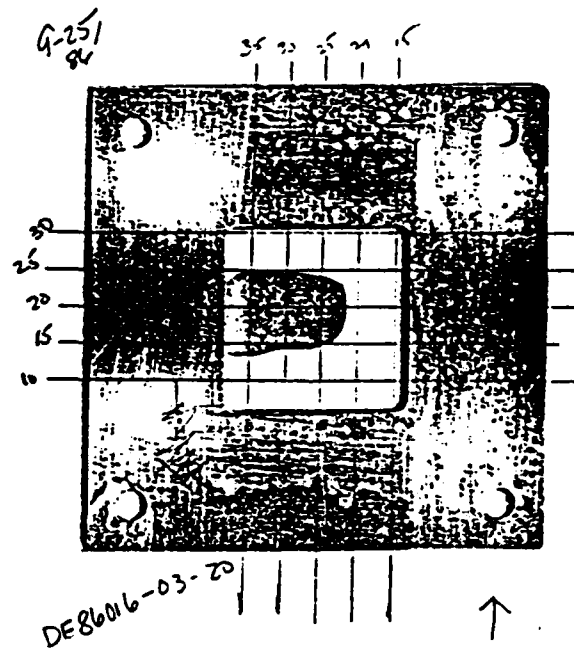
TWO SCANS

IR scan of GAs sample

A3-5

ATTACHMENT #4
PHOTOCOPIES OF SAMPLES IN THE
FEA HOLDER

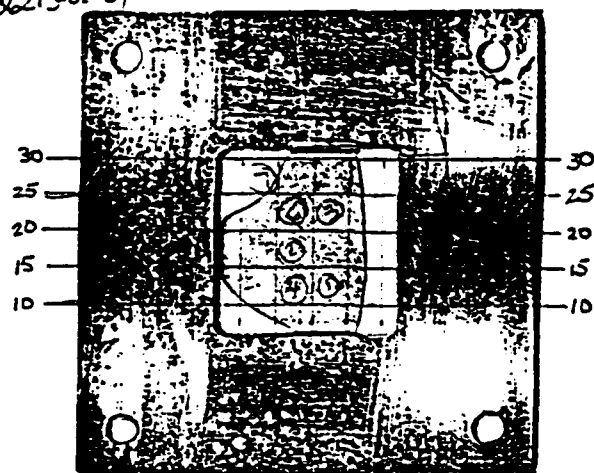
Page #	Content
A4-1	CdS-1 Sample
A4-2	CdS-2 Sample
A4-3	CdS-3 Sample
A4-4	InP Sample
A4-5	GaAs Sample



CdS-1 Sample

A4-1

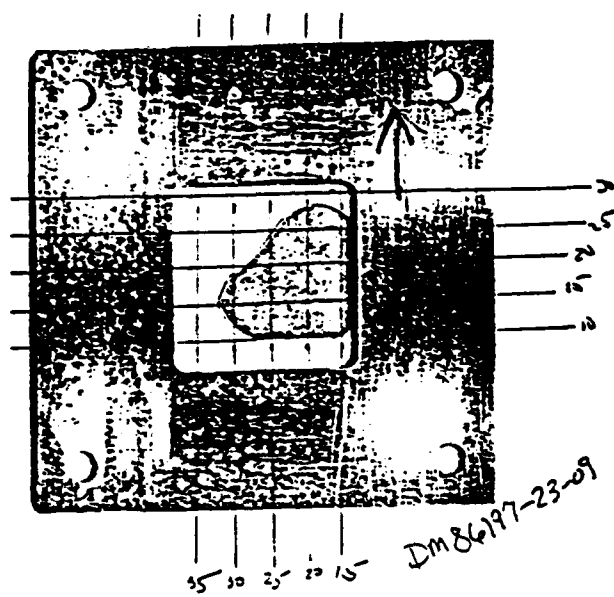
from Lazer to Detector
 cds
 DP86213-05-04



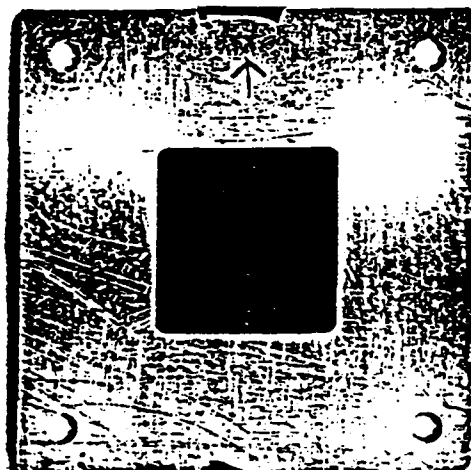
9-25-86

35 30 25 20 15

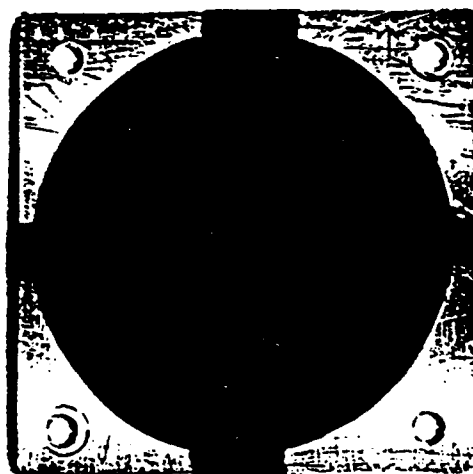
CdS-2 Sample



CdS-3 Sample

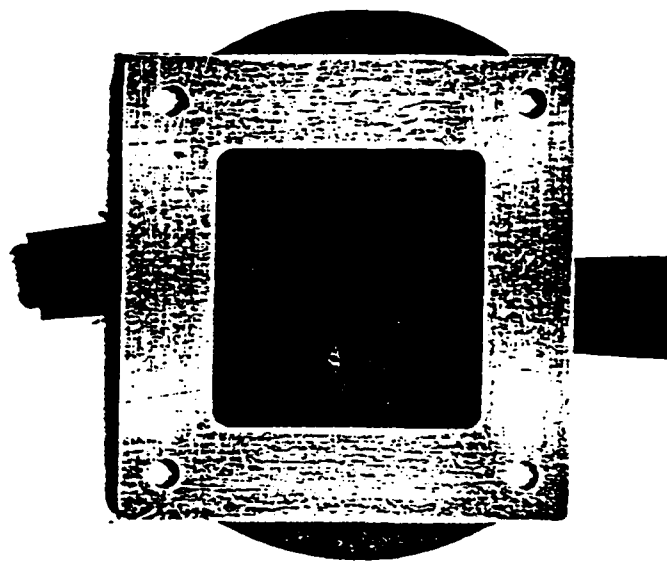


Laser Face

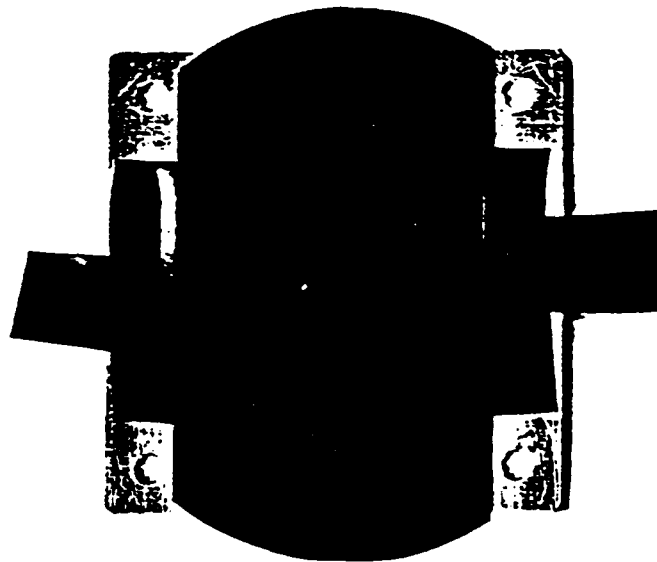


Detector Face

InP Sample
A4-4



Laser Face



Detector Face

Sample GaAs

ATTACHMENT #5
GRID WAFER DATA MAPS

Page #	Content
A5-1	Set-Up Grid for InP Wafer
A5-2	Spot Map for InP Wafer
A5-3	Select 1mm by 1mm Area of InP Wafer
A5-4	Select Areas 5mm by 5mm of GaAs Wafer
A5-5	Additional Areas 5mm by 5mm of GaAs Wafer
A5-6	More 5mm by 5mm Areas of GaAs Wafer
A5-7	Set-Up Grid for CDS-1
A5-8	Grid 14mm by 13mm of CDS-1
A5-9	Set-Up Grid Photocopy for CDS-2
A5-10	Grids 1mm by 1mm of CDS-2
A5-11	Set-Up Grid and 6mm by 6mm Maps of InP Wafer
A5-12	Set-Up Grid and 15mm by 10mm Map of CDS-3 Wafer
A5-13	Set-Up Grid and 10mm by 5mm Map of CDS-1 Wafer
A5-14	A 15mm by 5mm Map of CDS-2 Wafer

36

Project No. _____

Book No. _____

TITLE _____

125 min

Page No. _____

1.9

$I_0 = 110$

25.0	27.0	27.2	26.8	26.4	26.0	25.6	25.2	24.8	24.4	24.0			
25.0	61	61	62	62	61	60	61	61	64	63	61	25.0	
24.8													
24.6	61	62	62	61	61	61	63	62	64	62	68	24.6	
24.4													
24.2	62	62	61	61	60	62	63	64	61	63	60	24.2	
24.0													
23.2	63	62	61	61	62	62	63	61	61	60	63	23.8	
23.6													
23.4	61	62	60	60	61	62	61	62	61	58	58	60	60
23.2													
23.0	61	60	60	60	61	64	64	63	61	60	60	62	60
22.8													
22.6	60	60	61	60	62	63	63	63	61	60	63	64	64
22.4													
22.2	60	62	61	62	59	59	60	60	64	64	64		
22.0													
21.8	61	62	61	61	57	58	58	59	61	62	63		
21.6													
21.4	62	63	62	60	59	58	59	59	58	59	60		
21.2													
21.0	63	62	63	60	61	61	61	60	59	58	61		

28.0 27.8 27.6 27.4 27.2 27.0 26.8 26.6 26.4 26.2 26.0 25.8 25.6 25.4 25.2 25.0 24.8 24.6 24.4 24.2 24.0

gud in mm

Page 15-1

To Page No. _____

tnessed & Understood by me,

Date

Invented by

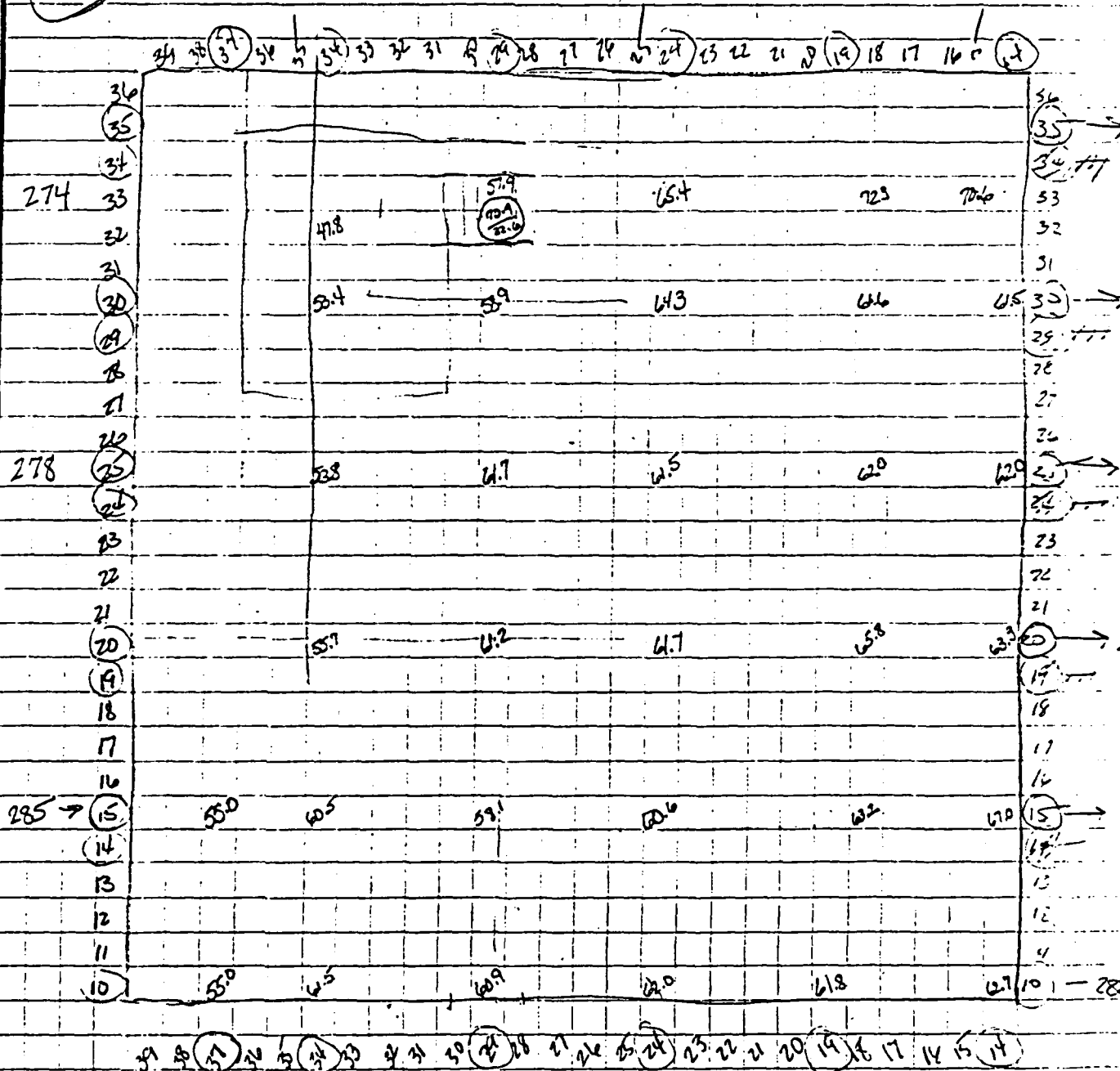
Date

Recorded by

9-10-86

$R_{ef} = 288$
~~9:00 km~~ $I_0 = 104$

using HP9835A



grid is in mm

P. A5-2

To Page No.

Witnessed & Understood by me,

Date _____

Invented by**Date**

Recorded by

From Page No.____

52

$$R_f = 289$$
$$I_0 = 91.3$$

289 →	32.2	32.2	32.1	32.4	32.1	32.0	32.2	32.1	32.0	32.9	33.0
288 ←	32.6	32.6	32.6	32.4	32.1	32.3	32.7	32.6	32.4	32.2	32.9
289 →	32.0	32.4	32.3	32.1	32.2	32.3	32.9	32.1	32.3	32.6	32.8
289 ←	32.0	32.1	32.7	32.0	32.2	32.6	32.9	32.6	32.0	32.7	32.7
288 →	32.6	32.3	32.0	32.7	32.5	32.6	32.7	32.6	32.3	32.4	32.6
288 ←	32.6	32.1	32.7	32.6	32.0	32.3	32.1	32.1	32.2	32.9	32.5
280 →	32.3	32.0	32.3	32.1	32.4	32.6	32.0	32.9	32.4	32.4	32.4
287 ←	32.3	32.1	32.3	32.3	32.7	32.6	32.7	32.7	32.9	32.4	32.3
288 →	32.6	32.3	32.1	32.2	32.3	32.7	32.6	32.1	32.4	32.7	32.2
289 ←	32.3	32.5	32.0	32.9	32.3	32.4	32.3	32.3	32.3	32.7	32.1
289 →	32.9	32.5	32.8	32.7	32.4	32.4	32.3	32.1	32.2	32.7	32.0

Wynah arrived
at 10 o'clock

		30.0	29.9	29.8	29.7	29.6	29.5	29.4	29.3	29.2	29.1	29.0
32												
40												
28												
289 ← 20												
289 → 24		28.1	28.8	28.7	28.1	28.4	28.1	28.4	28.1	28.4	28.1	28.4
280 ← 22		28.8	28.6	28.7	28.7	28.7	28.7	28.7	28.7	28.7	28.7	28.7
287 → 20		28.5	28.8	28.9	28.7	28.7	28.7	28.7	28.7	28.7	28.7	28.7
		31.0	30.0	29.0	28.0	27.0	26.0	25.0	24.0	23.0	22.0	

24

22

20.

18

16

60.8	66.4	65.8	64.6	79.8	6.1
83.4	75.6	76.8	77.2	72.8	10

→ 289
← 287

31 30 29 28 27 26 25 24 23 22

0. A5-3

Grids are in MW

To Page No.

Witnessed & Understood by me,

Date _____

Invented by

Date

Recorded by

TITLE

GATS

Project No. _____

Book No. _____

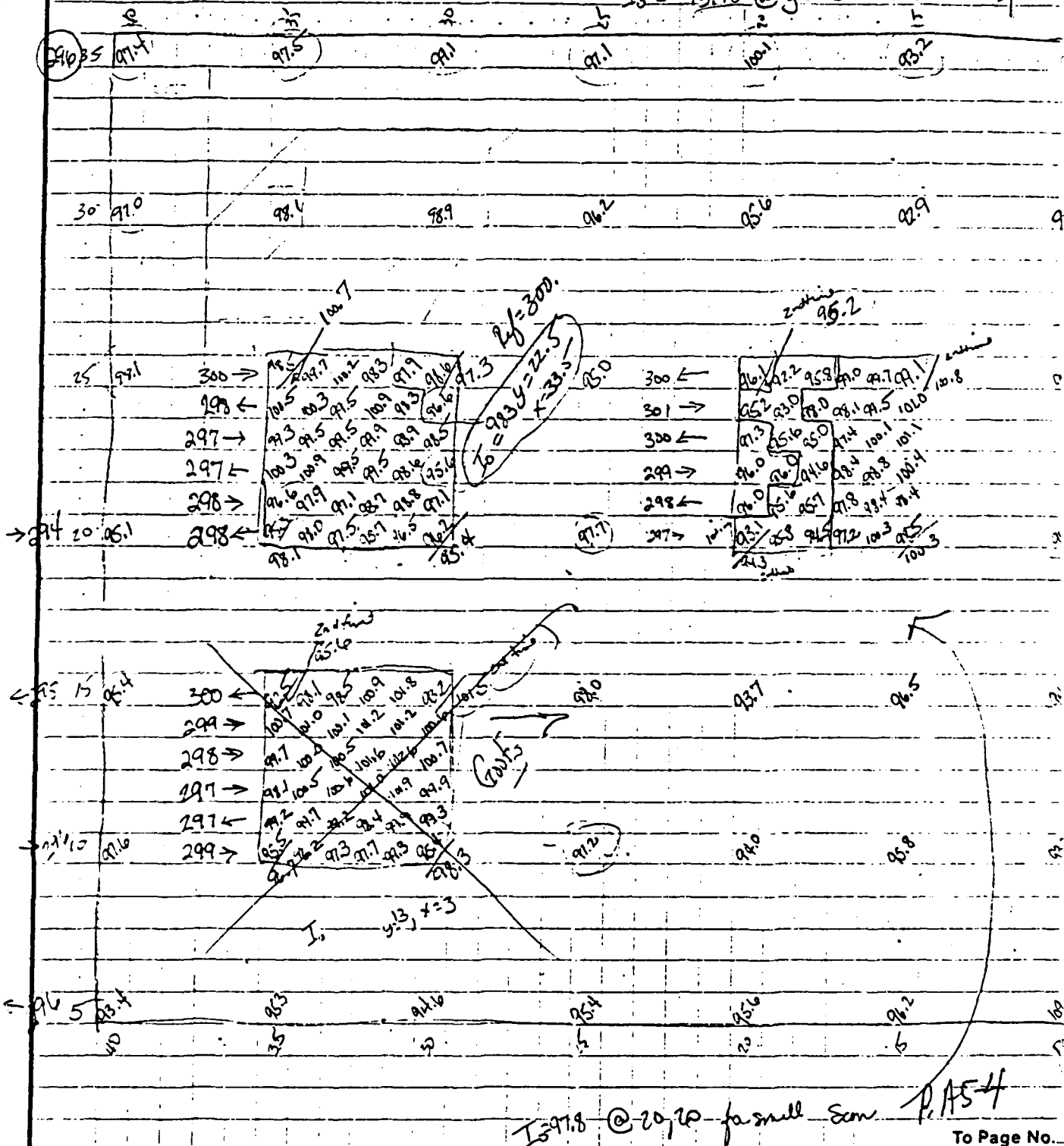
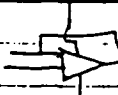
(39)

From Page No. _____

9-11-80

$I_0 = 117.5 @ y=5 x=10$

$I_0 = 93.48 @ y=20 x=25$



From Page No. 9-15-86

 $I_0 = 105.4$ $y = 22$ $x = 18$

Gals

Chopper at ~ 80

Gals

 $t = -0.06$ cm

104

3)

 $I_0 = 49.1$ $x = 35$
 $y = 15$

165 →	47.7	47.7	47.1	47.0	47.7	47.0
166 ←	47.2	47.7	47.8	48.4	47.8	46.0
165 →	46.1	47.9	47.6	47.6	48.1	47.4
164 ←	47.6	48.0	47.8	47.9	48.0	47.4
165 →	47.4	47.4	47.5	48.1	48.2	47.5
164 ←	47.2	47.3	47.9	47.7	47.7	47.4

40 35 35

 $I_0 = 105.4$ $y = 22$ $x = 18$

298 →	105.0	97.9	102.5	105.2	105.9	106.7	(300)
	101.1	100.2	101.8	104.2	105.5	106.2	← 298
296 →	105.1	104.9	104.2	103.9	107.3	107.0	
	104.0	105.7	104.1	106.2	104.9	104.6	← 296
295 →	105.4	106.8	107.0	102.3	106.2	105.3	
	105.4	105.3	106.0	104.3	106.7	106	← 297

Chopper 38.4

 $I_0 = 49.6$ $y = 10$ $x = 30$

166 →	48.2	48.9	49.0	48.9	49.0	48.3
165 ←	48.2	48.6	48.1	48.4	48.3	48.1
165 →	47.5	47.6	47.9	48.0	47.7	47.9
164 ←	47.2	47.9	46.8	47.1	47.7	47.3
166 →	47.7	47.2	46.7	46.9	46.1	46.2
167 ←	47.0	47.6	48.1	47.8	47.8	46.9

35 35 35

 $I_0 = 49.4$ $y = 13$ $x = 20$

166 →	46.9	48.0	47.8	49.1	48.5	48.3
165 ←	47.0	47.5	47.5	48.5	47.8	47.7
166 →	48.2	48.5	48.8	49.2	49.2	47.9
166 ←	48.9	50.1	49.1	47.9	47.0	47.5
166 →	49.0	48.0	47.0	47.5	46.8	47.2
165 ←	47.3	46.8	47.8	47.6	47.7	48.3

35 35 35

 $I_0 = 50.2$ $y = 10$ $x = 15$
Chopper 20

164 →	47.9	48.8	48.3	47.8	47.9	47.9
166 ←	47.4	48.5	47.4	46.8	48.0	46.3
165 →	49.0	47.6	47.4	48.2	47.6	47.0
166 ←	48.2	46.7	49.1	49.1	47.1	48.3
166 →	47.2	49.4	47.5	47.1	47.5	46.4
166 ←	48.6	47.5	47.3	49.2	46.9	47.3

15 15 15

2rid 2 mm

P. A. 5=5

To Page No. _____

Witnessed & Understood by me, _____

Date _____

Invented by _____

Date _____

Recorded by _____

|||

Project No. _____

TITLE _____

Book No. _____

4

From Page No. 9-18-86 CDS DE86016-03-22

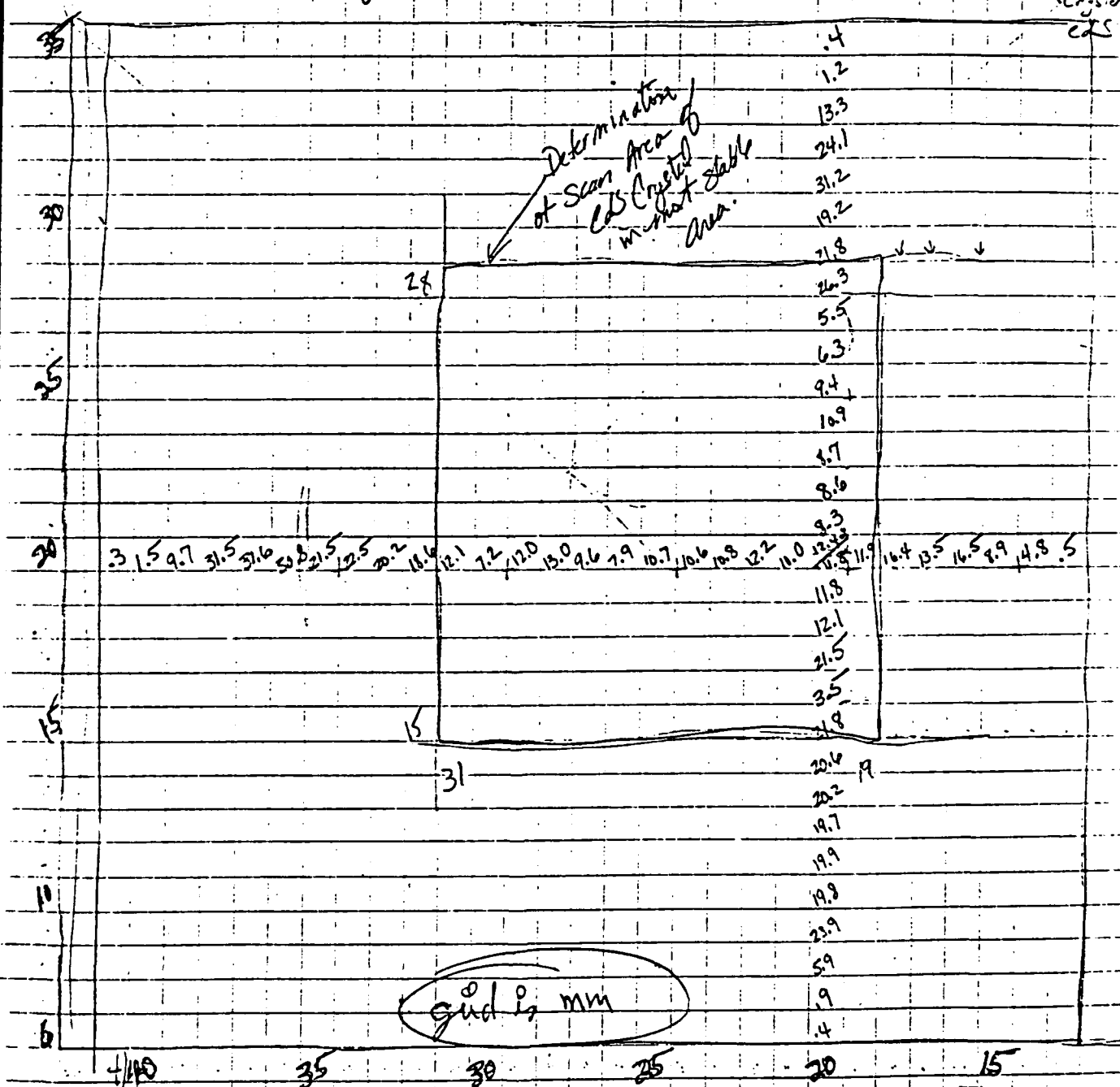
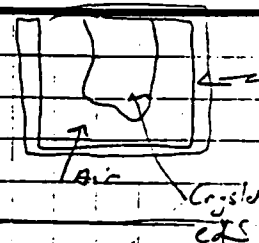
41.6

Suspended on a holder with tape 1"x1" holder

4.40

Ref @ 113.0 mm

CDS-1



Witnessed & Understood by me, OK

Date

Invented by

Date

Recorded by

To Page No. _____

PA57

From Page No. _____

9-18-80

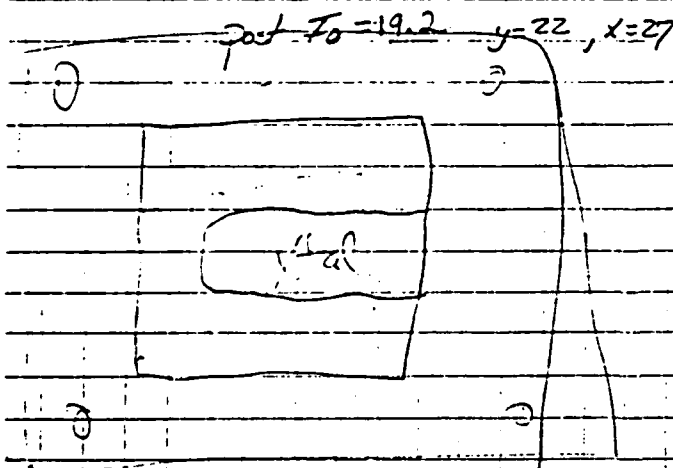
CdS Crystal DE 86014 -03-~~25~~

CDS-1

Def Apt = 0.037"

112.0 113.0 113.0 113.0 113.0

	31	30	29	28	27	26	25	24	23	22	21	20	19		28	27	26	25	24	23	22	21	20	19		18	17	16	15	14
28	19.7	19.8	20.0	19.7	19.3	21.0	19.7	17.5	19.1	22.2	25.5	25.9	25.7	28	25.2	25.2	23.9	21.2	22.2											
27	20.0	19.6	18.7	20.8	25.4	25.5	21.2	16.3	11.9	8.8	7.1	5.5	4.6	27	4.3	4.9	6.9	16.8	23.2											
26	20.2	23.9	20.1	11.1	6.9	4.7	3.8	3.6	5.1	5.3	6.4	10.5	12.0	26	11.5	9.0	5.5	2.8	2.2											
25	21.4	9.4	4.2	4.5	6.5	10.4	17.4	24.4	20.3	17.6	15.7	11.0	11.4	25	11.6	12.6	23.5	16.3	1.5											
24	19.5	5.1	13.5	21.9	12.7	8.6	13.3	15.6	11.7	14.0	15.1	14.1	13.3	24	12.7	14.1	13.6	12.5	8.2											
23	17.4	7.0	18.9	13.1	12.7	11.2	12.1	12.8	12.8	14.1	13.7	12.3	13.6	23	14.0	14.0	13.6	12.5	9.3											
22	14.7	7.6	16.2	12.0	13.1	11.8	11.9	13.1	11.8	12.8	12.8	12.7	12.9	22	13.0	13.0	12.7	12.4	9.1											
21	14.9	7.7	13.4	11.4	12.3	12.4	11.0	12.2	12.3	12.7	12.4	12.5	12.0	21	13.3	13.4	12.6	12.5	7.6											
20	17.5	7.0	17.0	12.0	12.1	12.4	10.8	10.5	13.0	12.6	12.2	12.8	12.8	20	13.9	12.9	12.4	12.2	7.4											
19	21.5	6.9	15.7	11.3	12.0	11.9	12.1	11.8	12.7	12.6	12.5	12.3	12.2	19	13.2	13.4	12.7	12.0	6.5											
18	22.1	11.0	7.1	18.0	10.5	14.1	14.9	15.2	14.1	14.3	15.8	12.8	13.3	18	12.7	13.4	13.5	12.6	6.5											
17	19.9	22.1	8.5	7.2	2.5	14.6	20.8	19.1	14.4	13.0	20.5	13.5	21.0	17	17.2	14.4	22.4	26.6	8.2											
16	19.9	20.0	23.8	17.9	11.5	3.6	7.3	6.9	6.4	6.1	7.0	5.7	5.2	16	6.1	6.1	4.8	5.0	7.9											
15	20.0	20.4	20.8	19.8	21.8	25.5	21.0	22.2	26.1	26.0	26.5	24.5	15.5	15	13.3	10.2	10.3	10.9	14.7											
	31	30	29	28	27	26	25	24	23	22	21	20	19		18	17	16	15	14											



The very low readings in 4.0 - 5.0 or lower are the edges of the x-tal.

grid is mm

P. A5-8

To Page No. _____

Witnessed & Understood by me, _____

Date _____

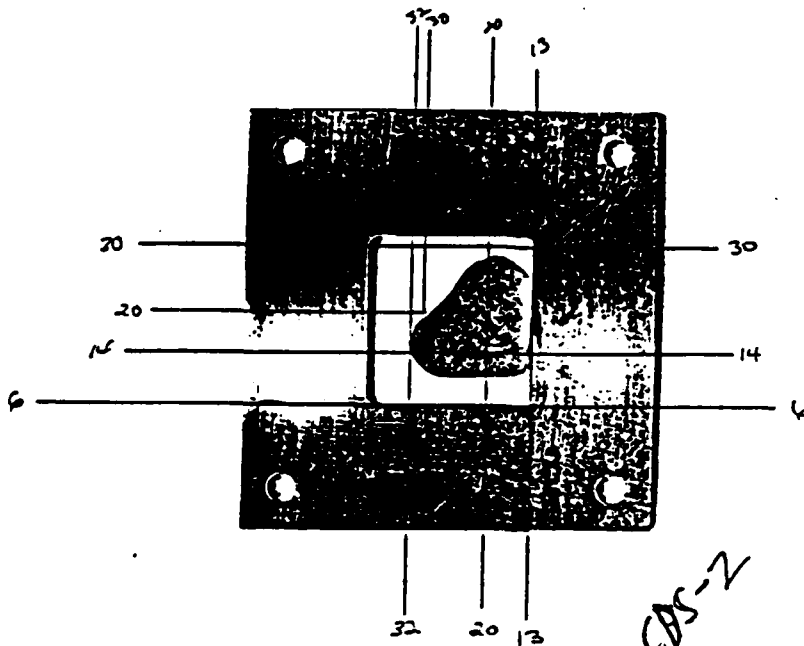
Invented by _____

Date _____

Recorded by _____

Project No. _____

45



CdS Crystal

looking from
Laser

$x=14$

$I_0 = 19.6$ $y = 20$
 $x = 20$

26	24	22	20	
2.0	20.3	12.3	5.1	4.3
19.6	5.8	23.0	2.4	17.0
10.7	31.2	18.0	18.3	15.7
12.3	15.0	14.1	17.9	14.6
20.5	16.7	19.0	14.5	17.0
12.3	14.6	15.4	16.6	17.3
17.3	18.6	17.5	16.6	16.8
17.0	16.4	15.4	16.0	16.2
14	21	12	2.3	11.9
11.4	15.3	13.3	16.3	16.3
32	30	28	26	24
22	20	18		

Looking from the Laser
information below

$x=25$
 $y=22$
 $@ 0^\circ$

$21.1 @ 0^\circ$

$I_0 = 20.3$
 $\Delta \approx 20^\circ$

$P_f = 102 \pm 101$

P. A5-9

To Page No. _____

essed & Understood by me,

Date

Invented by

Date

Recorded by

om Page No.

9/19/86

Dm 86197-23-09

CdS Crystal

Ref = 81.0

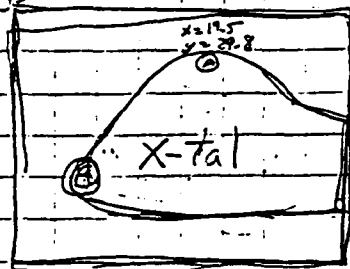
I₀ = 25.8 mV CIS-2

Sample holder in the center

x = 27 y = 22

12.4 at bottom edge of crystal

24.0 at the center of the crystal

looking from
Lazer

x = 14

(A) x = 19.5 y = 29.8 at top point X-Tal

B = x = ~~19.5~~ 32.30

17.40 y

x = 19 to 20

y = 17 to 18

I₀ = 19.6y = 20
x = 20

Ref	20.0	18	16	14	12	10.0		30	28	26	24	22	20	
101	18.0	15.9	14.3	12.4	10.1	15.1	18.0	102	21.0	21.6	21.0	20.3	12.9	5.1
100	16.1	15.4	14.4	13.1	11.3	15.1	17.8	102	21.5	21.8	19.6	5.8	3.6	2.4
101	15.8	14.3	12.7	11.2	9.2	6.2	17.6	101	21.4	20.3	10.7	3.2	18.0	18.3
101	16.2	15.5	15.3	15.5	15.1	14.5	17.4	101	21.7	18.5	12.3	1.5	1.1	1.9
100	15.2	14.9	15.6	14.9	14.6	14.1	17.2	100	22.2	13.5	2.5	16.7	19.0	14.5
79.0	14.7	14.9	14.3	13.9	14.3	14.7	17.0	100	10.6	20.9	18.3	14.6	15.4	14.6
	20.0	19.8	19.6	19.4	19.2	19.0		32	30	28	26	24	22	20
								18	18.1	20.0	17.3	18.6	17.5	16.6
								16	16.5	24.3	17.8	17.0	16.4	15.4
								14	21.1	21.2	21.3	11.9	11.4	10.3
								32	30	28	26	24	22	20

I₀ = 20.5
x = 25
y = 22
20°

21.1 @ 0°

I₀ = 20.3

21° @ 20°

good to mm

Ref = 102 to 101

P. A5-10

To Page No.

Witnessed & Understood by me,

Date

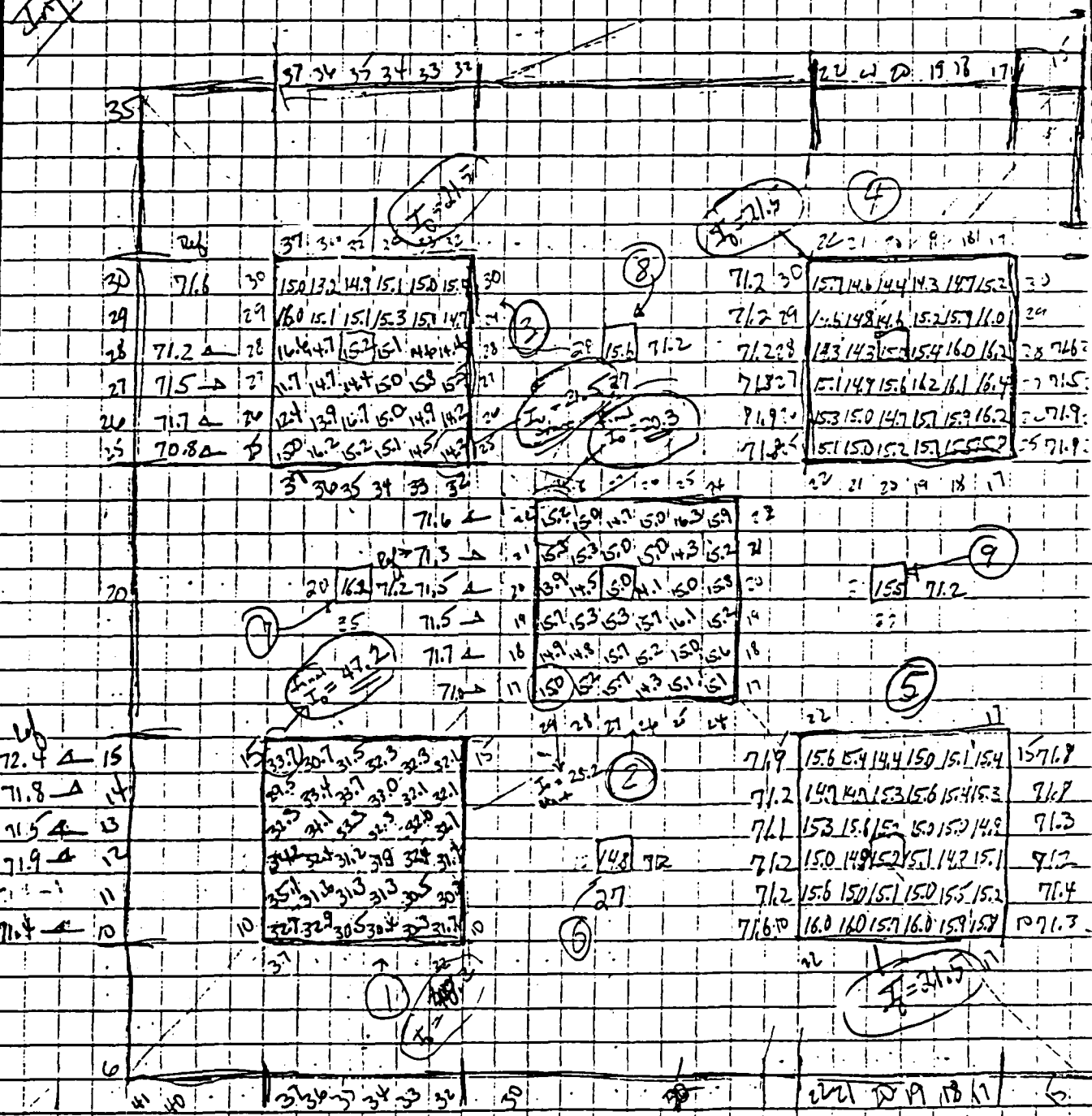
Invented by

Date

From Page No. 9-24-86

$I_0 = 48.2 \text{ mV}$
init

- ① Large Pinhole D625 $1/16$ " diameter det aperture
- ② Small Pinhole .037" pinhole



72.4 Δ 15
71.8 Δ 14
71.5 Δ 13
71.9 Δ 12
71.4 Δ 11
71.4 Δ 10

33.7 30.7 31.5 32.3 32.1
32.5 33.1 32.7 31.0 32.1 32.1
32.5 31.1 32.3 31.3 32.0 32.1
34.2 32.4 31.2 31.8 32.4 31.4
35.1 31.3 31.3 31.3 30.5 30.7
32.7 32.9 30.5 30.4 32.3 31.7

71.9 15.6 5.4 14.4 15.0 15.1 15.4 15.7 16.8
71.2 14.9 4.0 15.3 15.6 15.4 15.3 16.7
71.1 15.3 15.1 15.5 15.0 15.2 14.8 16.3
71.2 15.0 14.9 15.2 15.1 14.2 15.1 16.2
71.2 15.6 15.0 15.1 15.0 15.5 15.2 16.4
71.6 16.0 16.0 15.7 16.0 15.9 15.8 16.7

P. AS-11

To Page No. _____

Witnessed & Understood by me,	Date	Invented by	Date
		Recorded by	

Recorded by _____

52

Project No. _____

Book No. _____

TITLE _____

From Page No. 9-2586

DE86016-03-20

Chopper 200

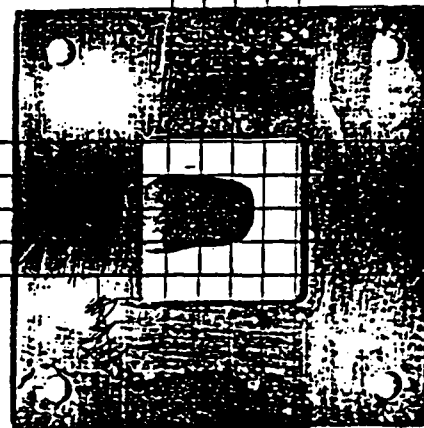
Layer 6mm

0.83 u - cm

4-251
80

CDS-1

35 30 25 20 15



DE86016-03-20



25

26

 $I_0 = 20.4$
 $y = 24, x = 30$
 $\begin{matrix} \rightarrow 72 \\ \leftarrow 72 \end{matrix}$

13.4	14.2	13.5	14.2	14.3
15.0	10.7	13.2	12.9	13.9

 $I_0 = 20.5$
 $y = 22, x = 32$
 $\begin{matrix} \rightarrow 72 \\ \leftarrow 72 \end{matrix}$

13.4	13.3	12.4	13.2	2.7
13.9	13.5	12.5	11.8	12.6

20

72

 $I_0 = 20.4$
 $y = 19, x = 34$
 $\begin{matrix} \rightarrow 72 \\ \leftarrow 72 \end{matrix}$

12.4	12.9	12.4	12.2	13.0
12.8	14.8	12.8	12.0	11.8

 $I_0 = 20.4$
 $y = 17, x = 32$
 $\begin{matrix} \rightarrow 73 \\ \leftarrow 72 \end{matrix}$

13.4	21.1	16.8	16.8	9.1
51.4	14.6	16.3	12.1	9.4

5

72

 $I_0 = 20.5$
 $y = 15, x = 30$
 $\begin{matrix} \rightarrow 72 \\ \leftarrow 72 \end{matrix}$

13.2	20.0	11.5	20.8	21.5
------	------	------	------	------

Guidance
mm

P. AS-13

To Page No. _____

Witnessed & Understood by me,

Date

Invented by

Date

Recorded by

11
TITLE

(53)

Project No.

CDS-2

From Page No.

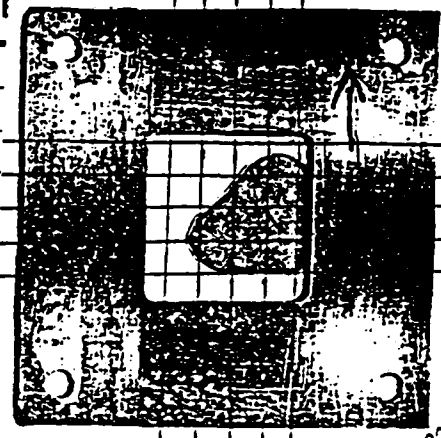
9-26-86

DM 86 197-23-09

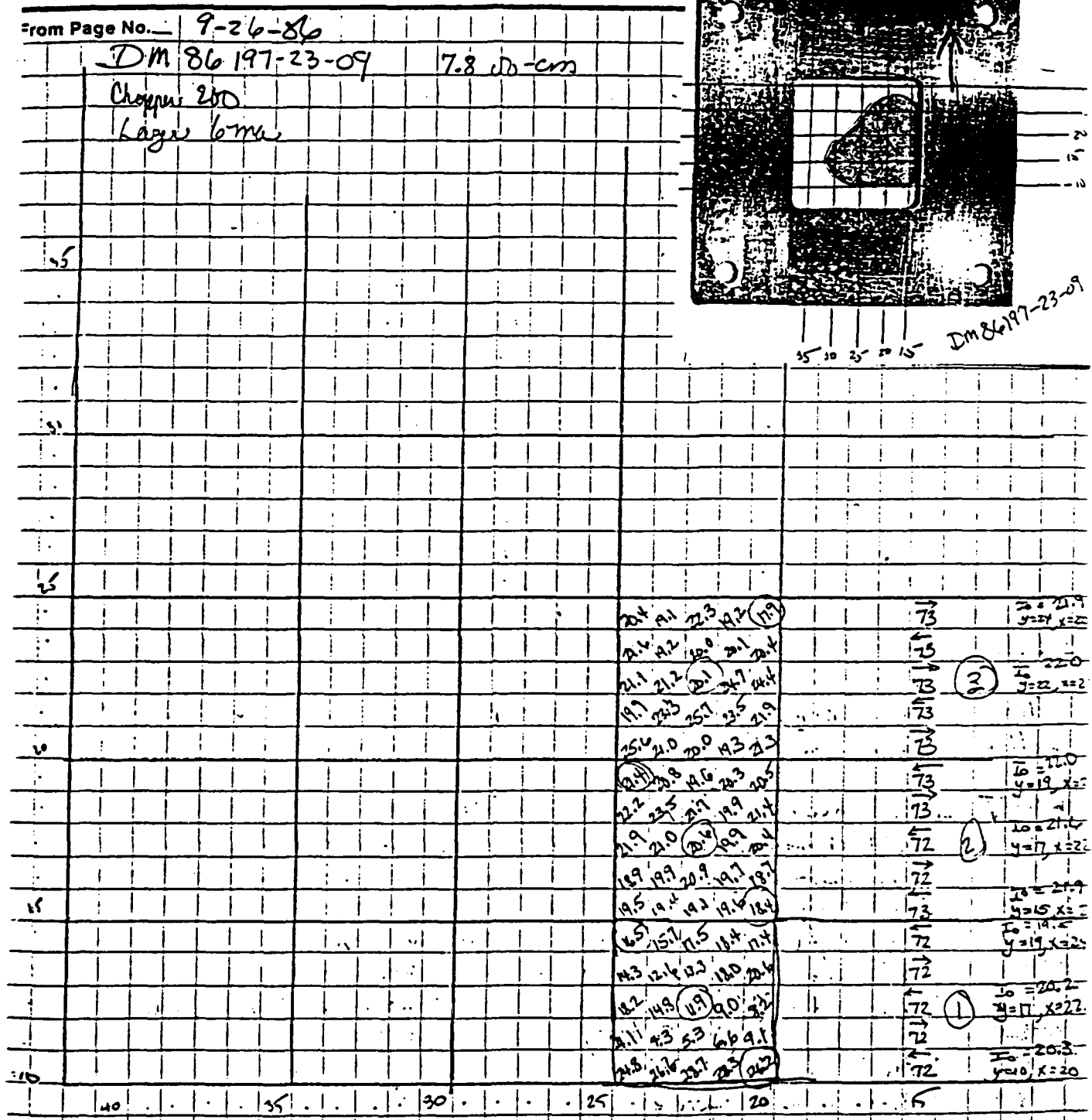
7.8 mm-cm

Chopper 250

Lager 6mm



DM 86 197-23-09



Witnessed & Understood by me,

Date

Invented by

Date

Recorded by

To Page No.

ATTACHMENT #6

HALL DATA

Page #	Content
A6-1	Photocopy of CdS Samples
A6-2	Electrical Data for CdS-1
A6-3	Electrical Data for CdS-2
A6-4	Electrical Data for CdS-3
A6-5	Photocopy of InP Hall Sample Sites
A6-6	Electrical Data for InP-1
A6-7	Electrical Data for InP-2
A6-8	Electrical Data for InP-3
A6-9	Electrical Data for InP-4
A6-10	Electrical Data for InP-5
A6-11	Photocopy of GaAs Hall Sample Sites
A6-12	Electrical Data for GaAs-A1
A6-13	Electrical Data for GaAs-A2
A6-14	Electrical Data for GaAs-A3
A6-15	Electrical Data for GaAs-B1
A6-16	Electrical Data for GaAs-B2
A6-17	Electrical Data for GaAs-B3



DE86016-03-20

(0.67 Ω -cm)

CDS-1



DM86197-23-09

(7.67 Ω -cm)

CDS-2



DP86213-02-04

(19.7 Ω -cm)

CDS-3

RESISTIVITY/HALL MOBILITY

DATE- 10/22/86 TIME- 12:32PM

MATERIAL- Cds-1

DE86016-03-20

LOT#- DE86016-03-20

THICKNESS= .055 cm

Contacts- In

Temp= 296 K

I= 1.000E-03 Amps

Bset= 3000 Gauss

Vr(1,1)= -.004047 Volts
Vr(1,2)= .003964 Volts
Vr(2,1)= -.001858 Volts
Vr(2,2)= .001749 Volts
Vr(3,1)= -.003934 Volts
Vr(3,2)= .004072 Volts
Vr(4,1)= -.001809 Volts
Vr(4,2)= .001795 Volts

Fa= .95

Fb= .95

Roa= 6.878E-01 ohm-cm

Rob= 6.874E-01 ohm-cm

Resistivity= 6.976E-01 ohm-cm

Vh(1,1)= .002398 Volts
Vh(1,2)= -.002245 Volts
Vh(2,1)= -.002035 Volts
Vh(2,2)= .002107 Volts
Vh(1,3)= .002156 Volts
Vh(1,4)= -.001991 Volts
Vh(2,3)= -.002288 Volts
Vh(2,4)= .00235 Volts

$$n = 2.75 \times 10^{16} / \text{cm}^3$$

Rhc= -2.264E+02 cm^3/coulomb

Mc= 3.293E+02 cm^2/v-sec

B+= 3017 Gauss

Rhd= -2.285E+02 cm^3/coulomb

Md= 3.324E+02 cm^2/v-sec

B-= 2982 Gauss

Rh= -2.275E+02 cm^3/coulomb

Mobility= 3.308E+02 cm^2/volt-second

DE86016-03-20

AD-A174 665

DEVELOPMENT OF A FREE CARRIER ABSORPTION MEASUREMENT
INSTRUMENT FOR INDIU (U) EAGLE-PICHER RESEARCH LAB
MIAMI OK SPECIALTY MATERIALS DIV 27 OCT 86

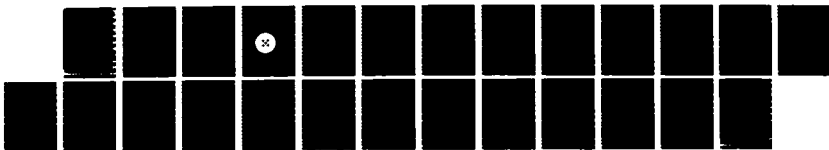
2/2

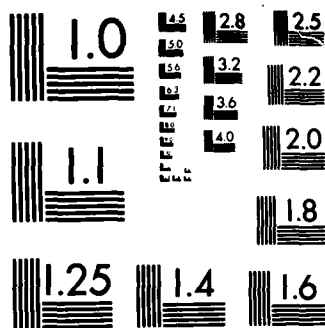
UNCLASSIFIED

N00014-85-C-2430

F/G 20/12

NL





MICROCOPY RESOLUTION TEST CHART
NATIONAL BUREAU OF STANDARDS-1963-A

RESISTIVITY/HALL MOBILITY

DATE- 10/22/86 TIME- 12:41PM

DM86197-23-09

MATERIAL- CdS-2

LOT#- DM86197-23-09

THICKNESS= .055 cm

Contacts- In

Temp= 296 K

I= 1.000E-04 Amps

Bset= 3000 Gauss

Vr(2,1)= -.003649 Volts
 Vr(2,2)= .003553 Volts
 Vr(3,1)= -.002539 Volts
 Vr(3,2)= .002693 Volts
 Vr(4,1)= -.003625 Volts
 Vr(4,2)= .003569 Volts

Fa= .99

Fb= .99

Roa= 7.671E+00 ohm-cm

Rob= 7.666E+00 ohm-cm

Resistivity= 7.669E+00 ohm-cm

Vh(1,1)= -.0007559 Volts
 Vh(1,2)= .000898 Volts
 Vh(2,1)= .001165 Volts
 Vh(2,2)= -.001108 Volts
 Vh(1,3)= -.001057 Volts
 Vh(1,4)= .001209 Volts
 Vh(2,3)= .0008527 Volts
 Vh(2,4)= -.0007995 Volts

$$n = 2.21 \times 10^{15} / \text{cm}^3$$

Rhc= -2.793E+03 cm^3/coulomb

Mc= 3.642E+02 cm^2/v-sec

B+= 3013 Gauss

Rhd= -2.868E+03 cm^3/coulomb

Md= 3.740E+02 cm^2/v-sec

B-= 2980 Gauss

Rh= -2.831E+03 cm^3/coulomb

Mobility= 3.691E+02 cm^2/volt-second

DM86197-23-09

RESISTIVITY/HALL MOBILITY

DATE- 10/22/86 TIME- 12:49PM

DP86213-02-04

MATERIAL- Cds-3

LOT#- DP86213-02-04

THICKNESS= .055 cm

Contacts- In

Temp= 296 K

I= 1.000E-04 Amps

Bset= 3000 Gauss

Vr(1,1)= -.007008 Volts
 Vr(1,2)= .006932 Volts
 Vr(2,1)= -.009042 Volts
 Vr(2,2)= .008933 Volts
 Vr(3,1)= -.006884 Volts
 Vr(3,2)= .007047 Volts
 Vr(4,1)= -.009007 Volts
 Vr(4,2)= .008952 Volts

Fa= .99

Fb= .99

Roa= 1.969E+01 ohm-cm

Rob= 1.968E+01 ohm-cm

Resistivity= 1.968E+01 ohm-cm

Vh(1,1)= -.001526 Volts
 Vh(1,2)= .001656 Volts
 Vh(2,1)= .002477 Volts
 Vh(2,2)= -.00241 Volts
 Vh(1,3)= -.002364 Volts
 Vh(1,4)= .002505 Volts
 Vh(2,3)= .001627 Volts
 Vh(2,4)= -.001563 Volts

$$n = 8.05 \times 10^{14} / \text{cm}^3$$

Rhc= -7.691E+03 cm^3/coulomb

Mc= 3.908E+02 cm^2/v-sec

B+= 3015 Gauss

Rhd= -7.829E+03 cm^3/coulomb

Md= 3.978E+02 cm^2/v-sec

B-= 2981 Gauss

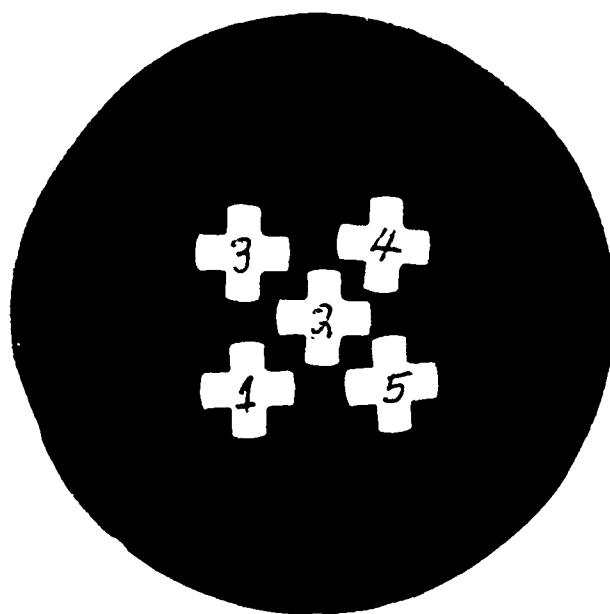
Rh= -7.760E+03 cm^3/coulomb

Mobility= 3.943E+02 cm^2/volt-second

DP86213-02-04

f

1



RESISTIVITY/HALL MOBILITY

DATE- 9/26/86

TIME- 2:57PM

FEA WAFER #1

MATERIAL- InP

LOT#- FEA WAFER #1

THICKNESS= .06 cm

Contacts- In

Temp= 296 K

I= 1.000E-02 Amps

Bset= 5000 Gauss

Vr(1,1)= -.002156 Volts
 Vr(1,2)= .002009 Volts
 Vr(2,1)= -.002171 Volts
 Vr(2,2)= .002054 Volts
 Vr(3,1)= -.001982 Volts
 Vr(3,2)= .002182 Volts
 Vr(4,1)= -.002152 Volts
 Vr(4,2)= .002076 Volts

Fa= 1

Fb= 1

Roa= 5.704E-02 ohm-cm

Rob= 5.706E-02 ohm-cm

Resistivity= 5.705E-02 ohm-cm

Vh(1,1)= .001899 Volts
 Vh(1,2)= -.001723 Volts
 Vh(2,1)= .001923 Volts
 Vh(2,2)= -.001834 Volts
 Vh(1,3)= -.001787 Volts
 Vh(1,4)= .001967 Volts
 Vh(2,3)= -.001763 Volts
 Vh(2,4)= .001849 Volts

$$n = 2.84 \times 10^{16} / \text{cm}^3$$

Rhc= -2.208E+02 cm^3/coulomb

Mc= 3.870E+03 cm^2/v-sec

B+= 5004 Gauss

Rhd= -2.197E+02 cm^3/coulomb

Md= 3.852E+03 cm^2/v-sec

B-= 5031 Gauss

Rh= -2.203E+02 cm^3/coulomb

Mobility= 3.861E+03 cm^2/volt-second

$$n = 2.84 \times 10^{16} / \text{cm}^3$$

FEA WAFER #1

RESISTIVITY/HALL MOBILITY

DATE- 9/26/86

TIME- 1:57PM

FEA WAFER- #2

MATERIAL- InP

LOT#- FEA WAFER- #2

THICKNESS= .06 cm

Contacts- In

Temp= 296 K

I= 1.000E-02 Amps

Bset= 5000 Gauss

FEA WAFER- #2

Vr(1,1)= -.00199 Volts
 Vr(1,2)= .001955 Volts
 Vr(2,1)= -.001988 Volts
 Vr(2,2)= .001951 Volts
 Vr(3,1)= -.001931 Volts
 Vr(3,2)= .002022 Volts
 Vr(4,1)= -.001981 Volts
 Vr(4,2)= .001962 Volts

Fa= 1

Fb= 1

Roa= 5.360E-02 ohm-cm

Rob= 5.368E-02 ohm-cm

Resistivity= 5.364E-02 ohm-cm

Vh(1,1)= .001947 Volts
 Vh(1,2)= -.001856 Volts
 Vh(2,1)= .001906 Volts
 Vh(2,2)= -.001882 Volts
 Vh(1,3)= -.001847 Volts
 Vh(1,4)= .001962 Volts
 Vh(2,3)= -.001896 Volts
 Vh(2,4)= .001929 Volts

$$n = 3.0 \times 10^{16} / \text{cm}^3$$

Rhc= -2.098E+02 cm^3/coulomb

Mc= 3.911E+03 cm^2/v-sec

B+= 5442 Gauss

Rhd= -2.075E+02 cm^3/coulomb

Md= 3.868E+03 cm^2/v-sec

B-= 5505 Gauss

Rh= -2.086E+02 cm^3/coulomb

Mobility= 3.890E+03 cm^2/volt-second

$$n = 3.0 \times 10^{16} / \text{cm}^3$$

RESISTIVITY/HALL MOBILITY

DATE- 9/26/86

TIME- 2:06PM

FEA WAFER- #3

MATERIAL- InP

LOT#- FEA WAFER- #3

THICKNESS= .06 cm

Contacts- In

Temp= 296 K

I= 1.000E-02 Amps

Bset= 5000 Gauss

FEA WAFER- #3

Vr(1,1)= -.002193 Volts
 Vr(1,2)= .002092 Volts
 Vr(2,1)= -.002186 Volts
 Vr(2,2)= .002111 Volts
 Vr(3,1)= -.002061 Volts
 Vr(3,2)= .002229 Volts
 Vr(4,1)= -.002177 Volts
 Vr(4,2)= .002113 Volts

Fa= 1

Fb= 1

Roa= 5.834E-02 ohm-cm

Rob= 5.833E-02 ohm-cm

Resistivity= 5.834E-02 ohm-cm

Vh(1,1)= .00211 Volts
 Vh(1,2)= -.00197 Volts
 Vh(2,1)= .002089 Volts
 Vh(2,2)= -.002017 Volts
 Vh(1,3)= -.001985 Volts
 Vh(1,4)= .002142 Volts
 Vh(2,3)= -.002018 Volts
 Vh(2,4)= .002087 Volts

$$n = 2.78 \times 10^{16} / \text{cm}^3$$

Rhc= -2.258E+02 cm^3/coulomb

Mc= 3.870E+03 cm^2/v-sec

B+= 5453 Gauss

Rhd= -2.237E+02 cm^3/coulomb

Md= 3.835E+03 cm^2/v-sec

B-= 5506 Gauss

Rh= -2.247E+02 cm^3/coulomb

Mobility= 3.852E+03 cm^2/volt-second

$$n = 2.78 \times 10^{16} / \text{cm}^3$$

RESISTIVITY/HALL MOBILITY

DATE- 9/26/86 TIME- 2:39PM

FEA WAFER #4

MATERIAL- InP

LOT#- FEA WAFER #4

THICKNESS- .06 cm

Contacts- In

Temp= 296 K

I= 1.000E-02 Amps

Bset= 5000 Gauss

FEA WAFER #4

Vr(1,1)= -.002099 Volts
 Vr(1,2)= .001982 Volts
 Vr(2,1)= -.002074 Volts
 Vr(2,2)= .002017 Volts
 Vr(3,1)= -.001953 Volts
 Vr(3,2)= .002125 Volts
 Vr(4,1)= -.002082 Volts
 Vr(4,2)= .002005 Volts

Fa= 1

Fb= 1

Roa= 5.556E-02 ohm-cm

Rob= 5.551E-02 ohm-cm

Resistivity= 5.554E-02 ohm-cm

$$n = 2.90 \times 10^{16} / \text{cm}^3$$

Vh(1,1)= .001879 Volts
 Vh(1,2)= -.001711 Volts
 Vh(2,1)= .001816 Volts
 Vh(2,2)= -.001794 Volts
 Vh(1,3)= -.0017 Volts
 Vh(1,4)= .001873 Volts
 Vh(2,3)= -.001762 Volts
 Vh(2,4)= .001792 Volts

Rhc= -2.150E+02 cm³/coulombMc= 3.871E+03 cm²/v-sec

B+= 4999 Gauss

Rhd= -2.158E+02 cm³/coulombMd= 3.886E+03 cm²/v-sec

B-= 4980 Gauss

Rh= -2.154E+02 cm³/coulombMobility= 3.878E+03 cm²/volt-second

$$n = 2.90 \times 10^{16} / \text{cm}^3$$

RESISTIVITY/HALL MOBILITY

DATE- 9/26/86 TIME- 2:47PM

MATERIAL- InP

FEA WAFER- #5

LOT#- FEA WAFER- #5

THICKNESS= .06 cm

Contacts- In

Temp= 296 K

I= 1.000E-02 Amps

Bset= 5000 Gauss

Vr(1,1)= -.002158 Volts
 Vr(1,2)= .002042 Volts
 Vr(2,1)= -.002144 Volts
 Vr(2,2)= .002064 Volts
 Vr(3,1)= -.002003 Volts
 Vr(3,2)= .002193 Volts
 Vr(4,1)= -.002146 Volts
 Vr(4,2)= .002062 Volts

Fa= 1

Fb= 1

Roa= 5.716E-02 ohm-cm

Rob= 5.714E-02 ohm-cm

Resistivity= 5.715E-02 ohm-cm

Vh(1,1)= .001924 Volts
 Vh(1,2)= -.001767 Volts
 Vh(2,1)= .00188 Volts
 Vh(2,2)= -.001841 Volts
 Vh(1,3)= -.001753 Volts
 Vh(1,4)= .001925 Volts
 Vh(2,3)= -.001803 Volts
 Vh(2,4)= .00185 Volts

$$n = 2.82 \times 10^{16} / \text{cm}^3$$

Rhc= -2.209E+02 cm^3/coulomb

Mc= 3.865E+03 cm^2/v-sec

B+= 5004 Gauss

Rhd= -2.221E+02 cm^3/coulomb

Md= 3.885E+03 cm^2/v-sec

B-= 4981 Gauss

Rh= -2.215E+02 cm^3/coulomb

Mobility= 3.875E+03 cm^2/volt-second

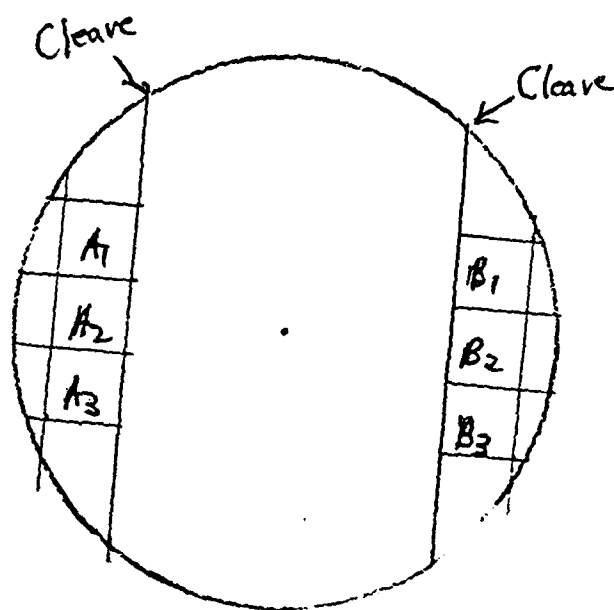
$$n = 2.82 \times 10^{16} / \text{cm}^3$$

FEA WAFER- #5

GaAs FEA Sample

0.060 cm Thick
chem/mechanical Polish

10-16-86
Mike Shaw



	ρ	μ	n
A ₁	$1.38 \times 10^4 \text{ g/cm}^3$	$3.42 \times 10^3 \text{ cm}^2/\text{Vs}$	$1.32 \times 10^{11}/\text{cm}^3$
A ₂	$2.01 \times 10^4 \text{ g/cm}^3$	$2.86 \times 10^3 \text{ cm}^2/\text{Vs}$	$1.08 \times 10^{11}/\text{cm}^3$
A ₃	$1.54 \times 10^4 \text{ g/cm}^3$	$3.44 \times 10^3 \text{ cm}^2/\text{Vs}$	$1.18 \times 10^{11}/\text{cm}^3$
	$2.50 \times 10^4 \text{ g/cm}^3$	$2.83 \times 10^3 \text{ cm}^2/\text{Vs}$	$8.83 \times 10^{10}/\text{cm}^3$
B ₁	$1.87 \times 10^4 \text{ g/cm}^3$	$6.98 \times 10^3 \text{ cm}^2/\text{Vs}$	$4.78 \times 10^{10}/\text{cm}^3$
B ₂	$2.49 \times 10^5 \text{ g/cm}^3$	$4.19 \times 10^3 \text{ cm}^2/\text{Vs}$	$5.79 \times 10^9/\text{cm}^3$
B ₃	$1.46 \times 10^4 \text{ g/cm}^3$	$3.84 \times 10^3 \text{ cm}^2/\text{Vs}$	$1.11 \times 10^{11}/\text{cm}^3$

RESISTIVITY/HALL MOBILITY

DATE: 9/18/ 86 TIME: 9:56.13

LOT #- 3300081-A1

MATERIAL TYPE- GaAs

THICKNESS= 0.060 cm

TEMP(K)= 296

I= 1.00E-06

Bsat= 5000 GAUSS

Vr(1,1)=-0.0501628 volts

Vr(1,2)= 0.0671019 volts

Vr(2,1)=-0.0350441 volts

Vr(2,2)= 0.0492447 volts

Vr(3,1)=-0.0707232 volts

Vr(3,2)= 0.0571253 volts

Vr(4,1)=-0.0440278 volts

Vr(4,2)= 0.0389428 volts

Fa=0.99 Fb=0.98

Roa= 1.36E+04 Rob= 1.40E+04

Resistivity= 1.38E+04 ohm-cm

Vh(1,1)= 0.0580377 volts

Vh(1,2)=-0.0642979 volts

Vh(2,1)=-0.0018663 volts

Vh(2,2)=-0.0366178 volts

Vh(1,3)=-0.0183204 volts

Vh(1,4)= 0.0155998 volts

Vh(2,3)=-0.0813092 volts

Vh(2,4)= 0.0433654 volts

$$n = 1.32 \times 10^{18} / \text{cm}^3$$

Rhc=-4.685E+07 Muc= 3.393E+03 +B=5003

Rhd=-4.759E+07 Mud= 3.447E+03 -B=5025

Rh=-4.722E+07 cm^3/coulomb

Mobility= 3.420E+03 cm^2/volt-sec

RESISTIVITY/HALL MOBILITY

DATE: 9/18/ 86 TIME: 8:58.79

LOT #- 3300081-A2

MATERIAL TYPE- GaAs

THICKNESS= 0.060 cm

TEMP(K)= 296

I= 1.00E-07

Bset= 5000 GAUSS

Vr(1,1)=-0.0022831 volts

Vr(1,2)= 0.0017783 volts

Vr(2,1)=-0.0172380 volts

Vr(2,2)= 0.0198334 volts

Vr(3,1)=-0.0030569 volts

Vr(3,2)= 0.0010635 volts

Vr(4,1)=-0.0188091 volts

Vr(4,2)= 0.0186515 volts

Fa=0.71 Fb=0.72

Roa= 1.99E+04 Rob= 2.04E+04

Resistivity= 2.01E+04 ohm-cm

Vh(1,1)=-0.0124911 volts

Vh(1,2)= 0.0132339 volts

Vh(2,1)= 0.0212315 volts

Vh(2,2)=-0.0234890 volts

Vh(1,3)=-0.0220450 volts

Vh(1,4)= 0.0230755 volts

Vh(2,3)= 0.0117816 volts

Vh(2,4)=-0.0139085 volts

Rhc=-5.811E+07 Muc= 2.890E+03 +B=5007

Rhd=-5.693E+07 Mud= 2.832E+03 -B=5015

Rh=-5.752E+07 cm^3/coulomb

Mobility= 2.861E+03 cm^2/volt-sec

$$n = 1.08 \times 10^{11} / \text{cm}^3$$

RESISTIVITY/HALL MOBILITY

DATE: 9/18/ 86 TIME: 9:31.5

LOT #- 3300081-A3

MATERIAL TYPE- GaAs

THICKNESS= 0.060 cm

TEMP(K)= 296

I= 1.00E-06

Bsat= 5000 GAUSS

Vr(1,1)=-0.0595898 volts

Vr(1,2)= 0.0642874 volts

Vr(2,1)=-0.0492702 volts

Vr(2,2)= 0.0531784 volts

Vr(3,1)=-0.0677472 volts

Vr(3,2)= 0.0584884 volts

Vr(4,1)=-0.0525705 volts

Vr(4,2)= 0.0523771 volts

Fa=0.99 Fb=0.99

Roa= 1.52E+04 Rob= 1.56E+04

Resistivity= 1.54E+04 ohm-cm

Vh(1,1)= 0.0498088 volts

Vh(1,2)=-0.0599107 volts

Vh(2,1)= 0.0257715 volts

Vh(2,2)=-0.0324392 volts

Vh(1,3)=-0.0364434 volts

Vh(1,4)= 0.0296412 volts

Vh(2,3)=-0.0627377 volts

Vh(2,4)= 0.0564539 volts

$$n = 1.18 \times 10^{11} / \text{cm}^3$$

Rhc=-5.286E+07 Muc= 3.433E+03 +B=4989

Rhd=-5.313E+07 Mud= 3.450E+03 -B=5009

Rh=-5.299E+07 cm^3/coulomb

Mobility= 3.442E+03 cm^2/volt-sec

RESISTIVITY/HALL MOBILITY

DATE: 9/18/ 86 TIME: 10:29.67

LOT #- 3300081-B1

MATERIAL TYPE- GaAs

THICKNESS= 0.060 cm

TEMP(K)= 296

I= 1.00E-07

Bset= 5000 GAUSS

Vr(1,1)=-0.0059434 volts

Vr(1,2)= 0.0040925 volts

Vr(2,1)=-0.0089946 volts

Vr(2,2)= 0.0110160 volts

Vr(3,1)=-0.0094158 volts

Vr(3,2)= 0.0019011 volts

Vr(4,1)=-0.0077167 volts

Vr(4,2)= 0.0311983 volts

Fa=0.96 Fb=0.89

Roa= 1.96E+04 Rob= 3.04E+04

Resistivity= 2.50E+04 ohm-cm

Vh(1,1)=-0.0027103 volts

Vh(1,2)=-0.0006171 volts

Vh(2,1)= 0.0288128 volts

Vh(2,2)=-0.0105760 volts

Vh(1,3)=-0.0137851 volts

Vh(1,4)= 0.0116723 volts

Vh(2,3)= 0.0161949 volts

Vh(2,4)= 0.0007680 volts

$$n = 8.83 \times 10^{10} / \text{cm}^3$$

Rhc=-6.996E+07 Muc= 2.798E+03 +B=5010

Rhd=-7.146E+07 Mud= 2.858E+03 -B=5031

Rh=-7.071E+07 cm^3/coulomb

Mobility= 2.828E+03 cm^2/volt-sec

RESISTIVITY/HALL MOBILITY

DATE: 9/18/ 86 TIME: 10:42.33

LOT #- 3300081-B2

MATERIAL TYPE- GaAs

THICKNESS= 0.060 cm

TEMP(K)= 296

I= 1.00E-08

Bsat= 5000 GAUSS

Vr(1,1)=-0.0232332 volts

Vr(1,2)= 0.0088491 volts

Vr(2,1)=-0.0018086 volts

Vr(2,2)= 0.0067191 volts

Vr(3,1)=-0.0123550 volts

Vr(3,2)= 0.0229757 volts

Vr(4,1)=-0.0043160 volts

Vr(4,2)= 0.0044830 volts

Fa=0.87 Fb=0.86

Roa= 2.40E+05 Rob= 2.58E+05

Resistivity= 2.49E+05 ohm-cm

Vh(1,1)= 0.0335859 volts

Vh(1,2)=-0.0169514 volts

Vh(2,1)=-0.0022388 volts

Vh(2,2)= 0.0150121 volts

Vh(1,3)= 0.0184366 volts

Vh(1,4)= 0.0007944 volts

Vh(2,3)=-0.0200140 volts

Vh(2,4)= 0.0331684 volts

$$n = 5.99 \times 10^9 / \text{cm}^3$$

Rhc=-1.006E+09 Muc= 4.038E+03 +B=4906

Rhd=-1.081E+09 Mud= 4.338E+03 -B=4988

Rh=-1.043E+09 cm^3/coulomb

Mobility= 4.188E+03 cm^2/volt-sec

RESISTIVITY/HALL MOBILITY

DATE: 9/18/ 86 TIME: 9:43.65

LOT #- 3300081-B3

MATERIAL TYPE- GaAs

THICKNESS= 0.060 cm

TEMP(K)= 296

I= 1.00E-06

Bset= 5000 GAUSS

Vr(1,1)=-0.0502822 volts
Vr(1,2)= 0.0567188 volts
Vr(2,1)=-0.0201842 volts
Vr(2,2)= 0.0589700 volts
Vr(3,1)=-0.0652197 volts
Vr(3,2)= 0.0926795 volts
Vr(4,1)=-0.0409547 volts
Vr(4,2)= 0.0431467 volts

Fa=0.99 Fb=0.97

Roa= 1.32E+04 Rob= 1.60E+04

Resistivity= 1.46E+04 ohm-cm

Vh(1,1)= 0.1274415 volts
Vh(1,2)=-0.0749840 volts
Vh(2,1)= 0.0160625 volts
Vh(2,2)=-0.0577560 volts
Vh(1,3)= 0.0298768 volts
Vh(1,4)= 0.0216091 volts
Vh(2,3)=-0.0600649 volts
Vh(2,4)= 0.0259571 volts

$$n = 6.11 \times 10^{11} / \text{cm}^3$$

Rhc=-5.817E+07 Muc= 3.989E+03 +B=5033

Rhd=-5.389E+07 Mud= 3.696E+03 -B=5006

Rh=-5.603E+07 cm^3/coulomb

Mobility= 3.843E+03 cm^2/volt-sec

ATTACHMENT #7

FEA Data and Free Electron Density Maps

Page #	Content
A7-1	Results for Sample CdS-1
A6-2	Results for Sample CdS-2
A7-3	Results for Sample CdS-3
A7-4	Results for Sample InP-1
A7-5	Results for Sample InP-2
A7-6	Results for Sample InP-3
A7-7	Results for Sample InP-4
A7-8	Results for Sample InP-5

FILE: CDS1

SAMPLE= DEB6016-03-20

I0= 20.5 Tas(3micron)= 73.0%ALPHA8D(AVE)= .405 C(ave)= 1.47E-17

R12= .1561 Tas(10.6micron)= 48.0%N(ave)= 2.75E+16

DATA	13.4	14.2	13.5	14.2	14.3	BETA	.916	.928	.918	.928	.930
	15.0	13.7	13.2	12.9	13.9		.941	.921	.913	.909	.924
	13.6	13.3	12.4	13.2	12.7		.919	.915	.901	.913	.906
	13.9	13.5	12.5	11.8	12.6		.924	.918	.903	.892	.904
	13.4	12.9	12.8	11.8	11.5		.916	.909	.907	.892	.887
	12.4	12.9	12.6	12.2	13.0		.901	.909	.904	.898	.910
	12.8	14.8	12.8	12.0	11.8		.907	.938	.907	.895	.892
	23.4	27.1	15.8	16.8	9.1		1.069	1.125	.953	.968	.851
	5.6	4.6	6.3	8.1	8.4		.797	.782	.808	.836	.840
	13.2	20.0	27.5	26.0	24.5		.913	1.017	1.131	1.108	1.085

Z T	65.4%	69.3%	65.9%	69.3%	69.8%EXP	.722	.756	.727	.756	.761
	73.2%	66.8%	64.4%	62.9%	67.8%	.790	.735	.714	.701	.744
	66.3%	64.9%	60.5%	64.4%	62.0%	.731	.718	.679	.714	.692
	67.8%	65.9%	61.0%	57.6%	61.5%	.744	.727	.683	.652	.688
	65.4%	62.9%	62.4%	57.6%	56.1%	.722	.701	.696	.652	.638
	60.5%	62.9%	61.5%	59.5%	63.4%	.679	.701	.688	.670	.705
	62.4%	72.2%	62.4%	58.5%	57.6%	.696	.781	.696	.661	.652
	114.1%	132.2%	77.1%	82.0%	44.4%	1.100	1.218	.822	.862	.525
	27.3%	22.4%	30.7%	39.5%	41.0%	.344	.287	.382	.475	.491
	64.4%	97.6%	134.1%	126.8%	119.5%	.714	.982	1.230	1.184	1.136

ALPHA8D	.325	.279	.319	.279	.274	n	2.20E+16	1.89E+16	2.16E+16	1.89E+16	1.86E+16
	.236	.307	.337	.355	.296		1.60E+16	2.09E+16	2.29E+16	2.41E+16	2.01E+16
	.313	.331	.387	.337	.368		2.12E+16	2.25E+16	2.63E+16	2.29E+16	2.50E+16
	.296	.319	.381	.428	.374		2.01E+16	2.16E+16	2.58E+16	2.90E+16	2.54E+16
	.325	.355	.362	.428	.449		2.20E+16	2.41E+16	2.45E+16	2.90E+16	3.04E+16
	.387	.355	.374	.401	.349		2.63E+16	2.41E+16	2.54E+16	2.72E+16	2.37E+16
	.362	.247	.362	.414	.428		2.45E+16	1.67E+16	2.45E+16	2.81E+16	2.90E+16
	-.095	-.197	.196	.149	.644		1.33E+16	1.01E+16	4.37E+16		
	1.068	1.247	.963	.743	.712		7.25E+16	8.46E+16	6.53E+16	5.04E+16	4.83E+16
	.337	.018	-.207	-.169	-.127		2.29E+16	1.23E+15			

FILE: CDS2

SAMPLE= DM86197-23-09

I0= 21.9 Tas(3micron)= 73.0%ALPHA#D(AVE)= .405 C(ave)= 1.47E-17

R12= .1561 Tas(10.6micron)= 48.0%Zn(ave)= 2.75E+16

DATA	20.4	19.1	22.3	19.2	17.9	BETA	1.003	.984	1.030	.986	.967
	21.6	19.2	20.0	20.1	20.4		1.020	.986	.997	.999	1.003
	21.1	21.2	20.1	24.7	24.4		1.013	1.014	.999	1.064	1.060
	19.9	23.3	25.7	23.5	21.9		.996	1.044	1.079	1.047	1.024
	25.6	21.0	20.0	19.3	21.3		1.077	1.012	.997	.987	1.016
	21.4	20.8	19.6	20.3	20.5		1.017	1.009	.992	1.002	1.004
	22.2	23.5	21.7	19.9	21.4		1.029	1.047	1.022	.996	1.017
	21.9	21.0	20.6	19.9	20.4		1.024	1.012	1.006	.996	1.003
	18.9	19.9	20.9	19.7	18.7		.982	.996	1.010	.993	.979
	19.5	19.4	19.1	19.6	18.4		.990	.989	.984	.992	.974

Z T	93.2%	87.2%	101.8%	87.7%	81.7%	EXP	.949	.904	1.013	.907	.860
	98.6%	87.7%	91.3%	91.8%	93.2%		.990	.907	.935	.939	.949
	96.3%	96.8%	91.8%	112.8%	111.4%		.973	.976	.939	1.090	1.081
	90.9%	106.4%	117.4%	107.3%	100.0%		.932	1.046	1.121	1.052	1.000
	116.9%	95.9%	91.3%	88.1%	97.3%		1.118	.970	.935	.911	.980
	97.7%	95.0%	89.5%	92.7%	93.6%		.983	.963	.921	.946	.953
	101.4%	107.3%	99.1%	90.9%	97.7%		1.010	1.052	.993	.932	.983
	100.0%	95.9%	94.1%	90.9%	93.2%		1.000	.970	.956	.932	.949
	86.3%	90.9%	95.4%	90.0%	85.4%		.896	.932	.966	.925	.889
	89.0%	88.6%	87.2%	89.5%	84.0%		.918	.914	.904	.921	.878

ALPHA#D	.052	.101	-.013	.098	.151	n	3.54E+15	6.88E+15	*****	6.61E+15	1.02E+16
	.010	.098	.067	.063	.052		6.84E+14	6.61E+15	4.54E+15	4.29E+15	3.54E+15
	.027	.024	.063	-.087	-.078		1.85E+15	1.61E+15	4.29E+15	*****	*****
	.071	-.045	-.115	-.051	.000		4.79E+15	*****	*****	*****	3.01E+01
	-.112	.031	.067	.094	.020		*****	2.09E+15	4.54E+15	6.35E+15	1.38E+15
	.017	.038	.082	.056	.049		1.15E+15	2.57E+15	5.56E+15	3.79E+15	3.30E+15
	-.010	-.051	.007	.071	.017		*****	*****	4.55E+14	4.79E+15	1.15E+15
	.000	.031	.045	.071	.052		3.01E+01	2.09E+15	3.05E+15	4.79E+15	3.54E+15
	.109	.071	.034	.078	.117		7.42E+15	4.79E+15	2.33E+15	5.31E+15	7.96E+15
	.086	.090	.101	.082	.130		5.82E+15	6.09E+15	6.88E+15	5.56E+15	8.79E+15

FILE: C053

SAMPLE= DP86213-02-04

I0= 20.5 Tas(3micron)= 73.0%ALPHA#D(AVE)= .405 C(ave)= 1.47E-17

R12= .1561 Tas(10.6micron)= 48.0%Zn(ave)= 2.75E+16

DATA	20.5	21.7	20.9	20.5	25.5	BETA	1.024	1.043	1.030	1.024	1.100
	20.2	20.3	21.2	21.2	21.7		1.020	1.021	1.035	1.035	1.043
	19.7	19.4	21.0	19.7	19.7		1.012	1.008	1.032	1.012	1.012
	19.0	19.2	20.5	18.9	21.7		1.002	1.005	1.024	1.000	1.043
	18.7	20.0	18.9	15.0	26.2		.997	1.017	1.000	.941	1.111
	18.4	19.2	20.3	18.8	22.7		.992	1.005	1.021	.998	1.058
	21.3	20.0	18.8	18.9	18.7		1.037	1.017	.998	1.000	.997
	19.8	20.2	20.2	18.7	18.8		1.014	1.020	1.020	.997	.998
	19.4	17.8	17.4	17.8	25.5		1.008	.983	.977	.983	1.100
	19.1	20.3	20.5	21.9	31.9		1.003	1.021	1.024	1.046	1.198

Z T	100.0%	105.9%	102.0%	100.0%	124.4%	EXP	1.000	1.042	1.014	1.000	1.168
	98.5%	99.0%	103.4%	103.4%	105.9%		.989	.993	1.025	1.025	1.042
	96.1%	94.6%	102.4%	96.1%	96.1%		.971	.960	1.018	.971	.971
	92.7%	93.7%	100.0%	92.2%	105.9%		.946	.953	1.000	.942	1.042
	91.2%	97.6%	92.2%	73.2%	127.8%		.934	.982	.942	.790	1.190
	89.8%	93.7%	99.0%	91.7%	110.7%		.923	.953	.993	.938	1.076
	103.9%	97.6%	91.7%	92.2%	91.2%		1.028	.982	.938	.942	.934
	96.6%	98.5%	98.5%	91.2%	91.7%		.975	.989	.989	.934	.938
	94.6%	86.8%	84.9%	86.8%	124.4%		.960	.901	.885	.901	1.168
	93.2%	99.0%	100.0%	106.8%	155.6%		.949	.993	1.000	1.049	1.357

ALPHA#D	.000	-.041	-.014	.000	-.155	n	3.01E+01	*****	3.01E+01	*****
	.011	.007	-.024	-.024	-.041		7.31E+14	4.86E+14	*****	*****
	.029	.041	-.018	.029	.029		1.98E+15	2.75E+15	*****	1.98E+15 1.98E+15
	.056	.048	.000	.060	-.041		3.80E+15	3.27E+15	3.01E+01	4.06E+15 *****
	.068	.018	.060	.236	-.174		4.60E+15	1.23E+15	4.06E+15	1.60E+16 *****
	.080	.048	.007	.064	-.074		5.42E+15	3.27E+15	4.86E+14	4.33E+15 *****
	-.028	.018	.064	.060	.068		*****	1.23E+15	4.33E+15	4.06E+15 4.60E+15
	.025	.011	.011	.068	.064		1.73E+15	7.31E+14	7.31E+14	4.60E+15 4.33E+15
	.041	.105	.122	.105	-.155		2.75E+15	7.11E+15	8.27E+15	7.11E+15 *****
	.052	.007	.000	-.048	-.305		3.53E+15	4.86E+14	3.01E+01	*****

FILE: INP1

SAMPLE= Y=10 TO 15 : X=32 TO 37

I0= 47.2 Tas(3micron)= 58.0% ALPHA&D(AVE)= .096 C(ave)= 3.35E-18

R12= .2658 Tas(10.6micron)= 52.0% n(ave)= 2.87E+16

DATA	33.7	30.7	31.5	32.3	32.3	32.1	BETA	.919	.885	.894	.903	.903
	29.5	33.4	33.7	33.0	32.1	32.1		.871	.915	.919	.911	.901
	32.3	34.1	33.3	32.3	32.6	32.7		.903	.923	.914	.903	.906
	34.2	32.4	31.2	31.9	32.4	31.7		.924	.904	.890	.898	.904
	35.1	31.6	31.3	31.3	30.5	30.2		.934	.895	.892	.892	.883
	32.7	32.9	30.5	30.4	30.3	31.7		.907	.910	.883	.881	.880

Z T	71.4%	65.0%	66.7%	68.4%	68.4%	68.0%	EXP	.814	.766	.779	.792	.792
	62.5%	70.8%	71.4%	69.9%	68.0%	68.0%		.745	.809	.814	.803	.788
	68.4%	72.2%	70.6%	68.4%	69.1%	69.3%		.792	.820	.807	.792	.796
	72.5%	68.6%	66.1%	67.6%	68.6%	67.2%		.821	.793	.774	.785	.793
	74.4%	66.9%	66.3%	66.3%	64.6%	64.0%		.835	.780	.775	.775	.762
	69.3%	69.7%	64.6%	64.4%	64.2%	67.2%		.798	.801	.762	.761	.759

ALPHA&D	.206	.267	.250	.234	.234	.238	n	6.17E+16	7.99E+16	7.48E+16	6.99E+16	6.99E+16
	.294	.212	.206	.220	.238	.238		8.78E+16	6.34E+16	6.17E+16	6.57E+16	7.11E+16
	.234	.199	.214	.234	.228	.226		6.99E+16	5.94E+16	6.40E+16	6.99E+16	6.81E+16
	.197	.232	.257	.242	.232	.246		5.88E+16	6.93E+16	7.67E+16	7.23E+16	6.93E+16
	.180	.248	.254	.254	.272	.278		5.39E+16	7.42E+16	7.61E+16	7.61E+16	8.12E+16
	.226	.222	.272	.274	.276	.246		6.75E+16	6.63E+16	8.12E+16	8.18E+16	8.25E+16

FILE: INP2

SAMPLE= Y=17 TO 22 : X=24 TO 29

I0= 20.8 Tas(3micron)= 58.0% ALPHA#D(AVE)= .096 C(ave)= 3.35E-18

R12= .2658 Tas(10.6micron)= 52.0% n(ave)= 2.87E+16

DATA	15.2	15.0	14.7	15.0	16.3	15.9	BETA	.928	.922	.915	.922	.956
	15.3	15.3	15.0	15.0	14.3	15.2		.930	.930	.922	.922	.905
	13.9	14.5	15.0	14.1	15.0	15.8		.894	.910	.922	.899	.922
	15.7	15.3	15.3	15.7	16.1	15.2		.940	.930	.930	.940	.951
	14.9	14.8	15.7	15.2	15.0	15.6		.920	.917	.940	.928	.922
	15.0	15.2	15.7	14.3	15.1	15.1		.922	.928	.940	.905	.925

Z T	73.1%	72.1%	70.7%	72.1%	78.4%	76.4%	EXP	.826	.819	.808	.819	.863
	73.6%	73.6%	72.1%	72.1%	68.8%	73.1%		.829	.829	.819	.819	.794
	66.8%	69.7%	72.1%	67.8%	72.1%	76.0%		.779	.801	.819	.787	.819
	75.5%	73.6%	73.6%	75.5%	77.4%	73.1%		.843	.829	.829	.843	.857
	71.6%	71.2%	75.5%	73.1%	72.1%	75.0%		.815	.812	.843	.826	.819
	72.1%	73.1%	75.5%	68.8%	72.6%	72.6%		.819	.826	.843	.794	.822

ALPHA#D	.191	.200	.213	.200	.147	.163	n	5.72E+16	5.97E+16	6.36E+16	5.97E+16	4.40E+16
	.187	.187	.200	.200	.231	.191		5.60E+16	5.60E+16	5.97E+16	5.97E+16	6.90E+16
	.249	.222	.200	.240	.200	.167		7.45E+16	6.63E+16	5.97E+16	7.17E+16	5.97E+16
	.171	.187	.187	.171	.155	.191		5.10E+16	5.60E+16	5.60E+16	5.10E+16	4.63E+16
	.204	.208	.171	.191	.200	.175		6.10E+16	6.23E+16	5.10E+16	5.72E+16	5.97E+16
	.200	.191	.171	.231	.196	.196		5.97E+16	5.72E+16	5.10E+16	6.90E+16	5.85E+16

FILE: INP3

SAMPLE= Y=25 TO 30 : X=32 TO 37

I0= 21.5 Tas(3micron)= 58.0% ALPHA#D(AVE)= .096 C(ave)= 3.35E-18

R12= .2658 Tas(10.6micron)= 52.0% n(ave)= 2.87E+16

DATA	15.0	13.2	14.9	15.1	15.0	15.4	BETA	.910	.865	.907	.912	.910
	16.0	15.1	15.1	15.3	15.0	14.7		.935	.912	.912	.917	.910
	16.6	14.7	15.2	15.1	14.6	14.4		.949	.903	.915	.912	.900
	11.7	14.7	14.4	15.0	15.8	15.5		.828	.903	.895	.910	.930
	12.4	13.9	16.7	15.0	14.9	14.2		.846	.883	.952	.910	.907
	15.0	16.2	15.2	15.1	14.5	14.2		.910	.940	.915	.912	.898

Z T	69.8%	61.4%	69.3%	70.2%	69.8%	71.6%	EXP	.802	.737	.798	.805	.802
	74.4%	70.2%	70.2%	71.2%	69.8%	68.4%		.835	.805	.805	.812	.802
	77.2%	68.4%	70.7%	70.2%	67.9%	67.0%		.855	.791	.808	.805	.788
	54.4%	68.4%	67.0%	69.8%	73.5%	72.1%		.678	.791	.780	.802	.829
	57.7%	64.7%	77.7%	69.8%	69.3%	66.0%		.706	.762	.858	.802	.798
	69.8%	75.3%	70.7%	70.2%	67.4%	66.0%		.802	.842	.808	.805	.784

ALHPA#D	.221	.306	.226	.217	.221	.204	n	6.61E+16	9.14E+16	6.74E+16	6.48E+16	6.61E+16
	.180	.217	.217	.208	.221	.234		5.37E+16	6.48E+16	6.48E+16	6.23E+16	6.61E+16
	.156	.234	.213	.217	.239	.248		4.68E+16	7.01E+16	6.36E+16	6.48E+16	7.14E+16
	.388	.234	.248	.221	.188	.200		1.16E+17	7.01E+16	7.41E+16	6.61E+16	5.61E+16
	.348	.271	.153	.221	.226	.257		1.04E+17	8.11E+16	4.56E+16	6.61E+16	6.74E+16
	.221	.172	.213	.217	.243	.257		6.61E+16	5.14E+16	6.36E+16	6.48E+16	7.27E+16

FILE: INP4

SAMPLE= Y=25 TO 30 : X=17 TO 22

10= 21.5 Tas(3micron)= 58.0% ALPHA#D(AVE)= .096 C(ave)= 3.35E-18

R12= .2658 Tas(10.6micron)= 52.0% n(ave)= 2.87E+16

DATA	15.7	14.6	14.4	14.3	14.7	15.2	BETA	.927	.900	.895	.893	.903
	14.6	14.8	14.6	15.2	15.9	11.0		.900	.905	.900	.915	.932
	14.3	14.3	15.0	15.4	16.0	16.2		.893	.893	.910	.920	.935
	15.1	14.9	15.6	16.2	16.1	16.4		.912	.907	.925	.940	.937
	15.3	15.0	14.7	15.1	15.9	16.2		.917	.910	.903	.912	.932
	15.1	15.0	15.2	15.1	15.5	15.8		.912	.910	.915	.912	.922

Z T	73.0%	67.9%	67.0%	66.5%	68.4%	70.7%	EXP	.825	.788	.780	.777	.791
	67.9%	68.8%	67.9%	70.7%	74.0%	51.2%		.788	.795	.788	.808	.832
	66.5%	66.5%	69.8%	71.6%	74.4%	75.3%		.777	.777	.802	.815	.835
	70.2%	69.3%	72.6%	75.3%	74.9%	76.3%		.805	.798	.822	.842	.839
	71.2%	69.8%	68.4%	70.2%	74.0%	75.3%		.812	.802	.791	.805	.832
	70.2%	69.8%	70.7%	70.2%	72.1%	73.5%		.805	.802	.808	.805	.819

ALHPA#D	.192	.239	.248	.252	.234	.213	n	5.73E+16	7.14E+16	7.41E+16	7.55E+16	7.01E+16
	.239	.230	.239	.213	.184	.431		7.14E+16	6.87E+16	7.14E+16	6.36E+16	5.49E+16
	.252	.252	.221	.204	.180	.172		7.55E+16	7.55E+16	6.61E+16	6.10E+16	5.37E+16
	.217	.226	.196	.172	.176	.164		6.48E+16	6.74E+16	5.86E+16	5.14E+16	5.25E+16
	.208	.221	.234	.217	.184	.172		6.23E+16	6.61E+16	7.01E+16	6.48E+16	5.49E+16
	.217	.221	.213	.217	.200	.188		6.48E+16	6.61E+16	6.36E+16	6.48E+16	5.98E+16

FILE: INP5

SAMPLE= Y=10 TO 15 : X=17 TO 22

I0= 21.5 Tas(3micron)= 58.0% ALPHA#D(AVE)= .096 C(ave)= 3.35E-18

R12= .2658 Tas(10.6micron)= 52.0% n(ave)= 2.87E+16

DATA	15.6	15.4	14.4	15.0	15.1	15.4	BETA	.925	.920	.895	.910	.912
	14.7	14.7	15.3	15.6	15.4	15.3		.903	.903	.917	.925	.920
	15.3	15.6	15.7	15.0	15.0	14.9		.917	.925	.927	.910	.910
	15.0	14.8	15.0	15.1	14.8	15.1		.910	.905	.910	.912	.905
	15.6	15.0	15.1	15.0	15.5	15.2		.925	.910	.912	.910	.922
	16.0	16.0	15.7	16.0	15.9	15.8		.935	.935	.927	.935	.932

Z T	72.6%	71.6%	67.0%	69.8%	70.2%	71.6%	EXP	.822	.815	.780	.802	.805
	68.4%	68.4%	71.2%	72.6%	71.6%	71.2%		.791	.791	.812	.822	.815
	71.2%	72.6%	73.0%	69.8%	69.8%	69.3%		.812	.822	.825	.802	.802
	69.8%	68.8%	69.8%	70.2%	68.8%	70.2%		.802	.795	.802	.805	.795
	72.6%	69.8%	70.2%	69.8%	72.1%	70.7%		.822	.802	.805	.802	.819
	74.4%	74.4%	73.0%	74.4%	74.0%	73.5%		.835	.835	.825	.835	.832

ALHPA#D	.196	.204	.248	.221	.217	.204	n	5.86E+16	6.10E+16	7.41E+16	6.61E+16	6.48E+16
	.234	.234	.208	.196	.204	.208		7.01E+16	7.01E+16	6.23E+16	5.86E+16	6.10E+16
	.208	.196	.192	.221	.221	.226		6.23E+16	5.86E+16	5.73E+16	6.61E+16	6.61E+16
	.221	.230	.221	.217	.230	.217		6.61E+16	6.87E+16	6.61E+16	6.48E+16	6.87E+16
	.196	.221	.217	.221	.200	.213		5.86E+16	6.61E+16	6.48E+16	6.61E+16	5.98E+16
	.180	.180	.192	.180	.184	.188		5.37E+16	5.37E+16	5.73E+16	5.37E+16	5.49E+16

END

1-87

DTIC